REPORT DOCUMENTATION PAGE

Form Approved OMB NO. 0704-0188

1. REPORT DATE (DD-MM-YYYY)	2. REPORT TYPE	3. DATES COVERED (From - To)
12-12-2014	Final Report	16-Sep-2009 - 15-Sep-2014

4. TITLE AND SUBTITLE
Final Report: Novel Quantum Phases at Interfaces

5a. CONTRACT NUMBER
W911NF-09-1-0527

5b. GRANT NUMBER

5c. PROGRAM ELEMENT NUMBER
611103

6. AUTHORS
Gregory A. Fiete

5d. PROJECT NUMBER

5e. TASK NUMBER

5f. WORK UNIT NUMBER

7. PERFORMING ORGANIZATION NAMES AND ADDRESSES
University of Texas at Austin
101 East 27th Street
Suite 5.300
Austin, TX 78712 -1532

8. PERFORMING ORGANIZATION REPORT NUMBER

9. SPONSORING/MONITORING AGENCY NAME(S) AND ADDRESS (ES)
U.S. Army Research Office
P.O. Box 12211
Research Triangle Park, NC 27709-2211

10. SPONSOR/MONITOR'S ACRONYM(S)
ARO

11. SPONSOR/MONITOR'S REPORT NUMBER(S)
54680-PH-PCS.74

12. DISTRIBUTION AVAILIBILITY STATEMENT
Approved for Public Release; Distribution Unlimited

13. SUPPLEMENTARY NOTES
The views, opinions and/or findings contained in this report are those of the author(s) and should not contrued as an official Department of the Army position, policy or decision, unless so designated by other documentation.

14. ABSTRACT
In this project we studied topological phases at transition metal oxide interfaces. Over the course of the 5-year project, a fairly detailed understanding of these systems was acquired. By using a combination of model Hamiltonian studies and first-principles calculations, we made a number of predictions for specific material systems that might exhibit topological phases, with the most promising candidate being the zero magnetic field quantum Hall state known as a Chern insulator or quantum anomalous Hall state. [111] grown thin films of LaNiO3 and Y2Ir2O7 may support this phase under the right conditions (which appear to be close to current experimental

15. SUBJECT TERMS
Topological phases, oxide interfaces, electron correlations

16. SECURITY CLASSIFICATION OF:			17. LIMITATION OF ABSTRACT	15. NUMBER OF PAGES	19a. NAME OF RESPONSIBLE PERSON
a. REPORT	b. ABSTRACT	c. THIS PAGE			Gregory Fiete
UU	UU	UU	UU		19b. TELEPHONE NUMBER 512-232-8084

Report Title

Final Report: Novel Quantum Phases at Interfaces

ABSTRACT

In this project we studied topological phases at transition metal oxide interfaces. Over the course of the 5-year project, a fairly detailed understanding of these systems was acquired. By using a combination of model Hamiltonian studies and first-principles calculations, we made a number of predictions for specific material systems that might exhibit topological phases, with the most promising candidate being the zero magnetic field quantum Hall state known as a Chern insulator or quantum anomalous Hall state. [111] grown thin films of LaNiO3 and Y2Ir2O7 may support this phase under the right conditions (which appear to be close to current experimental conditions). The main technological advantage of this topological phase is that its one-dimensional edge state allows for dissipationless current flow, and can be used for low-power electronics, potentially at room temperature (which a superconductor cannot do).

Enter List of papers submitted or published that acknowledge ARO support from the start of the project to the date of this printing. List the papers, including journal references, in the following categories:

(a) Papers published in peer-reviewed journals (N/A for none)

Received		Paper
02/05/2010	6.00	g. Fiete, A. deLozanne. Seeing Quantum Fractals, Science, (02 2010): . doi:
02/27/2013	52.00	Seth Whitsitt, Victor Chua, Gregory A Fiete. Exact chiral spin liquids and mean-field perturbations of gamma matrix models on the ruby lattice, New Journal of Physics, (11 2012): 115029. doi: 10.1088/1367-2630/14/11/115029
02/27/2013	57.00	Andreas Rüegg, Emanuel Gull, Gregory A. Fiete, Andrew J. Millis. Sum rule violation in self-consistent hybridization expansions, Physical Review B, (02 2013): 75124. doi: 10.1103/PhysRevB.87.075124
02/27/2013	56.00	Dimitrios Koumoulis, Thomas C. Chasapis, Robert E. Taylor, Michael P. Lake, Danny King, Nanette N. Jarenwattananon, Gregory A. Fiete, Mercouri G. Kanatzidis, Louis-S. Bouchard. NMR Probe of Metallic States in Nanoscale Topological Insulators, Physical Review Letters, (01 2013): 26602. doi: 10.1103/PhysRevLett.110.026602
02/27/2013	55.00	Rex Lundgren, Victor Chua, Gregory A. Fiete. Entanglement entropy and spectra of the one-dimensional Kugel-Khomskii model, Physical Review B, (12 2012): 224422. doi: 10.1103/PhysRevB.86.224422
02/27/2013	54.00	Andreas Rüegg, Gregory A. Fiete, Xiang Hu. Topological phases in layered pyrochlore oxide thin films along the [111] direction, Physical Review B, (12 2012): 235141. doi: 10.1103/PhysRevB.86.235141
02/27/2013	53.00	Mehdi Kargarian, Abdollah Langari, Gregory A. Fiete. Unusual magnetic phases in the strong interaction limit of two-dimensional topological band insulators in transition metal oxides, Physical Review B, (11 2012): 205124. doi: 10.1103/PhysRevB.86.205124
04/22/2013	58.00	Mehdi Kargarian, Gregory A. Fiete. Topological Crystalline Insulators in Transition Metal Oxides, Physical Review Letters, (04 2013): 156403. doi: 10.1103/PhysRevLett.110.156403
04/22/2013	59.00	Hsiang-Hsuan Hung, Lei Wang, Zheng-Cheng Gu, Gregory A. Fiete. Topological phase transition in a generalized Kane-Mele-Hubbard model: A combined quantum Monte Carlo and Green's function study, Physical Review B, (03 2013): 121113. doi: 10.1103/PhysRevB.87.121113
08/10/2012	40.00	Andreas Rüegg, Gregory Fiete. Topological insulators from complex orbital order in transition-metal oxides heterostructures, Physical Review B, (11 2011): 0. doi: 10.1103/PhysRevB.84.201103
08/10/2012	47.00	Gregory A. Fiete, Victor Chua, Mehdi Kargarian, Rex Lundgren, Andreas Rüegg, Jun Wen, Vladimir Zyuzin. Topological insulators and quantum spin liquids, Physica E: Low-dimensional Systems and Nanostructures, (02 2012): 0. doi: 10.1016/j.physe.2011.11.011
08/10/2012	46.00	Chih-Kang Shih, Jungdae Kim, Victor Chua, Gregory A. Fiete, Hyoungdo Nam, Allan H. MacDonald. Visualization of geometric influences on proximity effects in heterogeneous superconductor thin films, Nature Physics, (04 2012): 0. doi: 10.1038/nphys2287

08/10/2012 45.00 Andreas Rüegg, Chandrima Mitra, Alexander Demkov, Gregory Fiete. Electronic structure of (LaNiO_{3})_{2}/(LaAlO_{3})_{N} heterostructures grown along [111],
Physical Review B, (06 2012): 0. doi: 10.1103/PhysRevB.85.245131

08/10/2012 44.00 Gregory Fiete, Vladimir Zyuzin. Spatially anisotropic kagome antiferromagnet with Dzyaloshinskii-Moriya interaction,
Physical Review B, (03 2012): 0. doi: 10.1103/PhysRevB.85.104417

08/10/2012 43.00 Andreas Rüegg, Gregory Fiete. Topological Order and Semions in a Strongly Correlated Quantum Spin Hall Insulator,
Physical Review Letters, (01 2012): 0. doi: 10.1103/PhysRevLett.108.046401

08/10/2012 41.00 Gregory Fiete, Victor Chua. Exactly solvable topological chiral spin liquid with random exchange,
Physical Review B, (11 2011): 0. doi: 10.1103/PhysRevB.84.195129

08/24/2012 42.00 Jun Wen, Mehdi Kargarian, Abolhassan Vaezi, Gregory Fiete. Doping the Kane-Mele-Hubbard model: A slave-boson approach,
Physical Review B, (12 2011): 0. doi: 10.1103/PhysRevB.84.235149

10/05/2011 23.00 Jungdae Kim, Gregory Fiete, Hyoungdo Nam, A. H. MacDonald, Chih-Kang Shih. Universal quenching of the superconducting state of two-dimensional nanosize Pb-island structures,
Physical Review B, (7 2011): 0. doi: 10.1103/PhysRevB.84.014517

10/05/2011 24.00 Gregory Fiete, Stuart Sevier. Non-Fermi-liquid quantum impurity physics from non-Abelian quantum Hall states,
Physical Review B, (7 2011): 0. doi: 10.1103/PhysRevB.84.035101

10/05/2011 25.00 Victor Chua, Hong Yao, Gregory Fiete. Exact chiral spin liquid with stable spin Fermi surface on the kagome lattice,
Physical Review B, (5 2011): 0. doi: 10.1103/PhysRevB.83.180412

10/05/2011 26.00 G. A. Fiete. How Do You Want That Insulator?,
Science, (04 2011): 0. doi: 10.1126/science.1205251

10/05/2011 27.00 Andreas Rüegg, Gregory Fiete. Fractionally charged topological point defects on the kagome lattice,
Physical Review B, (4 2011): 0. doi: 10.1103/PhysRevB.83.165118

10/05/2011 28.00 Mehdi Kargarian, Jun Wen, Gregory Fiete. Competing exotic topological insulator phases in transition-metal oxides on the pyrochlore lattice with distortion,
Physical Review B, (4 2011): 0. doi: 10.1103/PhysRevB.83.165112

10/05/2011 29.00 Fan Zhang, Jeil Jung, Gregory Fiete, Qian Niu, Allan MacDonald. Spontaneous Quantum Hall States in Chirally Stacked Few-Layer Graphene Systems,
Physical Review Letters, (4 2011): 0. doi: 10.1103/PhysRevLett.106.156801

10/05/2011 30.00 Adrian Feiguin, Gregory Fiete. Spin-Incoherent Behavior in the Ground State of Strongly Correlated Systems,
Physical Review Letters, (4 2011): 0. doi: 10.1103/PhysRevLett.106.146401

10/05/2011 31.00 Vladimir Zyuzin, Gregory Fiete. Coulomb drag between helical edge states,
Physical Review B, (9 2010): 0. doi: 10.1103/PhysRevB.82.113305

10/05/2011 32.00 Jun Wen, Andreas Rüegg, C.-C. Wang, Gregory Fiete. Interaction-driven topological insulators on the kagome and the decorated honeycomb lattices,
Physical Review B, (8 2010): 0. doi: 10.1103/PhysRevB.82.075125

10/06/2011 33.00 Mehdi Kargarian, Gregory Fiete. Topological phases and phase transitions on the square-octagon lattice,
Physical Review B, (8 2010): 0. doi: 10.1103/PhysRevB.82.085106

10/06/2011 34.00 Gregory Fiete, Waheb Bishara, Chetan Nayak. Exotic resonant level models in non-Abelian quantum Hall states coupled to quantum dots,
Physical Review B, (7 2010): 0. doi: 10.1103/PhysRevB.82.035301

10/06/2011 35.00 Andreas Rüegg, Jun Wen, Gregory A. Fiete. Topological insulators on the decorated honeycomb lattice,
Physical Review B, (05 2010): 0. doi: 10.1103/PhysRevB.81.205115

10/06/2011 36.00 Adrian E. Feiguin. Spectral properties of a spin-incoherent Luttinger liquid,
Physical Review B, (02 2010): 0. doi: 10.1103/PhysRevB.81.075108

10/06/2011 37.00 Alexander A. Khajetoorians, Gregory A. Fiete, Chih-Kang Shih. Visualizing quantum well state perturbations of metallic thin films near stacking fault defects,
Physical Review B, (01 2010): 0. doi: 10.1103/PhysRevB.81.041413

10/06/2011 38.00 A. Rüegg, S. D. Huber, M. Sigrist. Z_{2} -slave-spin theory for strongly correlated fermions,
Physical Review B, (04 2010): 0. doi: 10.1103/PhysRevB.81.155118

12/12/2014 64.00 Hsin-Hua Lai, Hsiang-Hsuan Hung, Gregory A. Fiete. Short-ranged interaction effects on <math xmlns="http://www.w3.org/1998/Math/MathML"><msub><mi>Z</mi><mn>2</mn></msub></math> topological phase transitions,
Physical Review B, (11 2014): 195120. doi: 10.1103/PhysRevB.90.195120

12/12/2014 65.00 Rex Lundgren, Pontus Laurell, Gregory A. Fiete. Thermoelectric properties of Weyl and Dirac semimetals,
Physical Review B, (10 2014): 165115. doi: 10.1103/PhysRevB.90.165115

12/12/2014 66.00 Hsiang-Hsuan Hung, Victor Chua, Lei Wang, Gregory A. Fiete. Interaction effects on topological phase transitions via numerically exact quantum Monte Carlo calculations,
Physical Review B, (06 2014): 235104. doi: 10.1103/PhysRevB.89.235104

12/12/2014 67.00 Joseph Maciejko, Victor Chua, Gregory Fiete. Topological Order in a Correlated Three-Dimensional Topological Insulator,
Physical Review Letters, (01 2014): 16404. doi: 10.1103/PhysRevLett.112.016404

12/12/2014 68.00 Andreas Rüegg, Hsiang-Hsuan Hung, Emanuel Gull, Gregory A. Fiete. Comparative DMFT study of the <math><msub><mi>e</mi><mi>g</mi></msub></math>-orbital Hubbard model in thin films,
Physical Review B, (02 2014): 85122. doi: 10.1103/PhysRevB.89.085122

12/12/2014 69.00 Mehdi Kargarian, Gregory A. Fiete. Multiorbital effects on thermoelectric properties of strongly correlated materials,
Physical Review B, (11 2013): 205141. doi: 10.1103/PhysRevB.88.205141

12/12/2014 70.00 Andreas Rüegg, Chandrima Mitra, Alexander A. Demkov, Gregory A. Fiete. Lattice distortion effects on topological phases in (LaNiO_{3})_{2}/(LaAlO_{3})_{N} heterostructures grown along the [111] direction,
Physical Review B, (09 2013): 115146. doi: 10.1103/PhysRevB.88.115146

TOTAL: 40

Number of Papers published in peer-reviewed journals:

(b) Papers published in non-peer-reviewed journals (N/A for none)

Received		Paper
02/27/2013	51.00	Gregory A. Fiete. Topological insulators: Crystalline protection, Nature Materials, (11 2012): 1003. doi: 10.1038/nmat3473
10/06/2011	39.00	Gregory Fiete. In a tight spot, spin and charge separate, Physics, (4 2011): 0. doi: 10.1103/Physics.4.30
TOTAL:	**2**	

Number of Papers published in non peer-reviewed journals:

(c) Presentations

Over the course of this grant, I gave approximately 50 invited talks at meetings, conferences, workshops, and universities. All the work presented in these talks appeared (or will appear) in publications.

Number of Presentations: 50.00

Non Peer-Reviewed Conference Proceeding publications (other than abstracts):

Received	Paper
TOTAL:	

Number of Non Peer-Reviewed Conference Proceeding publications (other than abstracts):

Peer-Reviewed Conference Proceeding publications (other than abstracts):

Received	Paper
TOTAL:	

Number of Peer-Reviewed Conference Proceeding publications (other than abstracts):

(d) Manuscripts

Received		Paper
01/03/2011	15.00	Mehdi Kargarian. Implementation of Single-Qubit and CNOT Gates by Anyonic Excitations of Color Code Model with Two-Body Interactions, (12 2010)
01/10/2011	16.00	S. Sevier, G. Fiete. Non-Fermi Liquid Quantum Impurity Physics from non-Abelian Quantum Hall States, (01 2011)
01/11/2011	17.00	A. ruegg, G. Fiete. Fractionally charged topological point defects on the kagome lattice, (01 2011)
02/27/2013	48.00	Mehdi Kargarian, Gregory A. Fiete. Topological Crystalline Insulators in Transition Metal Oxides, arXiv:1212.4162 (12 2012)
02/27/2013	50.00	Dimitrios Koumoulis, Gerald D. Morris, Liang He, Xufeng Kou, Daniel King Jr, Kang L. Wang, Gregory A. Fiete, Mercouri G. Kanatzidis, Louis-S. Bouchard. Nanoscale nuclear spin probe of metallic and magnetic order in topological insulator heterostructures, Nature Physics (submitted) (02 2013)
02/27/2013	49.00	Hsiang-Hsuan Hung, Lei Wang , Zheng-Cheng Gu, Gregory A. Fiete. Topological phase transition in a generalized Kane-Mele-Hubbard model: A combined Quantum Monte Carlo and Green's function study, Phys Rev Lett (submitted) (02 2012)
05/21/2010	7.00	M. Kargarian, G. Fiete. Topological phases and phase transitions on the square-octagon lattice, (05 2010)
05/21/2010	8.00	J. Wen, A. Ruegg, G. Fiete. Interaction-driven topological insulators on the kagome and the decorated honeycomb lattices, (05 2010)
05/24/2010	9.00	A. Feiguin, G. Fiete. Spin-incoherent behavior in the ground state of strongly correlated systems, (05 2010)
06/06/2011	18.00	X. Hu, M. Kargarian, G. Fiete. Topological insulators and fractional quantum Hall effect on the ruby lattice, (05 2011)
06/07/2010	10.00	V. Zyuzin, G. Fiete. Coulomb drag between helical edge states, (06 2010)
06/07/2011	19.00	G. Fiete, V. Chua, X. Hu, M. Kargarian. Topological Insulators and Quantum Spin Liquids, (05 2011)
06/08/2011	20.00	A. Ruegg, G. Fiete. Topological Order and Semions in a Strongly Correlated Quantum Spin Hall Insulator, (06 2011)
07/28/2010	11.00	J. Kim, G. Fiete, H. Nam, A. MacDonald, C. Shih. Two-dimensional Nano-island Superconductivity, (07 2010)
08/17/2011	22.00	Victor Chua, Gregory A. Fiete. Exactly Solvable Topological Chiral Spin Liquid with Random Exchange , (submitted) (07 2011)

08/17/2011 21.00 Jun Wen,, Mehdi Kargarian,, Abolhassan Vaezi, , Gregory A. Fiete. Doping the Kane-Mele-Hubbard model: A Slave-Boson Approach ,
(submitted) (06 2011)

08/22/2013 60.00 Mehdi Kargarian, Gregory A. Fiete. Multi-orbital Effects on Thermoelectric Properties of Strongly Correlated Materials,
ArXiv e-prints (08 2013)

08/22/2013 62.00 Joseph Maciejko, Victor Chua, Gregory A. Fiete. Topological order in a correlated three-dimensional topological insulator,
ArXiv e-prints (07 2013)

08/22/2013 61.00 Hsiang-Hsuan Hung, Victor Chua, Lei Wang , Gregory A. Fiete. Finite-size and interaction effects on topological phase transitions via numerically exact quantum Monte Carlo calculations,
ArXiv e-prints (07 2013)

08/23/2013 63.00 Andreas Ruegg, Chandrima Mitra, Alexander A. Demkov, Gregory A. Fiete. Strain effects on topological phases in (LaNiO$_3$)$_2$/(LaAlO$_3$)$_N$ heterostructures grown along the [111] direction,
ArXiv e-prints (07 2013)

10/26/2009 1.00 A. Khajetoorians, G. Fiete, C. Shih. Visualizing Quantum Well State Perturbations of Metallic Thin Films near Stacking Fault Defects,
(10 2009)

10/26/2009 2.00 A. Feiguin, G. Fiete. Spectral properties of a spin-incoherent Luttinger Liquid,
(10 2009)

10/27/2010 12.00 G. Fiete, F. Zhang, J. Jung, A. Niu, A. MacDonald. Spontaneous Quantum Hall States in Chirally-stacked Few-Layer Graphene Systems,
(10 2010)

11/16/2009 3.00 G. Fiete, W. Bishara, C. Nayak. Exotic resonant level models in non-Abelian quantum Hall states coupled to quantum dots,
(11 2009)

11/27/2009 4.00 A. Ruegg, J. Wen, G. fiete. Topological Insulators on the Decorated Honeycomb Lattic,
(11 2009)

12/12/2014 71.00 Xiang Hu, Zhicheng Zhong, Gregory A. Fiete. First Principles Prediction of Topological Phases in Thin Films of Pyrochlore Iridates,
arXiv:1411.7333 (11 2014)

12/12/2014 73.00 Rex Lundgren , Jonathan Blair, Martin Greiter , Andreas Läuchli , Gregory A. Fiete , Ronny Thomale. Momentum Space Entanglement Spectrum of Bosons and Fermions with Interactions,
arXiv:1404.7545 (04 2014)

12/12/2014 72.00 Yao-Hua Chen, Hsiang-Hsuan Hung, Guoxiong Su, Gregory A. Fiete, C. S. Ting. Cellular dynamical mean-field theory study of an interacting topological honeycomb lattice model at finite temperature,
arXiv:1408.4847 (08 2014)

12/20/2010 13.00 V. Zyuzin, A. Zyuzin. Role of domain wall fluctuations in non-Fermi liquid behavior of metamagnets,
(12 2010)

12/22/2009 5.00 A. Ruegg, S. Huber, M. Sigrist. A Z2-slave-spin theory for strongly correlated fermions,
(12 2009)

12/30/2010 14.00 Mehdi Kargarian, Jun Wen, Gregory A. Fiete. Competing Exotic Topological Insulator Phases in Transition Metal Oxides on the Pyrochlore Lattice with Distortion,
(12 2010)

TOTAL: 31

Number of Manuscripts:

Books

Received Book

TOTAL:

Received Book Chapter

TOTAL:

Patents Submitted

Patents Awarded

Awards

While holding this grant, the PI received an NSF CAREER Award and a DARPA Young Faculty Award. He received a College of Natural Sciences teaching award, and was a finalist for a UT system-wide teaching award. He was invited to the address the US National Academy of Sciences on the topic of this grant. Many of this students received awards, include 3 NSF Graduate Research Fellowships and one student was an APS Apker Award Finalist. Prior group members have gone to Harvard, Stanford, UC Berkeley, and University of Illinois-Urbana Champaign.

Graduate Students

NAME	PERCENT_SUPPORTED	Discipline
Xiang Hu	1.00	
Qi Chen	0.80	
FTE Equivalent:	**1.80**	
Total Number:	**2**	

Names of Post Doctorates

NAME	PERCENT_SUPPORTED
Xiaoting Zhou	1.00
Hsiang-Hsuan	0.80
FTE Equivalent:	**1.80**
Total Number:	**2**

Names of Faculty Supported

NAME	PERCENT_SUPPORTED	National Academy Member
Gregory A. Fiete	0.15	
FTE Equivalent:	**0.15**	
Total Number:	**1**	

Names of Under Graduate students supported

NAME	PERCENT_SUPPORTED
FTE Equivalent:	
Total Number:	

Student Metrics

This section only applies to graduating undergraduates supported by this agreement in this reporting period

The number of undergraduates funded by this agreement who graduated during this period: 3.00

The number of undergraduates funded by this agreement who graduated during this period with a degree in science, mathematics, engineering, or technology fields:..... 3.00

The number of undergraduates funded by your agreement who graduated during this period and will continue to pursue a graduate or Ph.D. degree in science, mathematics, engineering, or technology fields:..... 2.00

Number of graduating undergraduates who achieved a 3.5 GPA to 4.0 (4.0 max scale):..... 3.00

Number of graduating undergraduates funded by a DoD funded Center of Excellence grant for Education, Research and Engineering:..... 0.00

The number of undergraduates funded by your agreement who graduated during this period and intend to work for the Department of Defense 0.00

The number of undergraduates funded by your agreement who graduated during this period and will receive scholarships or fellowships for further studies in science, mathematics, engineering or technology fields:..... 3.00

Names of Personnel receiving masters degrees

NAME
Total Number:

Names of personnel receiving PHDs

NAME	
Jun Wen	
Victor Chua	
Vladimir Zyzuin	
Ran Cheng	
Total Number:	**4**

Names of other research staff

NAME	PERCENT_SUPPORTED
FTE Equivalent:	
Total Number:	

Sub Contractors (DD882)

Inventions (DD882)

Scientific Progress

Please see attachment.

Technology Transfer

The PI currently serves as a consultant to the DoD, and many results from his research have been relayed to various points throughout the DoD.

ARO PECASE Research Summary

Gregory A. Fiete
University of Texas at Austin

The title of my PECASE project was "Novel quantum phases at interfaces". The main focus of this project was the exploration of novel quantum phenomena in correlated materials at the interface of transition metal oxides, but over the 5-year duration of the award many closely related projects were undertaken that could help to inform the understanding of quantum behavior at interfaces. In particular, the study of topological phases featured prominently throughout; I believe the work funded here has had a broader impact on the field of condensed matter physics by bringing others into this line of inquiry and by laying some of the initial (and current) expectations for how likely one is to find certain correlated electronic phases in the interfaces and heterostructures we studied. For the DoD, and Army in particular, I hope the research summarized here will ultimately be useful for next generation technologies, particularly in the areas of communication and sensing.

Approximately 50 papers—and a similar number of invited talks—resulted from this award (including works in *Nature Physics*, *Nature Materials*, *Science*, and *Physical Review Letters*), so it is not possible to summarize all of the results in detail. The most important results were conveyed in real-time to the program manager for this project, Dr. Marc Ulrich. In order to best facilitate the internalization of some of the most important results, I have provided a "lay" summary in the text that immediately follows, and I have also attached 3 review articles (either in draft form, or the final published form, if available). Together, they provide an excellent summary, with references, of the most important technical accomplishments of this project. The first, "Topological Phases in Oxide Heterostructures with Light and Heavy Transition metal ions" highlights work at the core of this project. The second, "Fractionalized Topological Phases", highlights some of the new ground broken on the fundamental influence of interactions on topological phases. The third, "Topological Insulators and Quantum Spin Liquids", highlights deep connections between frustrated magnetic systems with no magnetic order and topological insulators. In addition to the technical accomplishments, many students and postdocs were trained, and countless informal discussions were held with professional colleagues in the dissemination of these results.

Some Specific Accomplishments from the Last Few Years

Recently, I have focused my group's research efforts on two main topics at the forefront of research in condensed matter physics:

(i) Topological Insulators
(ii) Quantum Spin Liquids

These names may not be especially meaningful to scientists outside of condensed matter physics, so I will briefly summarize what they are, as well as a few key contributions of my group to each of these areas.

Topological Insulators

Most materials fall into one of two categories—a metal (conductor) or an insulator. (Semiconductors are not "half-conductors", but rather insulators that are in a certain sense "weakly" insulating.) For about half a century, physicists thought they understood insulators of the semiconducting variety rather well. We have designed the transistor

around their properties, and most electronic devices incorporate them in some way. Such insulators are commonplace.

It thus came as a major surprise in the first decade of the 21st century that physicists had missed something huge in this class of materials: The full breadth of relativistic effects. The theory of Special Relativity, for which Einstein is famous, plays a role in solids when the nuclei are heavy, and this modifies the electronic motion in highly non-trivial ways. In the language of solid state physics, this effect is called "spin-orbit coupling" because the spin, or magnetic moment of the electron, is coupled to its motion through a relativistic transformation of the nuclear electric field to a magnetic field in the reference frame of the electron. As the electron moves through the solid, the direction of its spin changes in response to the varying magnetic field in its frame. While this effect has been known for some time, it was previously thought have a very weak on the overall physics of materials. Physicists have since learned that spin-orbit coupling can drive a phase transition from an ordinary insulator to a "topological insulator".

A topological insulator (of the most common variety—"Z_2") has a precise mathematical description, but its salient property is that it is insulating in the bulk and *conducting on its boundary* (surface). Moreover, its conducting surface is unlike any previously known conductor, and it is predicted to have a number of potentially novel uses in electronic devices, including nearly dissipationless charge and spin transport at room temperature.

In a rare chapter of physics history, the existence of the topological insulator was predicted theoretically before it was discovered experimentally (only a year after its prediction). The usual order in condensed matter physics is experimental discovery first, theoretical explanation (if any—high temperature superconductivity still does not have one) second. Today, the study of topological insulators is still dominated by theoretical physicists, and many open questions remain, particularly involving what happens in materials with strong electron correlations and additional symmetries (crystalline, for example) that may enrich or further protect topological properties.

The issue of electron interactions lies at the heart of my group's effort in this area, and more generally in all the problems we investigate in my group. Our work has so far focused primarily on model Hamiltonian studies in which we predict new phases of matter driven by the presence of both strong interactions and spin-orbit coupling. We have we predicted a new phase known as a "weak topological Mott insulator", a new phase known as "QSH*", a new phase known as "TCMI", a new phase known as "TI*". Each of these phases possesses some unusual properties that are related to topological properties of the many-body wave function that originate in strong interactions and strong spin-orbit coupling. These phases cannot exist without the presence of significant electron-electron interactions, and in this sense are truly distinct from the class of topological phases reported in bulk Bi_2Se_3 and HgTe/CdTe quantum wells.

Electronic wave functions with topological properties are heavily sought after because they endow usually "fragile" quantum properties with orders of magnitude improvements in their robustness. Materials with topological electronic properties can open the door to transformative technologies in sensing and computing, for example.

A new direction undertaken by my group recently is the theoretical search for materials that will exhibit topological properties predicted in model Hamiltonian studies that

incorporate interactions in a fundamental way. This new effort will bridge theoretical studies my group has carried out with the latest developments in materials growth (for example, molecular beam epitaxy—used to grow new materials atomic layer-by-atomic layer). Our work now combines state-of-the-art numerical methods, such as DFT+DMFT and DFT+Gutzwiller, with input from leading experimental groups to advance technology in this direction. In addition, we are also studying non-equilibrium physics in models (many relevant to topological phases) that are aimed at bringing a higher degree of experimental relevance than many of those studied to date, including the ``Floquet" states.

Quantum Spin Liquids

Quantum spin liquids are a rare class of systems with local magnetic moments or "spins" which are not macroscopically magnetic in any way—even at the absolute zero of temperature. In effect, the magnetic degrees of freedom are disordered and random, much like the atomic positions in a liquid, hence the name. In a ferromagnetic material like iron, most of the magnetic degrees of freedom (spins) orient themselves in the same direction to form a material with a net magnetization at room temperature. We have all seen how this magnetization can be used to pick up or move small iron filings, for example. It turns out that in materials with local spins, the *spins nearly always order in some way*—ferromagnetic, antiferromagnetic, spiral, etc. at some finite temperature. This is because of the presence of a characteristic interaction (exchange) energy scale between spins (think dipole-dipole interactions from electricity and magnetism, for simplicity) that will become important once the temperature drops below this energy scale.

However, in some interacting spin systems competing energies make the lowest energy configuration of spins difficult to ``find". This feature goes under the general name "frustration". For example, consider a triangle with spins on each vertex (for a total of three). Suppose the energy of two spins is minimized if they are oriented in exactly the opposite direction (as would occur in an ideal antiferromagnet). By drawing a simple picture, it is clear that it is not possible to have each of the three spins oriented opposite to the two other spins. This is an example of "frustration". In physical systems with frustration, it is possible that the system is never able to find a configuration that minimizes the total energy as the temperature is lowered, and it fluctuates (quantum mechanically) between many different configurations. When this happens at zero temperature, the system is referred to as a quantum spin liquid.

Why would one be interested in studying quantum spin liquids? The study of quantum spin liquids is vibrant because they are among the richest (in terms of phenomenology) known interacting, quantum many-particle systems. As a result, the study of quantum spin liquids has revealed many fundamental aspects of quantum mechanics. It is probably fair to say that over the last two decades a fair fraction of the theoretical advances in our knowledge of many-body quantum mechanics is related to quantum spin liquids in some way. There are deep connections to string theory via the technical tool of conformal field theory, connections to high-energy particle physics via lattice gauge theories, connections to the fractional quantum Hall effect via fractionalized quantum numbers, connections to quantum information through entanglement studies, and promising potential for quantum computing via non-Abelian excitations (notably Majorana fermions) in some quantum spin liquids. Moreover, quantum spin liquids display a cornucopia of topological properties.

My group has focused on exploring the topological properties of the many-body wave functions of quantum spin liquids. We have established some rather general statements

and powerful relations between quantum spin liquids and topological insulators, unifying these two areas of research, which are most often thought of as disjoint. It is one concrete example of the benefits of working outside the traditional boundaries of sub-fields within condensed matter physics. We have also established some important results in quantum spin liquids, such as that disorder in the Hamiltonian can help stabilize certain types of topological phases,and we have established a first example of a quantum spin liquid phase.

Summary and Future Directions

In the short description above of my research, I left out a number of other areas in which my group has made contributions. In the interest of brevity, and to highlight the diversity of our research efforts, I will just flag the work on the entanglement spectrum of strongly correlated one-dimensional systems in references.

In addition to the basic research activity described here, I have also written invited "Perspective" articles in *Science*, "News & Views" in *Nature Materials* and invited "Viewpoint" articles in *Physics* intended to bring important developments to a wide audience. I have also received an invitation from the *US National Academy of Sciences* to address the Board of Physics and Astronomy in a 45 minute talk on the potential applications of topological insulators in devices: http://sites.nationalacademies.org/BPA/BPA_067816. Former group members have gone to **Harvard, Stanford**, **UC Berkeley**, and **UIUC** among other places. Among former undergraduates, three have received **NSF Graduate Research Fellowships**, and one was an **APS Apker Award Finalist**.

In the immediate future, my group will be devoting a significant portion of its research effort to studying the physics of transition metal oxides with heavy transition metals that incorporate both strong electron-electron interactions and strong spin-orbit coupling—widely acknowledged as key ingredients for novel quantum phenomena in materials. The transition metal oxides have already given us high-temperature superconductivity, colossal magnetoresistance, metal-insulator transitions, and (through molecular beam epitaxial growth) can be used to produce "materials by design" with layer-by-layer growth. It is widely thought that *if* the fundamental physics of this class of materials can be understood and controlled, it will lead to a new generation of electronics with greater functionality, sensitivity, and capability than currently available.

Finally, there is no need to restrict research effort to equilibrium phenomena in this or other classes of materials. The rapid development of laser technology in the last decade combined with the productive cross-fertilization between cold atom physics (where non-equilibrium, time-dependent phenomena are readily studied) and solid state physics makes the time ripe for a push by the condensed matter community to address non-equilibrium phenomena in correlated materials. My current funding from the ARO is in this direction. We have already developed a non-equilibrium DMFT code that presently few groups in the world possess. We hope that we will be able to settle a range of questions of both fundamental interest and practical relevance to real experimental systems.

Topological Phases in Oxide Heterostructures with Light and Heavy Transition Metal Ions

Gregory A. Fiete[1, a)] and Andreas Rüegg[2]
[1)] *Department of Physics, The University of Texas at Austin, Austin, Texas 78712, USA*
[2)] *Theoretische Physik, ETH Zürich, CH-8093 Zürich, Switzerland*

(Dated: 4 November 2014)

Using a combination of density functional theory, tight-binding models, and Hartree-Fock theory, we predict topological phases with and without time-reversal symmetry breaking in oxide heterostructures. We consider both heterostructures containing light transition metal ions, and those containing heavy transition metal ions. We find the (111) growth direction naturally leads to favorable conditions for topological phases in both perovskite structures and pyrochlore structures. For the case of light transition metal elements, Hartree-Fock theory predicts the spin-orbit coupling is effectively enhanced by on-site multiple-orbital interactions and may drive the system through a topological phase transition, while heavy elements with intrinsically large spin-orbit coupling require much weaker, or even vanishing electron interactions to bring about a topological phase.

I. INTRODUCTION

Topological insulators (TI) have now been studied for nearly a decade and there are a number of excellent reviews available, from both an experimental and theoretical perspective.[1–4] Aside from the important example of SmB_6,[5–8] all other experimental examples of topological insulators are weakly correlated. The most important reason for the weak correlation effects is that the bands of topological insulators near the Fermi energy are derived from s and p-type orbitals, which are rather extended. By contrast, the bands about the Fermi energy in SmB_6 are predominantly derived from f-orbitals, which are more localized, and therefore lead to flatter bands and enhanced interaction effects.[9]

One of the persistent challenges in experimental studies of TI is the problem of high bulk conductivity.[4] While some progress has been made on this front over the past few years, it has largely been incremental, and for the most part has been focused on bismuth-based TI. An alternative route is to look for new classes of strongly insulating materials that might support topological insulator phases. If one is also interested in studying interaction effects that could possibly take one beyond the "band theory" description of topological insulators, materials with orbitals more localized than the s and p-orbitals are highly desirable. Transition metal oxides, which typically have bands derived from d-orbitals close to the Fermi energy, are excellent candidates: There are a large number of insulating oxides, and interaction effects are known to be important in many of them–the high temperature cuprate superconductors serving as an excellent example.[10,11] Indeed, there have been a number of theoretical proposals for strongly correlated topological insulators in transition metal oxide systems.[12–20] A recent review of the prospects for such exotic phases in the context of three dimensional iridium (and other heavy transition metals) oxides is given in Ref.[21].

In this article, we focus on topological phases in thin film (two-dimensional) oxide heterostructures that can be described within the band theory picture. There are three prime candidates: (1) The time-reversal invariant topological insulator characterized by a single Z_2 invariant, (2) The time-reversal symmetry broken Chern insulator characterized by a quantized Chern number and quantized Hall conductance, and (3) The mirror symmetry protected (with respect to the center of the plane of the thin film[22]) topological crystalline insulator characterized by a mirror Chern number.[23–26] Combinations of these are possible as well for a "doubly topological" system, though clearly (1) and (2) are mutually exclusive. The Chern insulator differs from the quantum Hall insulator in that the former has time-reversal symmetry spontaneously broken by interactions (that is, a spontaneous magnetization of some sort), while the latter has time-reversal symmetry broken by the application of an external magnetic field. As a result, a Chern insulator requires interactions (because there is no spontaneous magnetism without electron-electron interactions), while a (integer) quantum Hall system does not. A topological crystalline insulator may possess time-reversal symmetry or have it broken by magnetic order; the only restriction is that any magnetic order present must respect the mirror symmetry.[24]

In the remainder of this article, we will consider two transition metal oxide structures, the perovskite with formula ABO_3 and the pyrochlore oxide $A_2B_2O_7$, where A is typically a rare-earth element, B is a transition metal element, and O is oxygen. Two specific examples we study are $LaNiO_3$ and $Y_2Ir_2O_7$, which are both materials that have been grown and are well characterized in bulk form. Our new angle is to study the properties of thin films of these materials that are grown along the (111) crystalline axis. We find the physical properties of these films are

[a)] Electronic mail: fiete@physics.utexas.edu

rather different from the bulk. Moreover, there does not appear to be an obvious way to infer the film properties from the bulk. As a result, these systems appear to be excellent candidates for exploring novel phenomena, such as topological phases, even when the bulk (non-thin film) materials possess strikingly different properties, such as a conducting behavior. We are thus presented with the exciting possibility of finding "new physics" in "old materials".

II. THIN FILM OXIDE HETEROSTRUCTURES

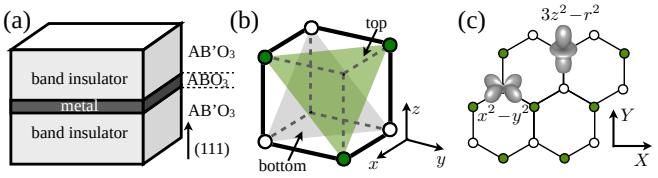

FIG. 1. (Color online.) (a) We consider oxide heterostructures grown along the (111) direction of the form $AB'O_3/ABO_3/AB'O_3$ for the perovskite structure and $A_2B'_2O_7/A_2B_2O_7/A_2B'_2O_7$ for the pyrochlore structure. Both $AB'O_3$ and $A_2B'_2O_7$ are assumed to be non-magnetic, wide band gap (band) insulators. The shaded region consists of a (111) bilayer of the metallic ABO_3 perovskite, such as $LaNiO_3$, or in the case of pyrochlore structures, a bilayer or a trilayer of a material such as $Y_2Ir_2O_7$. (b) Shown are the locations of the transition-metal ions (B) for the ABO_3 structure. (c) The ABO_3 bilayer system forms a "buckled honeycomb" lattice, which appears as a honeycomb lattice when projected to the plane perpendicular to (111). We assume that the relevant orbital degrees of freedom are the e_g orbitals of the transition-metal ions for ABO_3. For $A_2B_2O_7$ with heavy transition metal ions, the relevant orbitals come from the spin-orbit split t_{2g} manifold in the class of materials we study in this paper.

We are interested in a heterostructure similar to that shown in Fig.1, where the film is grown along the (111) direction. Most experimental studies of thin films in the perovskite systems ABO_3 are grown along the (001) (or symmetry related) direction because aligning the growth direction along a cubic axis generally favors high quality films. On the other hand, growing along (111) effectively changes the crystal structure in a single layer thin film from a square lattice of transition metal ions for (001) to a triangular lattice of transition metal ions for (111), as shown in Fig.1. For a bilayer grown along (001), one will have two square lattices of transition metal ions stacked directly on top of each other, but for growth along (111) a second "shifted" triangular lattice will sit on top of the original one. The combination of the two shifted triangular lattices is a "buckled" honeycomb lattice. In this example, growing along the (111) direction allows one to effectively "engineer" the lattice of the thin film, with important implications for the band structure in the weak coupling limit and the magnetic order in the strong coupling limit.

Likewise, the (111) growth direction for the $A_2B_2O_7$ pyrochlores leads to alternating planes of triangular and kagome lattices for the transition metal ions. [See Fig.5(a).] To the best of our knowledge, there have been no published experimental results on bilayer or trilayer films of $A_2B_2O_7$ grown along (111), though there are a number of systems where (111) growth of ABO_3 films has been demonstrated,[27–29] and also of AB_2O_4 spinels.[30] Various theoretical proposals now exist for topological phases in (111) grown transition metal oxide films,[31–44] and the list of candidate materials continues to grow. We believe it is likely that experiment will indeed find evidence of topological phases in this class of systems. Once a single example is found, experiments can be done to optimize material choices by "perturbing" around this material with different isovalent elements, substrates, etc, in order to achieve the maximum bulk gap. Our calculations suggest that the Chern insulator phase stands out as the mostly likely topological candidate for realistic conditions in thin film oxide heterostructures.

To be concrete, we will focus on the $LaNiO_3$ perovskite[31–34] and the $Y_2Ir_2O_7$ pyrchlore iridate.[35,37] (We note that an interesting theoretical study of Co-doped $LaNiO_3$ (111) grown bilayers suggest that correlation-driven odd parity superconductivity may appear in this system.[45]) First principles calculations show that the bands around the Fermi energy are predominately of d-orbital character in both $LaNiO_3$ and $Y_2Ir_2O_7$.[33,34,46] As a result, the spatial shape of the orbitals are highly asymmetric and can lead to interesting band features on the triangular, kagome, and honeycomb lattices that appear in the thin film structures of interest to us. In particular, a simple tight-binding model for the Ni d-orbitals leads to flat bands that touch dispersing bands quadratically[31] (the flat touching feature persists with more realistic first principles band calculations[33,34]), and also bands that cross in a Dirac point (see Fig.2). The stability of such band touching and crossing points with respect to interactions has been discussed recently in the literature in the context of interaction-generated topological phases.[31,32,47–51]

The central idea is that certain types of interactions, such as an on-site multi-orbital[31,32] interaction or different site density-density interaction in a single band[47–50] model, can generate an effective spin-orbit term (at the Hartree-Fock level) that favors topological phases. This is one of the ideas we will explore in the remainder of this article in the context of real materials, though we will find that for heavier transition elements, such as iridium, "interaction generated spin-orbit coupling terms" are not needed to access topological phases. Thus, any doubts about the reliability of the Hatree-Fock predictions for enhanced spin-orbit effects can be circumvented by focusing on classes of materials with intrinsically large spin-orbit coupling.

A. $LaNiO_3$ bilayers

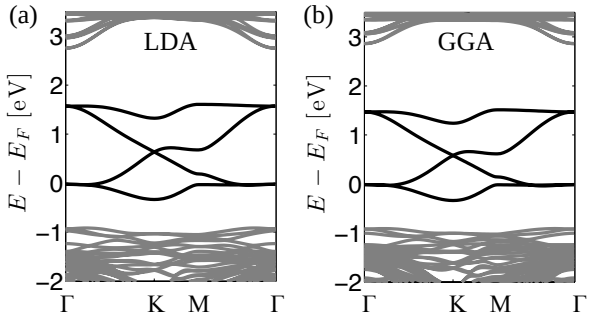

FIG. 2. First principles band structure of the fully lattice relaxed $(LaAlO_3)_{10}/(LaNiO_3)_2/(LaAlO_3)_{10}$ system within (a) LDA and (b) GGA, which are essentially indistinguishable. Note the quadratic band touching at the Γ point as well as the linear crossings at K and K′.[34] For a spin unpolarized system the Fermi energy lies right at the quadratic band touching point, while for a fully polarized (ferromagnetic) system the Fermi energy lies right at the Dirac point. Our Hartree-Fock calculations suggest that for realistic interaction values, the system is very close to a fully spin-polarized state with a quantized Chern number–a quantum anomalous Hall state.[33,34] See Fig.4(b).

The band structure obtained with the local density approximation (LDA) and the generalized gradient approximation (GGA)[34] for the fully relaxed $LaNiO_3$ (111) bilayer is shown in Fig. 2. The two are nearly indistinguishable. Rotations of the octahedral oxygen cages are known to be important for large classes of transition metal oxides,[52] including $LaNiO_3$ for which the adjacent oxygen cages counter-rotate about the (111) axis, as shown in Fig.3(a). To perform Hartree-Fock calculations with this band structure, we consider a tight-binding model based only on the nickel e_g orbitals that includes nearest-neighbor hopping via the oxygen p-orbitals and second-neighbor hopping via the oxygen p-orbitals. We find a a good fit by including the small differences in the hopping to "outer" versus "inner" oxygen atoms.[33] Assuming trigonal symmetry is preserved (a result consistent with our fully relaxed DFT results), we take the nearest-neighbor Slater-Koster parameters for hopping along the z-direction to be described by the matrix

$$\hat{t}_z = -\begin{pmatrix} t & 0 \\ 0 & t_\delta \end{pmatrix} \tag{1}$$

in the basis $(d_{z^2}, d_{x^2-y^2})$. Here t includes predominantly the hopping via the intermediate oxygen while t_δ arises from the direct overlap and is small. We set $t_\delta = 0$ in the following. Assuming that the nearest-neighbor hopping in the x and y directions are equivalent to the hopping along the z direction, we obtain the corresponding matrices by a rotation of the e_g-orbitals around (111) by $\pm 2\pi/3$. The matrix for the rotation

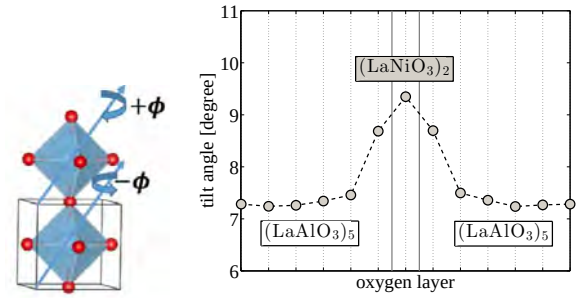

(a) ϕ about (111) (b) Title angle ϕ with layer index

FIG. 3. (Color online.) (a) The pattern of the octahedral tilts/counter rotations present in the fully relaxed structure. (b) Layer resolved octahedral rotation angles for the $(LaNiO_3)_2/(LaAlO_3)_{10}$ supercell obtained within the LDA approximation to DFT. As Fig. 2 shows, these rotations do not lift the quadratic band touching at the Γ point or the Dirac points at K, K' in the Brillouin zone because they preserve the trigonal point group symmetry.[34] This, in turn, implies the predictions for interaction-driven topological phases in the $(LaNiO_3)_2/(LaAlO_3)_N$ system remain qualitatively unchanged compared to the "ideal" lattice structure.[33]

by $2\pi/3$ is $\hat{R} = \begin{pmatrix} -1/2 & \sqrt{3}/2 \\ -\sqrt{3}/2 & -1/2 \end{pmatrix}$. As a result, we find $\hat{t}_x = \hat{R}^T \hat{t}_z \hat{R}, \quad \hat{t}_y = \hat{R}^T \hat{t}_x \hat{R}$. The Slater-Koster parameters for second-neighbor hopping define the matrix[33]

$$\hat{t}_{xy} = -\begin{pmatrix} t'/2 & \sqrt{3}\Delta/2 \\ -\sqrt{3}\Delta/2 & -3t'/2 \end{pmatrix}. \tag{2}$$

The off-diagonal entries proportional to Δ are allowed in the bilayer system discussed here (as opposed to a perfect cubic system) because the two possible paths connecting second-neighbor transition-metal ions are not equivalent: they either involve "inner" or "outer" oxygens.[33] Note that $\hat{t}_{xy}$ is not symmetric if $\Delta \neq 0$ which means that there is an associated direction for the hopping. We use the convention that $\hat{t}_{xy}$ denotes the hopping of an electron along a second neighbor bond which is reached by first following the y-axis and then the x-axis of the cube. By rotating the orbitals, we also obtain the second-neighbor hopping along the other directions: $\hat{t}_{yz} = \hat{R}^T \hat{t}_{xy} \hat{R}, \quad \hat{t}_{zx} = \hat{R}^T \hat{t}_{yz} \hat{R}$.

The generalized tight-binding model now takes the form

$$\begin{aligned} H_0 = &\sum_{\boldsymbol{r}\in A}\sum_{s}\sum_{u=xyz}\left(\vec{d}^{\dagger}_{s,\boldsymbol{r}}\hat{t}_u\vec{d}_{s,\boldsymbol{r}+\boldsymbol{e}_u} + \text{h.c.}\right) \\ &+ \sum_{\boldsymbol{r}\in A}\sum_{s}\sum_{u=xyz}\left(\vec{d}^{\dagger}_{s,\boldsymbol{r}}\hat{t}_{u,u+1}\vec{d}_{s,\boldsymbol{r}+\boldsymbol{e}_u-\boldsymbol{e}_{u+1}} + \text{h.c.}\right) \\ &+ \sum_{\boldsymbol{r}\in B}\sum_{s}\sum_{u=xyz}\left(\vec{d}^{\dagger}_{s,\boldsymbol{r}}\hat{t}_{u,u+1}\vec{d}_{s,\boldsymbol{r}-\boldsymbol{e}_u+\boldsymbol{e}_{u+1}} + \text{h.c.}\right), \end{aligned} \tag{3}$$

where $\vec{d}_s = (d_{z^2,s}, d_{x^2-y^2,s})^T$ is a vector in orbital space, $s = \uparrow, \downarrow$ is the spin and the notation $u+1$ refers to y if $u = x$ with a cyclic extension to the other elements.

fit	t [eV]	t' [eV]	Δ [eV]	E_F [eV]
unrelaxed (LDA)	0.598	0.062	-0.023	-0.693
fully relaxed (LDA)	0.541	0.045	-0.017	-0.641
fully relaxed (GGA)	0.508	0.046	-0.016	-0.593

TABLE I. Parameters obtained in tight-binding fits to the e_g DFT band structure of the unrelaxed and fully relaxed superlattice. There are very little changes between the unrelaxed and relaxed parameters, with t'/t nearly invariant implying negligible change in the phase diagram shown in Fig.4.

Using the tight-binding model H_0 with parameters t, t', and Δ (with $t_\delta = 0$), we fitted both the LDA and GGA band structures of the fully relaxed system near the Fermi level. The fitting parameters are listed in Table I and Fig. 4(a) shows the LDA together with the tight-binding band structure for the best fit. To study the multi-orbital interactions within Hartree-Fock theory, we use an on-site interaction of the form[10,53]

$$H_{\rm int}= \sum_{\boldsymbol{r}} \Big[U \sum_{\alpha} n_{\boldsymbol{r}\alpha\uparrow} n_{\boldsymbol{r}\alpha\downarrow} + (U'-J) \sum_{\alpha>\beta,s} n_{\boldsymbol{r}\alpha s} n_{\boldsymbol{r}\beta s} + U' \sum_{\alpha\neq\beta} n_{\boldsymbol{r}\alpha\uparrow} n_{\boldsymbol{r}\beta\downarrow} + J \sum_{\alpha\neq\beta} d^\dagger_{\boldsymbol{r}\alpha\uparrow} d_{\boldsymbol{r}\beta\uparrow} d^\dagger_{\boldsymbol{r}\beta\downarrow} d_{\boldsymbol{r}\alpha\downarrow} + I \sum_{\alpha\neq\beta} d^\dagger_{\boldsymbol{r}\alpha\uparrow} d_{\boldsymbol{r}\beta\uparrow} d^\dagger_{\boldsymbol{r}\alpha\downarrow} d_{\boldsymbol{r}\beta\downarrow} \Big]. \quad (4)$$

We assume $U' = U - 2J$ and $I = J$, which are valid in free space and believed to be approximately true in the solid state environment. The total multi-orbital Hubbard Hamiltonian for the e_g electrons is given by $H = H_0 + H_{\rm int}$, where H_0 is given in Eq. (3). The results[33,34] are shown in Fig.4(b). Studying a model that explicitly includes oxygen p-orbitals (where charge-transfer physics may appear) leads to similar results.[33]

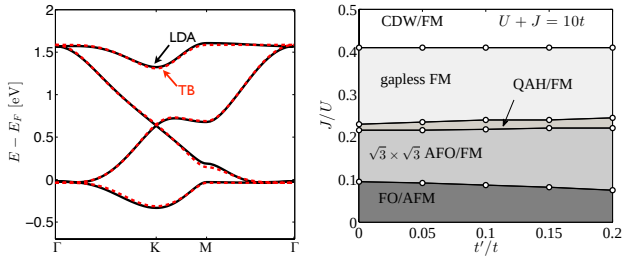

(a) LDA Tight Binding Fit (b) Hartree-Fock Phase Diagram

FIG. 4. (color online) (a) Fully relaxed LDA band structure and tight-binding (TB) fit. (b) Hartree-Fock phase diagram of the $LaNiO_3$ bilayer. We estimate the experimental system has parameters $t'/t \approx 0.1$ and $J/U \approx 0.1-0.2$, which is rather close to the quantum anomalous Hall (QAH) phase with ferromagnetic order. FO=ferro-orbital, AFM=antiferromagnetic, AFO=antiferro-orbital, FM=ferromagnetic, CDW=charge density wave.

B. $Y_2Ir_2O_7$ bilayers and trilayers

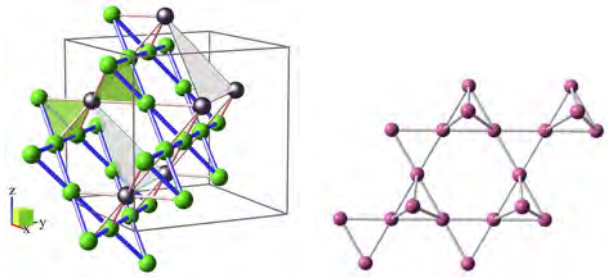

(a) Pyrochlore structure (b) Bilayer structure

FIG. 5. (Color online.) (a) Bulk pyrochlore lattice structure showing the alternation of kagome planes (green balls on lattice sites) and triangular lattice planes (grey balls on lattice sites) along the (111) direction. (b) A bilayer film viewed from the (111) direction. We focus on the bilayer and the triangular-kagome-triangular structure, which show the most promise for topological phases.

In order to study the (111) films of the pyrochlore in a set-up similar to that shown in Fig. 1(a), we consider a tight-binding model

$$H_0 = \sum_{\langle i,j\rangle,\alpha,\beta} t_{i\alpha,j\beta} c^\dagger_{i\alpha} c_{j\beta} - \lambda \sum_i \mathbf{l}_i \cdot \mathbf{s}_i, \quad (5)$$

where the d-orbital hopping takes the form[19,54]

$$t_{i\alpha,j\beta} = t^{in}_{i\alpha,j\beta} + t^{dir}_{i\alpha,j\beta}, \quad (6)$$

which contains both an indirect and a direct hopping term between the d-orbitals.[12,13,55] Here, $\lambda > 0$ is the intrinsic spin-orbit coupling in the system which acts within the t_{2g} manifold so $|\mathbf{l}| = 1$, and $\mathbf{s}_i$ is the spin of the electron in a t_{2g} d-orbital on site i.[12,13,55] In the $5d$ oxides, the strength of the spin-orbit coupling is estimated to be 0.2-0.7 eV and the hopping strength is on the order of 0.4-0.6 eV.[13,20] The hopping amplitude in Eq. (6) contains a direct d-d hopping, $t^{dir}_{i\alpha,j\beta}$, in addition to the indirect hopping via the oxygen orbitals.[19,54] The direct hopping is parameterized by the strength of the σ-bonds, t_s, and the π-bonds, t_p. Following Refs. [19] and [54], we consider a set of representative ratios to explore a realistic parameter space: We set $t_p = -2t_s/3$ and consider the cases of $t_s = -t$ and $t_s = t$. Our preliminary GGA calculations for the thin-films suggest the band structure is most similar to that for $t_s = -t$, though the further neighbor hopping is considerably more important for the $5d$ orbitals in $Y_2Ir_2O_7$ than it is for the $3d$ orbitals in $LaNiO_3$.

To carry out Hartree-Fock calculations for the $Y_2Ir_2O_7$ films, we use the tight-binding model in Eq.(5) with $t_s = -t$ supplemented by an on-site Hubbard term, $H_U = U \sum_i n_{i\uparrow} n_{i\downarrow}$, and further restrict ourselves to the $j = 1/2$ manifold.[35] The results are shown in Fig. 6. Note the triangular-kagome-triangular (TKT) film supports a

fairly wide region of a quantum anomalous Hall (Chern insulator=CI) state. We find that if one includes fluctuations beyond the Hartree-Fock approximation, this region moves to larger U values, close to what is reasonable for $Y_2Ir_2O_7$. Therefore, we conclude that both the (111) grown $LaNiO_3$ bilayer and the (111) grown $Y_2Ir_2O_7$ TKT trilayer are candidates for a quantum anomalous Hall state. Moreover, we find that small changes to the kinetic terms in Eq.(3) can lead to a Z_2 topological insulator in the (111) grown $Y_2Ir_2O_7$ bilayer for small U.[35]

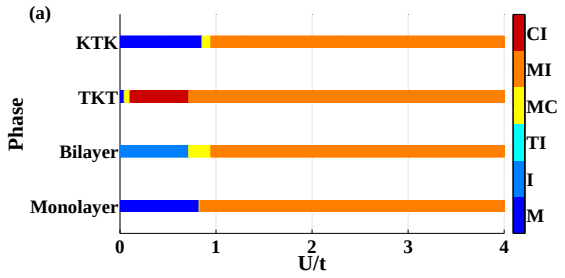

FIG. 6. (Color online.) Hartree-Fock phase diagrams for the single kagome layer (monolayer), bilayer, triangular-kagome-triangular (TKT), and kagome-triangular-kagome (KTK) systems. We have used $t_s = -t$ and restricted ourselves to the $j = 1/2$ manifold. M=metallic, I=trivial insulator, TI=topological insulator, MC=magnetic conductor, MI=magnetic insulator, CI=Chern insulator (same as QAH).

III. CONCLUSIONS

In conclusion, we have shown both the (111) grown $LaNiO_3$ bilayer and the (111) grown $Y_2Ir_2O_7$ TKT trilayer are candidates for a quantum anomalous Hall state, which will show a quantize Hall conductance. We also found that realistic changes to the kinetic terms of $Y_2Ir_2O_7$ can also lead to a Z_2 topological insulator in the (111) grown $Y_2Ir_2O_7$ bilayer. The most natural way to detect these states is through transport measurements, as has been done for the few known Z_2 TI[56,57] and QAH systems.[58] From the point-of-view of technology applications, there is clearly a need in the field for more systems known to possess these phases. The huge variety of transition metal oxides, combined with existing theoretical results, would seem to suggest it may only be a matter of time before a topological phase is discovered in a system similar to those we considered here.

ACKNOWLEDGMENTS

We are grateful to our collaborators in this area, A.A. Demkov, X. Hu, P. Jaduan, M. Kargarian, C. Mitra, and Z. Zhong. Our work was generously funded by ARO Grant No. W911NF-09-10527, NSF Grant No. DMR-0955778, and DARPA grant No. D13AP00052. The Texas Advanced Computng Center (TACC) at The University of Texas at Austin for provided the necessary computing resources. URL:http://www.tacc.utexas.edu.

[1] J. E. Moore, "The birth of topological insulators," Nature **464**, 194–198 (2010).
[2] M. Z. Hasan and C. L. Kane, "Colloquium: Topological insulators," Rev. Mod. Phys. **82**, 3045–3067 (2010).
[3] X. L. Qi and S. C. Zhang, "Topological insulators and superconductors," Rev. Mod. Phys. **83**, 1057–1110 (2011).
[4] Y. Ando, "Topological insulator materials," J. Phys. Soc. Jpn. **82**, 102001 (2013).
[5] M. Dzero and V. Galitski, "A new exotic state in an old material: a tale of SmB_6," JETP **117**, 499–507 (Sep. 2013), ISSN 1063-7761, 1090-6509, http://link.springer.com/article/10.1134/S1063776113110083.
[6] Maxim Dzero, Kai Sun, Victor Galitski, and Piers Coleman, "Topological kondo insulators," Phys. Rev. Lett. **104**, 106408 (Mar 2010), http://link.aps.org/doi/10.1103/PhysRevLett.104.106408.
[7] M. Neupane, N. Alidoust, S-Y. Xu, T. Kondo, Y. Ishida, D. J. Kim, Chang Liu, I. Belopolski, Y. J. Jo, T-R. Chang, H-T. Jeng, T. Durakiewicz, L. Balicas, H. Lin, A. Bansil, S. Shin, Z. Fisk, and M. Z. Hasan, "Surface electronic structure of the topological kondo-insulator candidate correlated electron system smb6," Nat. Comm. **4**, 2991 (2013).
[8] Xiaohang Zhang, N. P. Butch, P. Syers, S. Ziemak, Richard L. Greene, and Johnpierre Paglione, "Hybridization, inter-ion correlation, and surface states in the kondo insulator smb6," Phys. Rev. X **3**, 011011 (Feb 2013), http://link.aps.org/doi/10.1103/PhysRevX.3.011011.
[9] Feng Lu, JianZhou Zhao, Hongming Weng, Zhong Fang, and Xi Dai, "Correlated topological insulators with mixed valence," Phys. Rev. Lett. **110**, 096401 (2013), http://link.aps.org/doi/10.1103/PhysRevLett.110.096401.
[10] M. Imada, A. Fujimori, and Y. Tokura, "Metal-insulator transitions," Rev. Mod. Phys. **70**, 1039–1263 (1998).
[11] P. A. Lee, N. Nagaosa, and X. G. Wen, "Doping a Mott insulator: Physics of high-temperature superconductivity," Rev. Mod. Phys. **78**, 17–85 (Jan 2006).
[12] D. Pesin and L. Balents, "Mott physics and band topology in materials with strong spin-orbit coupling," Nature Phys. **6**, 376 (2010).
[13] M. Kargarian, J. Wen, and G. A. Fiete, "Competing exotic topological insulator phases in transition-metal oxides on the pyrochlore lattice with distortion," Phys. Rev. B **83**, 165112 (2011).
[14] M. Kargarian and G. A. Fiete, "Topological crystalline insulators in transition metal oxides," Phys. Rev. Lett. **110**, 156403 (2013).
[15] W. Witczak-Krempa, T. P. Choy, and Y. B. Kim, "Gauge field fluctuations in three-dimensional topological Mott insulators," Phys. Rev. B **82**, 165122 (2010).
[16] J. Maciejko and A. Rüegg, "Topological order in a correlated Chern insulator," Phys. Rev. B **88**, 241101 (Dec 2013), http://link.aps.org/doi/10.1103/PhysRevB.88.241101.
[17] A. Rüegg and G. A. Fiete, "Topological order and semions in a strongly correlated quantum spin Hall insulator," Phys. Rev. Lett. **108**, 046401 (Jan 2012), http://link.aps.org/doi/10.1103/PhysRevLett.108.046401.
[18] J. Maciejko, V. Chua, and G. A. Fiete, "Topological order in a correlated three-dimensional topological insulator," Phys. Rev. Lett. **112**, 016404 (Jan 2014), http://link.aps.org/doi/10.1103/PhysRevLett.112.016404.
[19] Ara Go, William Witczak-Krempa, Gun Sang Jeon, Kwon Park, and Yong Baek Kim, "Correlation effects on 3d topological phases: From bulk to boundary," Phys. Rev. Lett. **109**, 066401 (2012).
[20] Atsuo Shitade, Hosho Katsura, Jan Kuneš, Xiao-Liang Qi, Shou-Cheng Zhang, and Naoto Nagaosa, "Quantum spin hall effect in a transition metal oxide na[sub 2]iro[sub 3]," Phys. Rev. Lett. **102**, 256403 (2009).

[21] W. Witczak-Krempa, G. Chen, Y. B. Kim, and L. Balents, "Correlated quantum phenomena in the strong spin-orbit regime," Annu. Rev. Condens. Matter Phys. **5**, 57–82 (2014), http://www.annualreviews.org/doi/abs/10.1146/annurev-conmatphys-020911-125138.

[22] Junwei Liu, Timothy H. Hsieh, Peng Wei, Wenhui Duan, Jagadeesh Moodera, and Liang Fu, "Spin-filtered edge states with an electrically tunable gap in a two-dimensional topological crystalline insulator," Nat. Mat. **13**, 178183 (2014).

[23] Jeffrey C. Y. Teo, Liang Fu, and C. L. Kane, "Surface states and topological invariants in three-dimensional topological insulators: Application to bi[sub 1 - x]sb[sub x]," Phys. Rev. B **78**, 045426 (2008).

[24] Timothy H. Hsieh, Hsin Lin, Junwei Liu, Wenhui Duan, Arun Bansil, and Liang Fu, "Topological crystalline insulators in the snte material class," Nat. Commun. **3**, 982 (2012).

[25] Junwei Liu, Wenhui Duan, and Liang Fu, "Two types of surface states in topological crystalline insulators," Phys. Rev. B **88**, 241303 (Dec 2013), http://link.aps.org/doi/10.1103/PhysRevB.88.241303.

[26] Timothy H. Hsieh, Junwei Liu, and Liang Fu, "Topological crystalline insulators and dirac octets in antiperovskites," Phys. Rev. B **90**, 081112 (Aug 2014), http://link.aps.org/doi/10.1103/PhysRevB.90.081112.

[27] S. Middey, D. Meyers, M. Kareev, E. J. Moon, B. A. Gray, X. Liu, J. W. Freeland, and J. Chakhalian, "Epitaxial growth of (111)-oriented laalo3/lanio3 ultra-thin superlattices," Appl. Phys. Lett. **101**, 261602 (2012).

[28] J. L. Blok, X. Wan, G. Koster, D. H. A. Blank, and G. Rijnders, "Epitaxial oxide growth on polar (111) surfaces," Appl. Phys. Lett. **99**, 151917 (2011).

[29] S. Middey, D. Meyers, D. Doennig, M. Kareev, X. Liu, Y. Cao, P. J. Ryan, R. Pentcheva, J. W. Freeland, and J. Chakhalian, "Geometrically engineered mott phases in (111) oriented nickelate superlattices," (2014), arXiv:1407.1570.

[30] Xiaoran Liu, M. Kareev, Yanwei Cao, Jian Liu, S. Middey, D. Meyers, J. W. Freeland, and J. Chakhalian, "Electronic and magnetic properties of (1 1 1)-oriented cocr2o4 epitaxial thin film," (2014), arXiv:1406.0523.

[31] A. Rüegg and G. A. Fiete, "Topological insulators from complex orbital order in transition-metal oxides heterostructures," Phys. Rev. B **84**, 201103 (2011).

[32] K.-Y. Yang, W. Zhu, D. Xiao, S. Okamoto, Z. Wang, and Y. Ran, "Possible interaction-driven topological phases in (111) bilayers of $LaNiO_3$," Phys. Rev. B **84**, 201104 (2011).

[33] Andreas Rüegg, Chandrima Mitra, Alexander A. Demkov, and Gregory A. Fiete, "Electronic structure of $(lanio_3)_2/(laalo_3)_N$ heterostructures grown along [111]," Phys. Rev. B **85**, 245131 (2012).

[34] Andreas Rüegg, Chandrima Mitra, Alexander A. Demkov, and Gregory A. Fiete, "Lattice distortion effects on topological phases in $(lanio_3)_2/(laalo_3)_N$ heterostructures grown along the [111] direction," Phys. Rev. B **88**, 115146 (Sep 2013), http://link.aps.org/doi/10.1103/PhysRevB.88.115146.

[35] Xiang Hu, Andreas Rüegg, and Gregory A. Fiete, "Topological phases in layered pyrochlore oxide thin films along the [111] direction," Phys. Rev. B **86**, 235141 (2012).

[36] Satoshi Okamoto, Wenguang Zhu, Yusuke Nomura, Ryotaro Arita, Di Xiao, and Naoto Nagaosa, "Correlation effects in (111) bilayers of perovskite transition-metal oxides," Phys. Rev. B **89**, 195121 (May 2014), http://link.aps.org/doi/10.1103/PhysRevB.89.195121.

[37] Bohm-Jung Yang and Naoto Nagaosa, "Emergent topological phenomena in thin films of pyrochlore iridates," Phys. Rev. Lett. **112**, 246402 (Jun 2014), http://link.aps.org/doi/10.1103/PhysRevLett.112.246402.

[38] Satoshi Okamoto, "Doped mott insulators in (111) bilayers of perovskite transition-metal oxides with a strong spin-orbit coupling," Phys. Rev. Lett. **110**, 066403 (Feb 2013).

[39] Di Xiao, Wenguang Zhu, Ying Ran, Naoto Nagaosa, and Satoshi Okamoto, "Interface engineering of quantum hall effects in digital heterostructures of transition-metal oxides," Nat. Comm. **2**, 596 (2011).

[40] David Doennig, Warren E. Pickett, and Rossitza Pentcheva, "Confinement-driven transitions between topological and mott phases in $(LaNiO_3)_N/(LaAl\%mathrmO_3)_M(111)$ superlattices," Phys. Rev. B **89**, 121110 (Mar 2014), http://link.aps.org/doi/10.1103/PhysRevB.89.121110.

[41] J. L. Lado, V. Pardo, and D. Baldomir, "Ab initio study of z2 topological phases in perovskite (111) (srtio3)/(sriro3)2 and (ktao3)7/(kpto3)2 multilayers," Phys. Rev. B **88**, 155119 (Oct 2013), http://link.aps.org/doi/10.1103/PhysRevB.88.155119.

[42] Qi-Feng Liang, Long-Hua Wu, and Xiao Hu, "Electrically tunable topological state in [111] perovskite materials with an antiferromagnetic exchange field," New Journal of Physics **15**, 063031 (2013).

[43] Fa Wang and Ying Ran, "Nearly flat band with chern number $c = 2$ on the dice lattice," Phys. Rev. B **84**, 241103 (2011).

[44] Yilin Wang, Zhijun Wang, Zhong Fang, and Xi Dai, "Interaction-induced quantum anomalous hall phase in (111) bilayer of $lacoo_3$," (2014), arXiv:1409.6797.

[45] Bing Ye, Andrej Mesaros, and Ying Ran, "Possible correlation-driven odd-parity superconductivity in $lani_{7/8}co_{1/8}o_3$ (111) bilayers," Phys. Rev. B **89**, 201111 (May 2014), http://link.aps.org/doi/10.1103/PhysRevB.89.201111.

[46] Xiangang Wan, Ari M. Turner, Ashvin Vishwanath, and Sergey Y. Savrasov, "Topological semimetal and fermi-arc surface states in the electronic structure of pyrochlore iridates," Phys. Rev. B **83**, 205101 (2011).

[47] S. Raghu, X.-L. Qi, C. Honerkamp, and S.-C. Zhang, "Topological Mott insulators," Phys. Rev. Lett. **100**, 156401 (2008).

[48] Y. Zhang, Y. Ran, and A. Vishwanath, "Topological insulators in three dimensions from spontaneous symmetry breaking," Phys. Rev. B **79**, 245331 (2009).

[49] K. Sun, H. Yao, E. Fradkin, and S. A. Kivelson, "Topological insulators and nematic phases from spontaneous symmetry breaking in 2D Fermi systems with a quadratic band crossing," Phys. Rev. Lett. **103**, 046811 (2009).

[50] J. Wen, A. Rüegg, C.-C. J. Wang, and G. A. Fiete, "Interaction-driven topological insulators on the kagome and the decorated honeycomb lattices," Phys. Rev. B **82**, 075125 (2010).

[51] R. Yu, W. Zhang, H.-J. Zhang, S.-C. Zhang, X. Dai, and Z. Fang, "Quantized anomalous Hall effect in magnetic topological insulators," Science **329**, 61–64 (2010).

[52] S. Maekawa, T. Tohyama, S. E. Barnes, S. Ishihara, W. Koshinbae, and G. Khaliullin, *Physics of Transition Metal Oxides* (Springer, Berlin, 2004).

[53] T. Mizokawa and A. Fujimori, "Electronic structure and orbital ordering in perovskite-type 3 d transition-metal oxides studied by hartree-fock band-structure calculations," Phys. Rev. B **54**, 5368–5380 (Aug 1996).

[54] William Witczak-Krempa and Yong Baek Kim, "Topological and magnetic phases of interacting electrons in the pyrochlore iridates," Phys. Rev. B **85**, 045124 (2012).

[55] Bohm-Jung Yang and Yong Baek Kim, "Topological insulators and metal-insulator transition in the pyrochlore iridates," Phys. Rev. B **82**, 085111 (2010).

[56] M. König, S. Wiedmann, C. Brune, A. Roth, H. Buhmann, L. Molenkamp, X.-L. Qi, and S.-C. Zhang, "Quantum spin hall insulator state in hgte quantum wells," Science **318**, 766 (2007).

[57] Andreas Roth, Christoph Brüne, Hartmut Buhmann, Laurens W. Molenkamp, Joseph Maciejko, Xiao-Liang Qi, and Shou-Cheng Zhang, "Nonlocal transport in the quantum spin hall state," Science **325**, 294 (2009).

[58] Cui-Zu Chang, Jinsong Zhang, Xiao Feng, Jie Shen, Zuocheng Zhang, Minghua Guo, Kang Li, Yunbo Ou, Pang Wei, Li-Li Wang, Zhong-Qing Ji, Yang Feng, Shuaihua, Xi Chen, Jinfeng Jia, Xi Dai, Zhong Fang, Shou-Cheng Zhang, Ke He, Yayu Wang,

Li Lu, Xu-Cun Ma, and Qi-Kun Xue, "Experimental observation of the quantum anomalous hall effect in a magnetic topological insulator," Science **167**, 167 (2013).

Fractionalized Topological Insulators

Joseph Maciejko[1,*] and Gregory A. Fiete[2,†]

[1]*Department of Physics, University of Alberta, Edmonton, Alberta T6G 2E1, Canada*
[2]*Department of Physics, The University of Texas at Austin, Austin, Texas 78712, USA*

(Dated: December 12, 2014)

Topological insulators have emerged as a major topic of condensed matter physics research with several novel applications proposed. Although there are now a number of established experimental examples of materials in this class, all of them can be described by theories based on electronic band structure, which implies that they do not possess electronic correlations strong enough to fundamentally change this theoretical description. Here, we review recent theoretical progress in the description of a class of strongly correlated topological insulators — fractionalized topological insulators — where band theory fails dramatically due to the fractionalization of the electron into other degrees of freedom.

The field of topological insulators (TI) is now approximately a decade old, and there are a number of excellent reviews available, from both an experimental and theoretical perspective[1–4]. Our goal in this article is to provide a progress report on a specific subdirection that has developed rapidly in the last few years—the theoretical study of phases of matter that, while conceptually related to topological insulators, cannot be described by an electronic band structure because of the fractionalization of the electron into other degrees of freedom, driven by strong electronic correlations. This latter scenario has earlier precedents in the Mott insulator (which exhibits the separation of spin and charge) and the fractional quantum Hall effect (which has excitations with only a fraction of the charge of the electron), but acquires a distinct flavor when applied to topological insulators. By taking fractionalized topological insulators as an example, we hope to convey the broader message that the class of materials commonly known as topological insulators barely scratches the surface of the possible types of topological materials, once electron correlations are taken into account.

SPLITTING THE ELECTRON APART

We restrict our discussion to two and three spatial dimensions, as fractionalized excitations in gapped one-dimensional systems are require additional considerations. Since we focus on systems not described by band theory, we merely note in passing that interactions can drive a topologically trivial phase into a topological band insulator through the spontaneous generation of spin-orbit coupling[5,6] or magnetic order[7], or through the renormalization of electronic bands[8]. By contrast, in the phases we highlight below the quantum numbers of the electron break apart, implying that the latter is not a sharply defined quasiparticle and the system cannot be adequately described by an electronic band structure. The chief theoretical challenges for the study of fractionalized topological insulators are: (i) to describe them in a conceptually convenient way, (ii) to predict the conditions under which they are expected (i.e., find the set of Hamiltonians that support them), and if possible (iii) to provide a list of specific candidate materials that can be investigated experimentally. The field is presently at the stage of tackling challenges (i) and (ii), with relatively little work on (iii).

A convenient way to describe the basic properties of fractionalized topological insulators is the slave-particle approach. In the present context, it answers the following question: What new state of matter does one get if electrons inside a topological insulator fractionalize into other degrees of freedom? The answer depends on the type of topological insulator with which one starts, as well as the assumed pattern of electron fractionalization. From these basic inputs, the slave-particle approach predicts the universal properties of the resulting fractionalized topological insulator, such as the quantum numbers and quantum statistics of low-energy excitations, the degeneracy of the ground state on surfaces of various topologies, and quantized electromagnetic, spin, and thermal response properties (Table I). The slave-particle approach does not, however, solve the much more difficult problem of the classification of all possible correlated topological phases—which goes beyond the scope of our focused review—because a generic correlated topological phase may not always be understood as originating via fractionalization from a noninteracting topological insulator. More sophisticated methods such as the group cohomology[9,10] and cobordism[11] approaches have been recently developed to address this considerable challenge.

Besides fractionalization, to obtain an exotic topological phase one typically assumes that some of the fractionalized degrees of freedom form a topological band insulator. The latter can thus be seen as a nonfractionalized parent state from which fractionalized daughter states can be constructed (Table I, first two columns). The nontrivial response properties of the parent state combine with the fractional quantum numbers of the fractionalized degrees of freedom to yield even more exotic response properties for the daughter state. This scenario occurs in slave-particle mean-field studies of models of topological band insulators subjected to strong electron-electron

parent state	fractionalized state	d	symmetry	EM response	spin response	thermal response
CI	CSL	2		$\sigma_{xy}=0$	$\sigma^s_{xy}=0$	$\kappa_{xy}/T=2$
QSH	fractionalized QSH	2	TRS	$\sigma_{xy}=0$	$\sigma^s_{xy}=0$	$\kappa_{xy}/T=0$
TI/WTI	TMI/WTMI	3	TRS	$\theta=0$		$\theta_{\rm grav}=\pi$ (TMI)
TCI	TCMI	3	mirror			
CI	CI*	2		$\sigma_{xy}=2$	$\sigma^s_{xy}=0$	$\kappa_{xy}/T=2$
QSH	QSH*	2	TRS	$\sigma_{xy}=0$	$\sigma^s_{xy}=2$	$\kappa_{xy}/T=0$
TI	TI*	3	TRS	$\theta=\pi$		$\theta_{\rm grav}=\pi$
CI	FCI	2		$\sigma_{xy}=1/3$	$\sigma^s_{xy}=0$	$\kappa_{xy}/T=1$
QSH	FQSH	2	TRS	$\sigma_{xy}=0$	$\sigma^s_{xy}=2/3$	$\kappa_{xy}/T=0$
TI	FTI	3	TRS	$\theta=\pi/3$		$\theta_{\rm grav}=\pi$

TABLE I. Summary of the d-dimensional fractionalized topological insulators discussed in this article and their universal response properties (acronyms are defined in the main text). σ_{xy}: Hall conductance in units of e^2/h; θ: coefficient of the $\boldsymbol{E}\cdot\boldsymbol{B}$ term in units of $e^2/2\pi h$; σ^s_{xy}: spin Hall conductance in units of $e/4\pi$ for a system with conserved z component of spin; κ_{xy}/T: thermal Hall conductance divided by the temperature, in units of $\pi^2k_B^2/3h$; $\theta_{\rm grav}$: coefficient of the gravitational equivalent of the $\boldsymbol{E}\cdot\boldsymbol{B}$ term, responsible for a surface quantized thermal Hall effect.

interactions. Besides interacting with external fields via their fractional quantum numbers such as spin or charge, the fractionalized degrees of freedom also interact with emergent gauge fields. As in quantum chromodynamics (QCD), these gauge fields are confining in a conventional phase where fractionalized degrees of freedom—"quarks" in the QCD analogy—do not exist at low energies as long-lived, propagating excitations. Inside a fractionalized topological insulator, the gauge fields are deconfined and allow the fractionalized degrees of freedom to lead an existence of their own. The gauge fields themselves admit propagating excitations—the gauge bosons—which can be gapless or gapped, depending on the type of gauge field and the nature of the parent topological phase.

FRACTIONALIZATION AND NEW PHASES OF MATTER

The first pattern of electron fractionalization to be considered in the context of strongly correlated topological insulators was spin-charge separation, originated in the study of the Luttinger liquid in 1D and the Mott transition in 2D[12,13]. The electron is assumed to fractionalize into a charged, spinless, bosonic rotor and an electrically neutral, spinful, fermionic spinon, coupled by a $U(1)$ gauge field (Fig. 1). The electronic quasiparticle weight is proportional to the expectation value of the rotor field. The resulting theory typically has two distinct stable phases: a weakly interacting phase where the rotors undergo Bose condensation and the rotor field acquires a nonzero expectation value, and a strongly interacting phase where the rotors are uncondensed. In the weakly interacting phase, the electronic quasiparticle weight is finite and the electronic band structure is well defined, while in the strongly interacting phase the quasiparticle weight vanishes due to strong rotor fluctuations, corresponding to a Mott phase. In the latter case, the spinons acquire a band structure of their own which, if gapped, can be classified by the usual topological invariants[2,3]. In 2D, Chern-insulator (CI) or $\mathbb{Z}_2$ topological insulator band structures for the spinons lead to a chiral spin liquid[14] (CSL) or a fractionalized quantum spin Hall (QSH) insulator[15,16], respectively. The fractionalized QSH insulator is only stable in the presence of additional layers containing enough gapless spinons to screen the $U(1)$ gauge field and avoid the instanton effect that causes confinement[15]. In 3D time-reversal invariant systems, the Mott phases are called strong topological Mott insulators[17] (TMI) or weak topological Mott insulators[18] (WTMI) depending on whether the spinons form a strong or weak $\mathbb{Z}_2$ topological insulator, respectively. The same analysis applied to systems with mirror crystalline symmetries leads to the concept of a topological crystalline Mott insulator[19] (TCMI). All these 3D fractionalized topological phases have gapless surface modes of spinons with the properties that electrons would have in the corresponding noninteracting topological phases, but in addition have a bulk gapless "photon" mode from the emergent $U(1)$ gauge field[17,20]. However, there is no quantized electromagnetic response of the $\boldsymbol{E}\cdot\boldsymbol{B}$ type[1–3] because the spinons are electrically neutral. To identify this class of spin-charge separated states experimentally, methods similar to those proposed or used to identify quantum spin liquids[21] should be applied. One should observe a bulk contribution to the low-temperature specific heat arising from the gapless photon mode, although it could be difficult to distinguish from the phonon contribution. In addition, one could imagine detecting the linearly dispersing surface spinon modes via

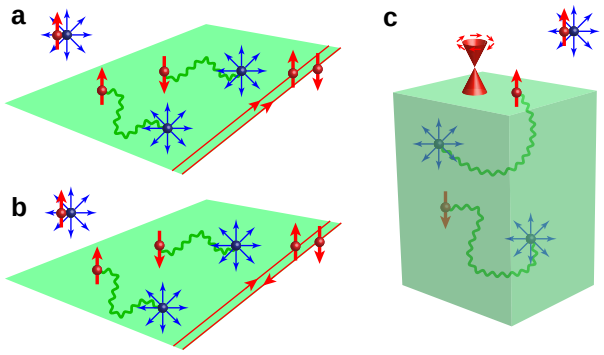

FIG. 1. Fractionalized topological insulators accessed by the $U(1)$ slave-rotor description. Outside the material, the charged bosonic rotor (blue sphere) and the neutral fermionic spinon (red sphere) are confined together to form an electron. Inside the material, they become deconfined particles and interact via an emergent $U(1)$ gauge field (green wiggly line). In the 2D chiral spin liquid (a), these particles acquire semionic (i.e., half-fermionic) statistics and there are chiral edge states of spinons. In the 2D fractionalized quantum spin Hall insulator (b), the spinon edge states are helical. In the 3D topological Mott insulator states (c), the $U(1)$ gauge field is gapless in the bulk, and there are gapless Dirac-like spinon surface states.

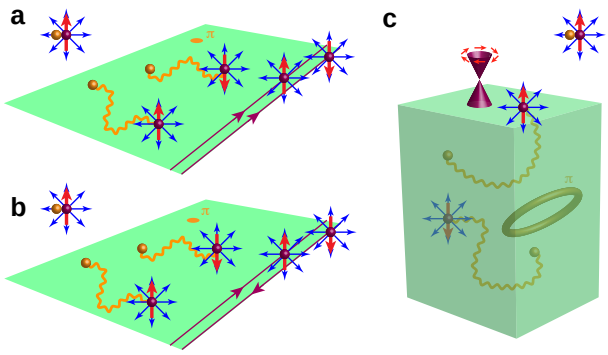

FIG. 2. Fractionalized topological insulators accessed by the $\mathbb{Z}_2$ slave-Ising description. Outside the material, the neutral bosonic slave-Ising particle (orange sphere) and the charged slave-fermion (purple sphere) are confined together to form an electron. Inside the material, they become deconfined particles and interact via an emergent $\mathbb{Z}_2$ gauge field (orange wiggly line) that supports π-flux vortex excitations (orange disk). In the 2D correlated Chern insulator (a), vortices acquire semionic statistics and there are chiral edge states of slave-fermions. In the 2D correlated quantum spin Hall insulator (b), vortices have semionic mutual statistics with slave-Ising particles and slave-fermions, and the slave-fermion edge states are helical. In the 3D correlated topological insulator (c), the π-flux vortex becomes a bulk vortex loop, and there are gapless Dirac-like slave-fermion surface states.

the observation of 2D spin or heat transport localized at the surface of the material.

A different pattern of electron fractionalization originating from theories of high-temperature superconductivity[22] assumes that the electron fractionalizes into a neutral, spinless, bosonic slave-Ising particle and a charged, spinful slave-fermion, coupled by a $\mathbb{Z}_2$ gauge field[23] (Fig. 2). This type of fractionalization may appear trivial, as the slave-Ising particle carries neither the charge nor the spin of the electron. The resulting fractionalized phases, however, are far from trivial. As in the $U(1)$ theory, the $\mathbb{Z}_2$ theory typically has a non-fractionalized weakly interacting phase where the slave-Ising particles Bose condense, and a fractionalized strongly interacting phase where they are uncondensed. By contrast with the $U(1)$ theory however, in the $\mathbb{Z}_2$ case the slave-fermion carries the charge of the electron, thus the fractionalized phases inherit the electromagnetic response properties of the parent topological band insulator. In 2D, Chern-insulator and $\mathbb{Z}_2$ topological insulator band structures for the slave fermions lead to a correlated Chern insulator[24] (CI*) with quantized Hall response and a correlated quantum spin Hall insulator[25] (QSH*), respectively. These are fully gapped phases with intrinsic topological order of the double-semion and toric-code type, respectively. In 3D time-reversal invariant systems, a $\mathbb{Z}_2$ topological insulator band structure leads to a strongly correlated topological insulator[26] (TI*) that, unlike the TMI described above, exhibits a quantized $\boldsymbol{E}\cdot\boldsymbol{B}$ electromagnetic response and has no gapless bulk excitations. The TI* is a true 3D topological phase whose bosonic sector is described by a topological BF theory[27,28] that imparts a relative statistical angle of π between bulk particle and loop excitations and is responsible for a nontrivial topological ground-state degeneracy.

Finally, there are even more exotic fractionalized phases in which the electron with charge e splits apart into three fermionic partons of charge $e/3$ (Fig. 3). In 2D, when these partons form noninteracting integer quantum Hall states one obtains the familiar fractional quantum Hall states. In the conceptually similar case of a Chern insulating band structure, one obtains fractional Chern insulators (FCI)—fractional quantum Hall states that exist in the absence of an external magnetic field. There is already a sizeable literature on FCI, and we direct the reader to existing review articles on the subject[29,30] for more information and original references. If the fractionally charged fermions form a time-reversal invariant $\mathbb{Z}_2$ topological insulator, one obtains a fractional quantum spin Hall insulator or 2D fractional topological insulator[31–35] (FTI), and in 3D a 3D FTI[36–39]. The relevant gauge theories in the example above are of the $U(1)\times U(1)$ or $\mathbb{Z}_3$ variety, leading to gapless bulk photons or no bulk gapless excitations, respectively (a non-Abelian $SU(3)$ gauge theory is formally possible but is typically plagued by the problem of confinement). In both cases the 3D FTI exhibits a quantized $\boldsymbol{E}\cdot\boldsymbol{B}$ electromagnetic response, but with a coefficient one-third that of a topological band insulator. From an experimental

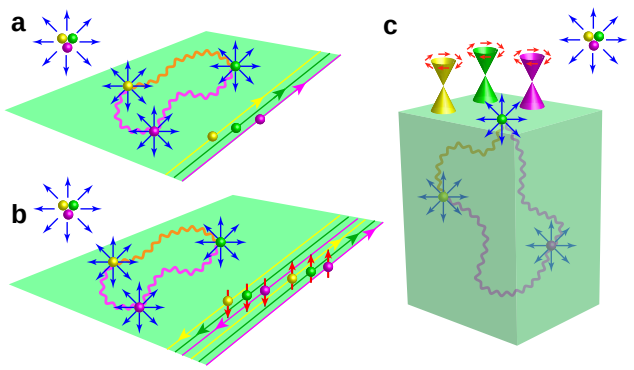

FIG. 3. Fractional topological insulators. Outside the material, the three fermionic partons of charge $e/3$ are confined together to form an electron. Inside the material and in the $U(1) \times U(1)$ description, they become deconfined particles and interact via two $U(1)$ gauge fields (orange and magenta wiggly lines). In the 2D phases (a) and (b), the partons acquire fractional statistics. In the fractional Chern insulator (a), there are chiral edge states of partons, while in the fractional quantum spin Hall insulator (b) the parton edge states are helical. In the 3D fractional topological insulator (c), the $U(1)$ gauge fields are gapless in the bulk, and there are gapless Dirac-like parton surface states. In the $\mathbb{Z}_3$ description, the gauge field would be gapped in the bulk with vortex loop excitations similar to those of Fig. 2(c).

standpoint, a 3D FTI should be easier to detect than a 3D TMI because its gapless surface states are electrically charged, leading to nontrivial signatures in photoemission, tunneling, and quantum oscillations[40].

Can the fractionalized topological insulators whose phenomenology we have described so far be reliably obtained as ground states of interacting electronic Hamiltonians? The answer is a partial yes. In 2D, FCI ground states have been reliably obtained as ground states of models of spinless electrons with nearest-neighbor repulsive interactions via numerical studies[29,30] and strong-coupling expansions[41]. 2D time-reversal invariant FTI ground states have likewise been found in numerical studies[42,43] and exactly soluble models[44,45] of interacting fermions and/or bosons (compressible, bosonic analogs of 2D FTI may have also been found in microscopic models of interacting bosons[46]). Progress has also been made in systematically designing Hamiltonians for which various spin-charge separated states such as the CSL are exact ground states[47,48], but these are models of interacting localized spins rather than models of interacting electrons. The challenge remains mostly open in 3D—where numerical studies come at a prohibitive computational cost—with the exception of exactly soluble models[44].

We have discussed a few examples of fractionalized topological insulators. While a list of specific materials that would harbor such phases is currently lacking, materials that combine the fundamental ingredients of strong spin-orbit coupling and strong electron correlations—such as the pyrochlore iridates[49] and samarium hexaboride[50]—do exist and are currently under intense experimental study. Such materials, as well as systems of ultracold atoms subjected to synthetic gauge fields, may unveil entirely novel quantum phases of matter, topological or otherwise.

We are grateful to our collaborators in this area, V. Chua, A. Karch, M. Kargarian, X.-L. Qi, A. Rüegg, T. Takayanagi, C.-C. J. Wang, J. Wen, and S.-C. Zhang. Our work was generously funded by the ARO, DARPA, DOE, NSF, the Simons Foundation, NSERC, CRC, and startup funds from the University of Alberta. J.M. and G.A.F. contributed equally to this work.

* maciejko@ualberta.ca
† fiete@physics.utexas.edu

[1] Moore, J. E. The birth of topological insulators. *Nature* **464**, 194–198 (2010).
[2] Hasan, M. Z. & Kane, C. L. Colloquium: Topological insulators. *Rev. Mod. Phys.* **82**, 3045–3067 (2010).
[3] Qi, X. L. & Zhang, S. C. Topological insulators and superconductors. *Rev. Mod. Phys.* **83**, 1057–1110 (2011).
[4] Ando, Y. Topological insulator materials. *J. Phys. Soc. Jpn.* **82**, 102001 (2013).
[5] Raghu, S., Qi, X.-L., Honerkamp, C. & Zhang, S.-C. Topological Mott insulators. *Phys. Rev. Lett.* **100**, 156401 (2008).
[6] Zhang, Y., Ran, Y. & Vishwanath, A. Topological insulators in three dimensions from spontaneous symmetry breaking. *Phys. Rev. B* **79**, 245331 (2009).
[7] Yu, R. *et al.* Quantized anomalous Hall effect in magnetic topological insulators. *Science* **329**, 61–64 (2010).
[8] Zhang, X., Zhang, H., Wang, J., Felser, C. & Zhang, S.-C. Actinide topological insulator materials with strong interaction. *Science* **335**, 1464–1466 (2012).
[9] Chen, X., Gu, Z.-C., Liu, Z.-X. & Wen, X.-G. Symmetry-protected topological orders in interacting bosonic systems. *Science* **338**, 1604–1606 (2012).
[10] Mesaros, A. & Ran, Y. Classification of symmetry enriched topological phases with exactly solvable models. *Phys. Rev. B* **87**, 155115 (2013).
[11] A. Kapustin, "Symmetry protected topological phases, anomalies, and cobordisms: Beyond group cohomology", preprint at http://arxiv.org/abs/1403.1467.
[12] Florens, S. & Georges, A. Slave-rotor mean-field theories of strongly correlated systems and the Mott transition in finite dimensions. *Phys. Rev. B* **70**, 035114 (2004).
[13] Lee, P. A., Nagaosa, N. & Wen, X. G. Doping a Mott insulator: Physics of high-temperature superconductivity. *Rev. Mod. Phys.* **78**, 17–85 (2006).
[14] He, J., Kou, S.-P., Liang, Y. & Feng, S. Chiral spin liquid in a correlated topological insulator. *Phys. Rev. B* **83**, 205116 (2011).
[15] Young, M. W., Lee, S.-S. & Kallin, C. Fractionalized quantum spin Hall effect. *Phys. Rev. B* **78**, 125316 (2008).
[16] Rachel, S. & Le Hur, K. Topological insulators and Mott

physics from the Hubbard interaction. *Phys. Rev. B* **82**, 075106 (2010).

[17] Pesin, D. & Balents, L. Mott physics and band topology in materials with strong spin-orbit coupling. *Nature Phys.* **6**, 376 (2010).

[18] Kargarian, M., Wen, J. & Fiete, G. A. Competing exotic topological insulator phases in transition-metal oxides on the pyrochlore lattice with distortion. *Phys. Rev. B* **83**, 165112 (2011).

[19] Kargarian, M. & Fiete, G. A. Topological crystalline insulators in transition metal oxides. *Phys. Rev. Lett.* **110**, 156403 (2013).

[20] Witczak-Krempa, W., Choy, T. P. & Kim, Y. B. Gauge field fluctuations in three-dimensional topological Mott insulators. *Phys. Rev. B* **82**, 165122 (2010).

[21] Balents, L. Spin liquids in frustrated magnets. *Nature* **464**, 199–208 (2010).

[22] Senthil, T. & Fisher, M. P. A. $\mathbb{Z}_2$ gauge theory of electron fractionalization in strongly correlated systems. *Phys. Rev. B* **62**, 7850 (2000).

[23] Rüegg, A., Huber, S. D. & Sigrist, M. $\mathbb{Z}_2$ slave-spin theory for strongly correlated fermions. *Phys. Rev. B* **81**, 155118 (2010).

[24] Maciejko, J. & Rüegg, A. Topological order in a correlated Chern insulator. *Phys. Rev. B* **88**, 241101 (2013).

[25] Rüegg, A. & Fiete, G. A. Topological order and semions in a strongly correlated quantum spin Hall insulator. *Phys. Rev. Lett.* **108**, 046401 (2012).

[26] Maciejko, J., Chua, V. & Fiete, G. A. Topological order in a correlated three-dimensional topological insulator. *Phys. Rev. Lett.* **112**, 016404 (2014).

[27] Hansson, T. H., Oganesyan, V. & Sondhi, S. L. Superconductors are topologically ordered. *Ann. Phys. (N.Y.)* **313**, 497–538 (2004).

[28] Cho, G. Y. & Moore, J. E. Topological BF field theory description of topological insulators. *Ann. Phys. (N.Y.)* **326**, 1515–1535 (2011).

[29] Parameswaran, S. A., Roy, R. & Sondhi, S. L. Fractional quantum Hall physics in topological flat bands. *C. R. Physique* **14**, 816–839 (2013).

[30] Bergholtz, E. J. & Liu, Z. Topological flat band models and fractional Chern insulators. *Int. J. Mod. Phys. B* **27**, 1330017 (2013).

[31] Bernevig, B. A. & Zhang, S.-C. Quantum spin Hall effect. *Phys. Rev. Lett.* **96**, 106802 (2006).

[32] Levin, M. & Stern, A. Fractional topological insulators. *Phys. Rev. Lett.* **103**, 196803 (2009).

[33] Karch, A., Maciejko, J. & Takayanagi, T. Holographic fractional topological insulators in 2+1 and 1+1 dimensions. *Phys. Rev. D* **82**, 126003 (2010).

[34] Lu, Y.-M. & Ran, Y. Symmetry-protected fractional Chern insulators and fractional topological insulators. *Phys. Rev. B* **85**, 165134 (2012).

[35] Chan, A., Hughes, T. L., Ryu, S. & Fradkin, E. Effective field theories for topological insulators by functional bosonization. *Phys. Rev. B* **87**, 085132 (2013).

[36] Maciejko, J., Qi, X.-L., Karch, A. & Zhang, S.-C. Fractional topological insulators in three dimensions. *Phys. Rev. Lett.* **105**, 246809 (2010).

[37] Swingle, B., Barkeshli, M., McGreevy, J. & Senthil, T. Correlated topological insulators and the fractional magnetoelectric effect. *Phys. Rev. B* **83**, 195139 (2011).

[38] Hoyos, C., Jensen, K. & Karch, A. Holographic fractional topological insulators. *Phys. Rev. D* **82**, 086001 (2010).

[39] Maciejko, J., Qi, X.-L., Karch, A. & Zhang, S.-C. Models of three-dimensional fractional topological insulators. *Phys. Rev. B* **86**, 235128 (2012).

[40] Swingle, B. Experimental signatures of three-dimensional fractional topological insulators. *Phys. Rev. B* **86**, 245111 (2012).

[41] McGreevy, J., Swingle, B. & Tran, K.-A. Wave functions for fractional Chern insulators. *Phys. Rev. B* **85**, 125105 (2012).

[42] Neupert, T., Santos, L., Ryu, S., Chamon, C. & Mudry, C. Fractional topological liquids with time-reversal symmetry and their lattice realization. *Phys. Rev. B* **84**, 165107 (2011).

[43] C. Repellin, B. A. Bernevig, and N. Regnault, "$\mathbb{Z}_2$ fractional topological insulators in two dimensions", preprint at http://arxiv.org/abs/1402.2652.

[44] Levin, M., Burnell, F. J., Koch-Janusz, M. & Stern, A. Exactly soluble models for fractional topological insulators in two and three dimensions. *Phys. Rev. B* **84**, 235145 (2011).

[45] Koch-Janusz, M., Levin, M. & Stern, A. Exactly soluble lattice models for non-Abelian states of matter in two dimensions. *Phys. Rev. B* **88**, 115133 (2013).

[46] Motrunich, O. I. & Fisher, M. P. A. d-wave correlated critical Bose liquids in two dimensions. *Phys. Rev. B* **75**, 235116 (2007).

[47] Schroeter, D. F., Kapit, E., Thomale, R. & Greiter, M. Spin Hamiltonian for which the chiral spin liquid is the exact ground state. *Phys. Rev. Lett.* **99**, 097202 (2007).

[48] J.-W. Mei and X.-G. Wen, "Design local spin models for Gutzwiller-projected parton wave functions", preprint at http://arxiv.org/abs/1407.0869.

[49] Witczak-Krempa, W., Chen, G., Kim, Y. B. & Balents, L. Correlated quantum phenomena in the strong spin-orbit regime. *Annu. Rev. Condens. Matter Phys.* **5**, 57–82 (2014).

[50] Dzero, M. & Galitski, V. A new exotic state in an old material: a tale of SmB_6. *JETP* **117**, 499–507 (2013).

Physica E 44 (2012) 845–859

Contents lists available at SciVerse ScienceDirect

Physica E

journal homepage: www.elsevier.com/locate/physe

Topological insulators and quantum spin liquids

Gregory A. Fiete *, Victor Chua, Mehdi Kargarian, Rex Lundgren, Andreas Rüegg, Jun Wen, Vladimir Zyuzin

Department of Physics, The University of Texas at Austin, Austin, TX 78712, USA

ARTICLE INFO

Article history:
Received 2 June 2011
Received in revised form
11 October 2011
Accepted 9 November 2011
Available online 18 November 2011

ABSTRACT

In this paper we review some connections recently discovered between topological insulators and certain classes of quantum spin liquids, focusing on two and three spatial dimensions. In two dimensions we show the integer quantum Hall effect plays a key role in relating topological insulators and chiral spin liquids described by fermionic excitations, and we describe a procedure for "generating" a certain class of topological states. In three dimensions we discuss interesting relationships between certain quantum spin liquids and interacting "exotic" variants of topological insulators. We focus attention on better understanding interactions in topological insulators, and the phases nearby in parameter space that might result from moderate to strong interactions in the presence of strong spin–orbit coupling. We stress that oxides with heavy transition metal ions, which often host a competition between electron interactions and spin–orbit coupling, are an excellent place to search for unusual topological phenomena and other unconventional phases.

Contents

1. Introduction

At first glance topological insulators and quantum spin liquids have nothing to do with each other. A topological insulator (TI) has properties that can be understood in the absence of any electron interactions [1–3], while quantum spin liquids (QSL) are largely understood theoretically in terms of lattice models of interacting spins [4]. Moreover, topological insulators explicitly possess charge and spin degrees of freedom, while spin liquids are understood only in terms of spin degrees of freedom. Quantum spin liquids come in both gapped and gapless varieties, but even for the gapped variety with topological order it would appear there is little to say by way of a relationship between TIs and QSLs. As a supporting argument, one might point out that the "type" of topological order is different: Topological insulators do not have any non-trivial ground state degeneracy, while some of the best understood topological spin liquids possess a non-trivial ground state degeneracy [5].

However, to dismiss any relationship between these two phases of matter is to ignore some beautiful, and we believe insightful, relationships. To help motivate why it is useful to look for connections between systems that apparently have no relationship to one another we need to look no further than

* Corresponding author.
E-mail address: fiete@physics.utexas.edu (G.A. Fiete).

1386-9477/$ - see front matter © 2011 Elsevier B.V. All rights reserved.
doi:10.1016/j.physe.2011.11.011

Laughlin's account of his discovery of the fractional quantum Hall effect [6]. According to Laughlin, a one-dimensional polymer known as polyacetylene (which displays charge fractionalization, at least theoretically [7]) was an important motivation for his inspired guess for a fractional quantum Hall state wavefunction [6]. As it so turns out, there are also deep connections between polyacetylene and topological insulators [8,9]. We believe analogous relationships between TIs and QSLs can also provide useful insights, and could play a key role in deepening our understanding of strongly interacting variants of topological insulators that are not adiabatically connected to the non-interacting TI limit.

In this topical review we will flush out some of the connections between TIs and QSLs recently established. In this paper, we will focus on a number of different lattice models of fermions. Some of the models are non-interacting, some are interacting, some have no intrinsic spin–orbit coupling, while some do have intrinsic spin–orbit coupling. We study a variety of lattices in two and three spatial dimensions and focus on the interplay of lattice geometry, interactions, and spin–orbit coupling. Our aim is to enlarge our understanding of the phase diagram of interacting fermions in two and three dimensions by solving different model problems and using them as points of generalization. For example, which features appear often and therefore are rather general, and which features appear to be model specific? This approach is complementary to directly develop an effective theory. Effective theories are extremely powerful because of their generality and efficient exploitation of the various symmetries present in a problem. However, it is not always straightforward to "guess" an effective theory of a new phase of matter so special cases derived from more microscopic lattice models can serve as a useful guide, particularly when strong interactions and/or correlations are present. That is the point-of-view we take in this paper.

A summary of our main results is as follows. For the case of two-dimensional lattices we show that under rather general conditions there is a connection between TIs and Kitaev-type [10,11] spin models. An earlier work by Lee et al. [12] connecting the honeycomb Kitaev model and the integer quantum Hall effect was an important inspiration for our studies. A relationship between the integer quantum Hall effect, TIs, and Kitaev models exists because the latter can be exactly solved by a mapping that reduces the interacting spin degrees of freedom to non-interacting Majorana degrees of freedom [11]. These Majorana fermions hop on the lattice and have a band structure similar to "normal" fermions (only with a redundancy in the labeling of the states). Therefore, one may study the topological properties of the energy bands, such as whether they possess a finite Chern number. Energy bands of finite Chern number will turn out to establish a connection between TIs and Kitaev-type spin liquids (and of course the integer quantum Hall effect).

Staying with two-dimensions, we will discuss recent results on obtaining a fractional quantum Hall effect in a flat-band lattice model with a partially filled band with a finite Chern number. This lattice model may prove useful in the studies of "fractional" topological insulators in two-dimensions with time-reversal symmetry [13–16]. We also describe a class of models in which spin–orbit coupling can be spontaneously generated at the mean-field level [17]. We contrast the relative instability to electron interactions of Dirac-like and quadratic band touching points in the non-interacting band structure. We find that when quadratic band touching points are present, topological phases often appear as the leading instability with interactions. Such mean-field studies reduce a many-particle problem to a single-particle problem and serve at least two key roles in the study of topological insulators: (1) They elucidate where topological phases can be expected to appear in the presence of electron interactions and (2) they help guide the class of non-interacting lattice models that contain interesting physics. We finish our discussion of two-dimensional systems with an example of theoretical TI studies guiding the discovery of a QSL with novel properties [18] and comment on the role that disorder can play in stabilizing topological quantum spin liquids [19] and topological insulators [20–24].

In the case of three-dimensions, we focus on systems with intrinsic spin–orbit coupling and intermediate strength interactions. With an eye towards transition metal oxides with 4d and 5d elements, we use the slave-rotor mean-field theory [25,26] to investigate the competition between interactions, spin–orbit coupling and lattice distortions on the pyrochlore lattice. We find that a new phase—the "weak topological Mott insulator"—appears [27] with topologically protected gapless modes that carry heat only along a certain class of bulk defects [28]. As a function of pressure, a complex set of transitions between conventional and exotic phases is possible in such systems. We discuss the connection of the slave-rotor mean-field states to quantum spin liquids describe by fermionic excitations and suggest some ways the latter may inform the study of interacting TIs in three dimensions [29]. We close with a discussion of a newly emerging direction in transition metal oxides: interaction-driven topological phases at interfaces [30–33].

Our paper is organized as follows. In Section 2 we set the convention for our use of the term "topological order" in this paper and provide some important general background, including TI-QSL connections in one-dimension and important results for interacting systems. In Section 3 we detail our main results for two-dimensions, and in Section 4 we describe our chief three-dimensional results. Finally, in Section 5 we summarize our main results and give our view of interesting future directions of study.

2. Preliminaries

2.1. Topological terminology

Our main goal in this paper is to provide examples of how TIs and QSLs are related to each other, and how the study of each can help deepen our understanding of the other. An important "connection" between these two types of phases is via their topological [34] properties. In Section 3, we will be more precise by what we mean by "connection". We note here that it *does not simply mean adiabatic connection* of the electronic states because TIs and QSLs are distinct phases of matter. In order to help avoid confusion later, we emphasize that we will use "topological" in the broadest sense of the word: there is some mathematical invariant characterizing the global properties of the system that cannot change unless a bulk gap in the energy spectrum closes. Those with a background in the fractional quantum Hall effect or exotic quantum spin liquids commonly take "topological order" to be synonymous with "non-trivial ground state degeneracy" and "non-trivial (*i.e.* fractional) quantum numbers/statistics" of excitations [5]. Since a large part of this paper deals with TIs which do not have a non-trivial ground state degeneracy, but nevertheless do have topological properties, we choose a more encompassing use of the terminology.

For purposes of this paper, we would say that Z_2 time-reversal invariant TIs, integer quantum Hall systems, fractional quantum Hall systems, and QSLs described at low energies by a Z_2 gauge theory all possess "topological order". We find this use of terminology convenient for highlighting the different roles that topological invariants and conventional order parameters play in describing a state of matter. This way, the quantities characterizing a phase are divided into "non-local" (topological) and "local" (conventional order parameter) types. (As an aside, we note that such divisions can be subtle and sometimes go against conventional wisdom. For example, superconductors should be classified as topologically ordered in the sense of Wen [5], as they have a

non-trivial ground state degeneracy and possess no *gauge invariant local order parameter* [35].)

2.2. General remarks on one-dimensional systems

In this topical review, we are mainly concerned with two and three-dimensional systems. However, a few remarks about one-dimensional systems are in order. One-dimensional Fermi systems are special for a number of reasons: (i) They are strongly correlated at low-energies regardless of the strength of the interactions, and they possess interesting properties such as spin–charge separation, a kind of fractionalization of fermion quantum numbers [36,37]. (ii) Their theoretical study is amenable to powerful, non-perturbative techniques based on Abelian and non-Abelian bosonization techniques [36,37]. A well-known gapless phase of one-dimensional fermions conveniently described with these techniques is the Luttinger liquid [38]. In recent years it has become clear that interesting, highly universal "spin-incoherent" Luttinger liquid regimes also appear [39–41].

Focusing our attention on gapped one-dimensional systems, a few results are suggestive of possible connections between TIs and QSLs. While there are no Z_2 topological insulators in one dimension [8,42,43], the more general Altland and Zirnbauer classifications [44,45] of non-interacting topological states has provided us with important results for other topological phases resulting from different sets of symmetries. Of particular interest is the class BDI (time-reversal symmetry with sublattice symmetry and integer spin), which has a Z classification in one dimension [42,43]. Fidkowski and Kitaev [46] have recently shown in a one-dimensional model in class BDI that the Z classification breaks down to Z_8 in the presence of interactions, and have further generalized these results to other symmetry classes [47]. In other words, phases that are topologically distinct at the non-interacting level can be adiabatically connected with interactions that are slowly turned on and off in a particular way. This example proves that interactions can lead to important modifications of the non-interacting topological classifications [48]. A similar breakdown may occur in two and three-dimensional systems, although to our knowledge there is not yet a concrete example.

2.3. Entanglement as a tool to study topological order

Because topological order is a global, non-local property, it is rather difficult to measure in the general situation. (Most physical responses are described by the *local* coupling of an order parameter to an external perturbation, or generalized "force" [49].) In a few important cases, such as the integer and fractional quantum Hall effects, and the Z_2 topological insulators, the topological properties give rise to certain quantized responses [5,8,50,51]. These examples have topologically protected gapless boundary modes that dominate the responses. However, often there is no obvious "nice" response that can be computed or observed in experiment. The challenge of understanding the many-body quantum mechanics in these cases has led to important advances in the understanding of quantum entanglement in recent years [52,53].

In particular, the entanglement entropy [54–56] and the entanglement spectrum [57] have emerged as two important measures of the quantum entanglement and the topological properties. Typically, a reduced density matrix of the ground state is computed by tracing over some degrees of freedom (usually real-space coordinates for part of the system). The topological entanglement entropy, computed by tracing over the reduced density matrix times the logarithm of the reduced density matrix, contains important information about the "quantum dimensions" of the excitations in the system [55,56]. This measure is useful for topological systems with excitations that have "exotic" quantum numbers, such as the fractional quantum Hall effect [58]. (The non-interacting Z_2 topological insulators do not have "exotic" quantum numbers, so the topological entanglement entropy is not a particularly revealing quantity in this case. However, in a recently identified strongly correlated QSH* phase not adiabatically connected to the QSH phase, the entanglement entropy can serve as a means to distinguish them [59].)

On the other hand, the entanglement spectrum (ES) [57] has proven to be useful in the study of topological insulators [22,60–64]. The ES is found by writing the reduced density matrix as an exponential of a fictitious Hamiltonian. The eigenvalues of this fictitious Hamiltonian constitute the entanglement spectrum. It is remarkable that the ES, which is determined only from the ground-state wave function, contains important information about the *excitations* of the system [57]. In particular, for non-interacting models (such as Z_2 topological insulators and superconductors) it has been shown that gapless boundary modes imply a gapless ES [60,61,65]. Moreover, it has recently been proved by Chandran et al. [66] that in fractional quantum Hall states the low-energy modes of the entanglement spectrum and edge-state excitation spectrum are in one-to-one correspondence. Qi et al. have obtained similar results [67].

One important result to emerge from the study of the ES of topological insulators is that a gapless ES can persist under some conditions where the physical edge spectrum becomes gapped. For example, applying a magnetic field to an inversion symmetric Z_2 topological insulator will gap the surface states but leave the entanglement spectrum gapless [61,62]. The same is true if time-reversal symmetry is broken in more subtle ways [62]. Strong interactions that gap the edge modes [68,69] will also leave a degeneracy in the ES [70]. Thus, the ES "remembers" the underlying state is topological. In this case, it turns out that the gapless nature of the ES is protected by an inversion symmetry [60–63]. In the case of three-dimensional insulators with inversion symmetry, a gapless entanglement spectrum implies an "$\mathbf{E}\cdot\mathbf{B}$" term in the action *even if the boundary contains no gapless modes* [61]. In this sense, the entanglement spectrum can be used to identify a phase of matter [63]. Recently it has been shown that the breakdown of the Z classification (to Z_8) of class BDI in the presence of interactions [46,47] can be understood via the ES [71].

We close this subsection on entanglement by returning once more to one dimension and QSLs. For aficianados of one-dimensional spin chains, Haldane's classification [72] of antiferromagnetically coupled Heisenberg spins is celebrated: half-odd integer multiple spin chains are gapless (Luttinger liquids) while integer spin chains are gapped and possess no long-range order, *i.e.* they are gapped QSLs. Technically, the two cases are distinguished by the Berry phase (topological) term in the effective low-energy action. Remarkably, the gapped integer spin systems contain *topological order* which manifests itself as a non-local string order parameter with long range order [73], and *protected gapless boundary modes* [74] (similar to TIs). In fact, ES studies of integer spin chains show phenomenology quite similar to TIs. For example, the physical edge state degeneracies lead to the same degeneracies in the ES [75]. Additionally, perturbations that destroy long-range order in the string parameter and edge-state degeneracy leave the ES degeneracy in tact, so long as inversion symmetry is preserved [75]. The ES results show that the perturbations to spin chains that destroy the conventional measures of the topological order in the Haldane phase, long-range string order and edge-state degeneracies, do not destroy the Haldane phase itself (so long as the bulk gap remains open). (Even in gapless one-dimensional systems the ES may provide useful information [76].)

Thus, the entanglement properties have emerged as a robust method of identifying a quantum phase [77]. It is remarkable that

the behaviors of the ES spectrum for TIs and QSLs exhibit such similar phenomenology, both with and without perturbations that destroy the edge modes. As we will see in the next section, there are more direct ways that TIs and QSLs can be related in higher spatial dimensions.

3. Two-dimensional systems

In this section we will describe a class of non-interacting and interacting lattice models with topological order in two spatial dimensions. Some of these are spin models of QSLs and some are tight-binding models of TIs. We will show that under a certain set of conditions there is a precise topological connection between them.

3.1. Orientation

The first prediction of a quantum spin Hall state (a two-dimensional TI) in a specific material was made by Bernevig et al. [78] for HgTe quantum wells. This prediction was soon verified experimentally in a series of beautiful experiments in Würzburg [79,80].

In this topical review, we will focus on models inspired by the earlier pioneering work of Kane and Mele [81,82], which first established the quantum spin Hall state as a new topological phase in a simple tight-binding model on the honeycomb lattice that preserves time-reversal symmetry. Their Hamiltonian is

$$\mathcal{H}_{\mathrm{K-M}} = -t\sum_{\langle ij\rangle,\sigma}(c^{\dagger}_{i\sigma}c_{j\sigma}+\mathrm{H.c.})+\mathcal{H}_{\mathrm{CDW}}+\mathcal{H}_{\mathrm{R}} +i\lambda_{\mathrm{SO}}\sum_{\langle\langle ij\rangle\rangle,\alpha,\beta}\vec{e}_{ij}\cdot\vec{s}_{\alpha\beta}c^{\dagger}_{i\alpha}c_{j\beta}, \quad (1)$$

where t is a real first-neighbor hopping, $c^{\dagger}_{i\sigma}$ creates a particle of spin σ on site i and $c_{i\sigma}$ annihilates the same particle, λ_{SO} is the (real) parameter representing the strength of the second-neighbor spin–orbit coupling, $\vec{e}_{ij}=(\mathbf{d}^1_{ij}\times\mathbf{d}^2_{ij})/|\mathbf{d}^1_{ij}\times\mathbf{d}^2_{ij}|$ is a vector normal to the $x-y$ plane describing how the path $\langle\langle ij\rangle\rangle$ was traversed, that is, either "bending" to the right or left [81,82]. Here, $\mathcal{H}_{\mathrm{CDW}}$ and $\mathcal{H}_{\mathrm{R}}$ are charge density wave and Rashba spin–orbit terms, respectively. The CDW term describes a mean-field staggered sublattice potential that would gap the Dirac points if $\lambda_{\mathrm{SO}}=0$ and put the model in a trivial insulator phase. The Rashba spin–orbit term breaks S^z conservation and is generally present if the physical system has broken inversion symmetry with respect to the plane of the honeycomb lattice.

A key precedent to Kane and Mele's work was a result from Haldane [83] in which it was shown that a tight-binding model of *spinless* fermions on the honeycomb lattice with broken time-reversal symmetry *but zero net magnetic field* could exhibit a quantum Hall effect. (In other words, it is the breaking of time-reversal symmetry that is key for the quantum Hall effect, not the net magnetic flux.) Haldane's model is

$$\mathcal{H}_{\mathrm{H}} = -t\sum_{\langle ij\rangle}(c^{\dagger}_{i}c_{j}+\mathrm{H.c.})+\mathcal{H}_{\mathrm{CDW}}+it_2\sum_{\langle\langle ij\rangle\rangle}\mathrm{sgn}(\vec{e}_{ij})c^{\dagger}_{i}c_{j}, \quad (2)$$

where t_2 is the (real) parameter describing the string of the second neighbor hopping and $\mathrm{sgn}(\vec{e}_{ij})$ is ±1 depending on whether the spinless fermion made a right or left "turn" along the path $\langle\langle ij\rangle\rangle$.

As Kane and Mele emphasized in their work [81,82], in a quantum spin Hall system that preserves S^z quantization [$\mathcal{H}_{\mathrm{R}}=0$ in Eq. (1)], the state can be represented as "two copies" of Haldane's model (2)—one for spin up and one for spin down—each of which sees an opposite sign of the effective magnetic field and therefore preserves time-reversal symmetry overall. The presence of a small but finite Rashba coupling does not change the phase; it only destroys the S^z conservation.

While the topological classification of the quantum Hall effect is based on the Chern number [58] (which takes the integers Z) and the two-dimensional time-reversal invariant TIs are classified by Z_2 [1–3], the Haldane–Kane–Mele correspondence shows that the integer quantum Hall effect in a lattice model is intimately related to the quantum spin Hall state. In particular, if a spin polarized tight-binding model realizes a quantum Hall effect, combining two time-reversed copies of it with spin degrees of freedom is guaranteed to produce a quantum spin Hall effect. This simple observation is actually a powerful tool for *generating* desired topological states in two-dimensional lattice models. We will use this approach in several different ways below, including generating TIs from QSLs [62,84], generating QSLs from TIs [18] (the Haldane–Kane–Mele correspondence in reverse), and generating *fractional* TIs from the fractional quantum Hall effect in lattice models [85].

3.2. "Non-interacting" lattice models

After the work of Kane and Mele on the honeycomb lattice [81,82] there was a flurry of activity exploring simple non-interacting tight-binding lattice models on a variety of different lattices in two and three spatial dimensions. For example, in two dimensions the decorated honeycomb lattice [84], the checkerboard lattice [86], the square-octagon lattice [62], the kagome lattice [87], the ruby lattice [85], and others [88] have been shown to support a TI phase in simple s-band models. If multiple orbitals on each site are used, even the simple square lattice can support a TI [78].

A natural question to ask is "What properties of a lattice model would allow it to support a TI phase?" One way to view this question in light of the discussion above is "What properties of a spinless fermion lattice model would allow it to support an integer quantum Hall effect?" When cast this way, there are immediate connections to so-called "chiral" QSLs, a class of spin liquids with broken time-reversal symmetry and a thermal Hall conductance. In fact, one of the early models relating spin liquids to the (fractional) quantum Hall effect was proposed by Laughlin himself [89].

In recent years, an important class of exactly solvable spin models known as "Kitaev" models has emerged [10,11]. These models can be used to generate concrete examples of various types of QSLs (previous studies often relied on uncontrolled approximations). In particular, chiral spin liquids with a quantized thermal Hall conductance can be found [18,90,91]. As we now show, such models can be adiabatically deformed to an integer quantum Hall "Haldane-type" model, which in turn can be used to construct a two-dimensional TI via the Haldane–Kane–Mele correspondence described above.

As a simple example, consider the Kitaev model on the honeycomb lattice [11],

$$\mathcal{H}_{\mathrm{Kitaev}} = \sum_{\langle ij\rangle_x}J\sigma^x_i\sigma^x_j+\sum_{\langle ij\rangle_y}J\sigma^y_i\sigma^y_j+\sum_{\langle ij\rangle_z}J\sigma^z_i\sigma^z_j, \quad (3)$$

where the spin-1/2 components $\sigma^x,\sigma^y,\sigma^z$ couple to each other along the x,y,z-labeled links, respectively. The symmetry of the Hamiltonian (3) is unusual (not Heisenberg, XY, or Ising, for example), but there are recent proposals suggesting it would arise naturally in some solid state contexts [92,93]. The main reason for choosing the form (3) is that it admits an exact solution with a spin-liquid ground state [11].

The Hamiltonian (3) is easily solved by choosing an alternate representation of the spin degrees of freedom: One can write the spins as

$$\sigma^x_j = i\eta^x_j\eta^0_j,\quad \sigma^y_j = i\eta^y_j\eta^0_j,\quad \sigma^z_j = i\eta^z_j\eta^0_j, \quad (4)$$

where the $\eta^0_j,\eta^x_j,\eta^y_j,\eta^z_j$ are four "flavors" of Majorana fermions on the site j. They have the properties $\eta^a=(\eta^a)^{\dagger}$, $(\eta^a)^2=1$ on each site for $a=0,x,y,z$, and they satisfy the anticommutation relations

$\{\eta_i^a,\eta_j^b\}=2\delta_{ab}\delta_{ij}$. They contain "half" the degrees of freedom of a "normal" fermion (one that satisfies the usual anticommutation relations). Importantly, the transformation (4) preserves the spin commutation relations $[\sigma_j^a,\sigma_j^b]=2i\epsilon^{abc}\sigma_j^c$ provided we impose the constraint $D_j\equiv-\eta_j^0\eta_j^x\eta_j^y\eta_j^z=1$ on each site. (The Majorana representation (4) actually doubles the Hilbert space, so one needs to project to the physical Hilbert space.) Under the representation (4) the Kitaev Hamiltonian is transformed to

$$\mathcal{H}_{\text{Kitaev}}=\sum_{\langle ij\rangle_x} iJu_{ij}\eta_i^0\eta_j^0+\sum_{\langle ij\rangle_y} iJu_{ij}\eta_i^0\eta_j^0+\sum_{\langle ij\rangle_z} iJu_{ij}\eta_i^0\eta_j^0, \tag{5}$$

where $u_{ij}=-i\eta_i^a\eta_j^a$ is a Z_2 gauge field with eigenvalues ±1 defined along an a-link. The product of six different u_{ij} around hexagonal plaquettes on the honeycomb lattice defines a Z_2 gauge flux through that plaquette, $W_p=\prod u_{ij}$. The usefulness of the representation (4) is that now

$$[u_{ij},u_{kl}]=[u_{ij},\mathcal{H}_{\text{Kitaev}}]=[W_p,\mathcal{H}_{\text{Kitaev}}]=0, \tag{6}$$

so that the u_{ij} are *non-dynamical* gauge fields and W_p are *non-dynamical* gauge fluxes. In other words, the u_{ij} in Eq. (5) can be taken to be constants, rather than operators where the value of the constants are determined (up to gauge equivalent choices) by the fluxes W_p around the plaquettes in the lattice. For a bipartite lattice (like the honeycomb lattice) it is known that the uniform flux configuration is lowest in energy [94], and for non-bipartite lattices detailed numerical studies indicate the same [18,90].

With the u_{ij} as constants, it is clear that the interacting spin Hamiltonian (3) has now been reduced to a *non-interacting hopping Hamiltonian* (5). (Recall that $\eta^a=(\eta^a)^\dagger$.) Of course, a non-interacting Hamiltonian can always be solved exactly. In the present case, it is useful to Fourier transform to momentum space as one would for any tight-binding Hamiltonian and determine the energy bands $E(\vec{k})$. Because of the self-adjoint property of the Majorana fermions, half of the states are redundant and $E(\vec{k})=-E(-\vec{k})$. One "unusual" property of the tight-binding model (5) is that the hopping amplitudes, iJu_{ij}, are purely imaginary (assuming J is real).

The procedure for solving any Kiteav-type model on any lattice is exactly the same as above, even if the lattice is different and/or the spin is larger [18,95–99]. Staying with the honeycomb lattice model for the moment, it is worth emphasizing that Kitaev's solution also determines whether the ground state of the spin system spontaneously breaks time-reversal symmetry [11]. The statement is the following: If the lattice contains plaquettes with only an even number of sides (such as the honeycomb lattice) the ground state will not break time-reversal symmetry. If there are any plaquettes with an odd number of links (such as the decorated honeycomb lattice [90] or kagome lattice [18]) the ground state will spontaneously break time-reversal symmetry [11]. This statement follows because time-reversal symmetry sends $u_{ij}\to-u_{ij}$, which will change the sign of W_p on odd-sided plaquettes, but not even-sided ones.

Applying this to the honeycomb lattice model (5) we can immediately infer that since the model does not break time-reversal symmetry, the band structure must have zero Chern number. On the other hand, the addition of the term [12]

$$\mathcal{H}'=\sum_{(ijk)\in\triangle} J'\sigma_i^y\sigma_j^z\sigma_k^x+\sum_{(ijk)\in\nabla} J'\sigma_i^x\sigma_j^z\sigma_k^y, \tag{7}$$

explicitly breaks time-reversal symmetry and leads to a *second-neighbor* hopping term

$$\mathcal{H}'=\sum_{\langle\langle ik\rangle\rangle\in\triangle} -ij'u_{ij}u_{jk}\eta_i^0\eta_k^0+\sum_{\langle\langle ik\rangle\rangle\in\nabla} ij'u_{ij}u_{jk}\eta_i^0\eta_k^0, \tag{8}$$

where $\triangle$ and ∇ denote up and down pointing triangles of (ijk), with i always taken to be the left most point. Remarkably, if the Majorana band structure of the Hamiltonian (5) with Eq. (8) are taken to represent spinless fermions (as opposed to Majorana fermions), the states can be adiabatically deformed into the Haldane model (2) (which contains purely real first-neighbor hopping and imaginary second-neighbor hopping) on the honeycomb lattice [12]. This implies that the Hamiltonian (5) with Eq. (8) is a topological chiral spin liquid with Chern number ±1!

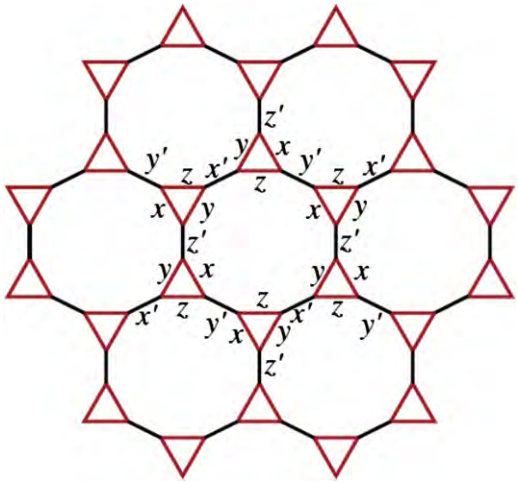

Fig. 1. (Color online) The decorated honeycomb (sometimes called the "star") lattice. An exactly solvable chiral spin liquid model with a finite Chern number and non-Abelian anions has been found on this lattice [90]. By the Kitaev–Haldane–Kane–Mele correspondence, this implies a topological insulator phase in a simple s-band model also exists on this lattice [84].

This result establishes a Kitaev–Haldane–Kane–Mele correspondence on the honeycomb lattice that generalizes the earlier Haldane–Kane–Mele correspondence to include chiral spin liquids with finite Chern numbers (provided the chiral spin liquids can be described by fermions with a band structure—there is not such an obvious connected to spin liquids described by a bosonic representation of the spin degrees of freedom). As we now show, the presence of a chiral spin liquid with finite Chern number on the honeycomb lattice [12] when there is also an integer quantum Hall effect [83] and a TI phase [81,82] is a special case of a more general result.

The first exactly solvable model of a chiral spin liquid with a finite Chern number that included only two-spin interactions was proposed by Yao and Kivelson [90] on the decorated honeycomb lattice shown in Fig. 1. The Hamiltonian is of the Kitaev type and is given by

$$\mathcal{H}_{\text{dhc}}=\sum_{\langle ij\rangle_x} J\sigma_i^x\sigma_j^x+\sum_{\langle ij\rangle_y} J\sigma_i^y\sigma_j^y+\sum_{\langle ij\rangle_z} J\sigma_i^z\sigma_j^z + \sum_{\langle ij\rangle_{x'}} J'\sigma_i^x\sigma_j^x+\sum_{\langle ij\rangle_{y'}} J'\sigma_i^y\sigma_j^y+\sum_{\langle ij\rangle_{z'}} J'\sigma_i^z\sigma_j^z, \tag{9}$$

where the exchange is given by J along the links of the triangles and J' along the links between triangles, as shown in Fig. 1. The Hamiltonian (9) is solved using the transformation (4) and a fermion hopping model with purely imaginary hopping parameter results, similar to what is found in Eq. (5). Because of the triangular plaquettes on the lattice, the ground state spontaneously breaks time-reversal symmetry. For $0<J'/J<\sqrt{3}$, the ground state is a gapped chiral spin liquid with Chern number ±1, while for $J'/J>\sqrt{3}$, the ground state is gapped chiral spin liquid with zero Chern number [90]. If the Kitaev–Haldane–Kane–Mele correspondence described above on the honeycomb lattice is to prove general, Yao and Kivelson's discovery of the chiral spin liquid with finite Chern number in a Kitaev model should imply that there is a TI in an s-band model on the

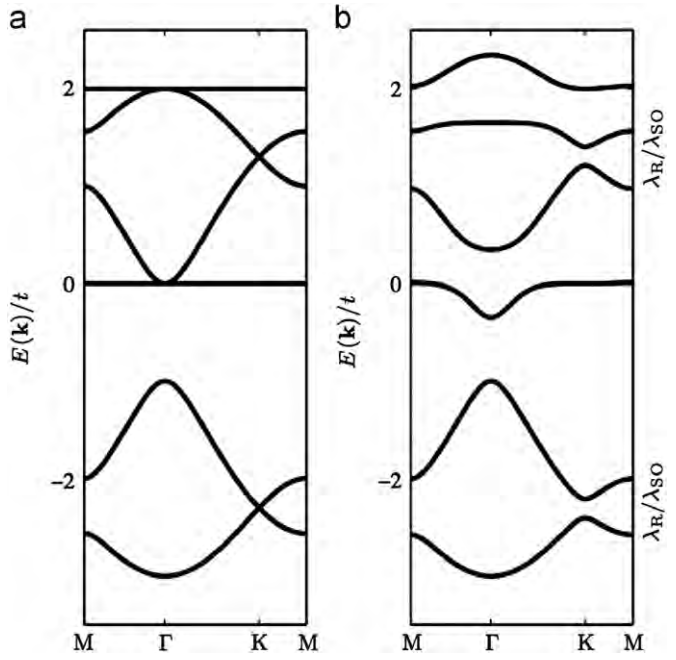

Fig. 2. The decorated honeycomb lattice energy bands along high symmetry directions in the Brillouin zone (from Ref. [84]). In (a) $\lambda_{SO}=0$ and in (b) $\lambda_{SO}=0.1t$. There are Dirac points at K and K' (not shown) and quadratic band crossing points (QBCP) at Γ in (a), while in (b) $\lambda_{SO}\neq 0$ opens up a gap at each of these points and destroys the flat bands.

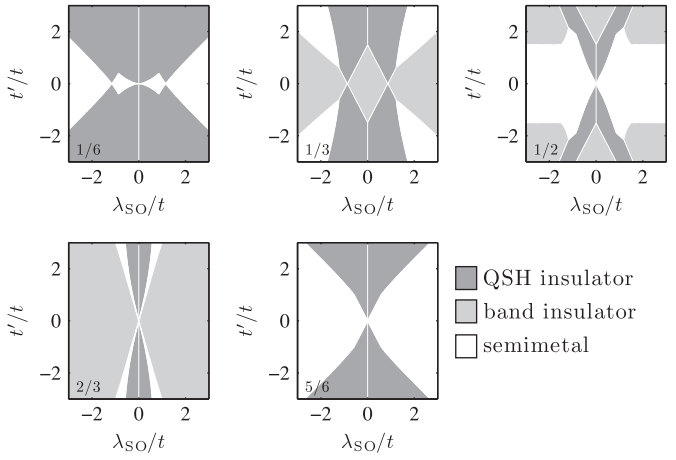

Fig. 3. Phase diagrams for the decorated honeycomb lattice with t and t' real in the absence of a staggered on-site potential and no Rashba coupling (from Ref. [84]). Several filling fractions f are shown (lower left corner). For fixed f and λ_{SO} it is possible to drive a transition between a topological insulator and a non-topological phase by varying the ratio t'/t.

decorated honeycomb lattice. We have shown this is indeed the case [84].

Consider the s-band Hamiltonian on the decorated honeycomb lattice,

$$\mathcal{H}_{\text{dhc-TB}} = -t\sum_{\langle ij\rangle,\sigma,\Delta} c^{\dagger}_{i\sigma}c_{j\sigma} - t'\sum_{\langle ij\rangle,\sigma,\Delta\to\Delta} c^{\dagger}_{i\sigma}c_{j\sigma} + \text{H.c} \quad ., \\ +\mathcal{H}_{\text{CDW}}+\mathcal{H}_{\text{R}}+i\lambda_{\text{SO}}\sum_{\langle\langle ij\rangle\rangle,\alpha,\beta}\vec{e}_{ij}\cdot\vec{s}_{\alpha\beta}c^{\dagger}_{i\alpha}c_{j\beta}, \tag{10}$$

which describes nearest-neighbor hopping on the triangles "△" with amplitude t and between triangles "△→△" with amplitude t', and the remaining terms describe the same physics as represented in Eq. (1). The bands for $\mathcal{H}_{\text{CDW}}=\mathcal{H}_{\text{R}}=0$ are shown in Fig. 2, and the phase diagrams at various filling fractions are shown in Fig. 3. Note that at all filling fractions there is a finite region of parameter space occupied by a TI (QSH) phase.

We now show that the TI phase at 1/2 filling is "connected" to the chiral spin liquid phase of Eq. (9) via the Kitaev–Haldane–Kane–Mele correspondence demonstrated on the honeycomb lattice by Lee et al. [12]. We do this by showing that the Hamiltonian describing the band structure of Eq. (9) (with "normal" spinless fermions replacing the Majorana fermions) with only purely imaginary first-neighbor hopping can be adiabatically deformed to one spin component of Eq. (10) (with $\mathcal{H}_{\text{CDW}}=\mathcal{H}_{\text{R}}=0$) which has purely real first-neighbor hopping and purely imaginary second-neighbor hopping. This is done by applying a combination of gauge transformations and adiabatic tuning of the real and imaginary components of first and second neighbor hopping parameters. The

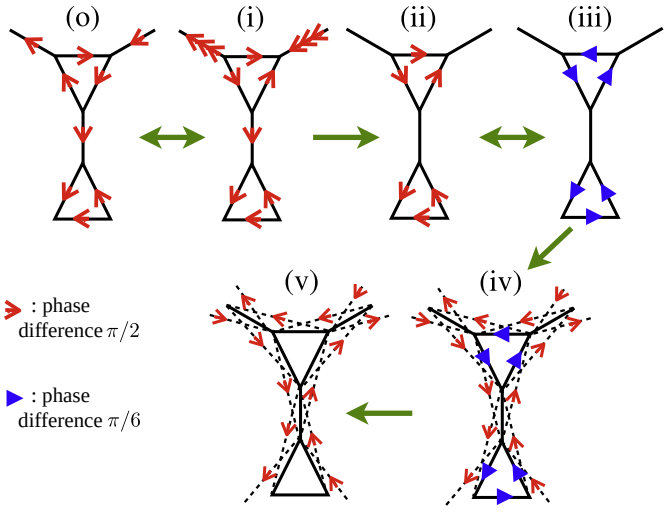

Fig. 4. (Color online) (from Ref. [84]) Schematic illustration of the continuous path which adiabatically connects the representative free fermion model of the Kitaev model on the decorated Honeycomb lattice with the spinless model with real t, t' and λ_{SO}. The patterns (o) and (i) are equivalent and correspond to Kitaev's model whereas (v) represents the model with real t, t' and λ_{SO}. The adiabatic deformation does not lead to a gap closing and the Chern number stays constant. See Fig. 5. This establishes the topological connection between the two models.

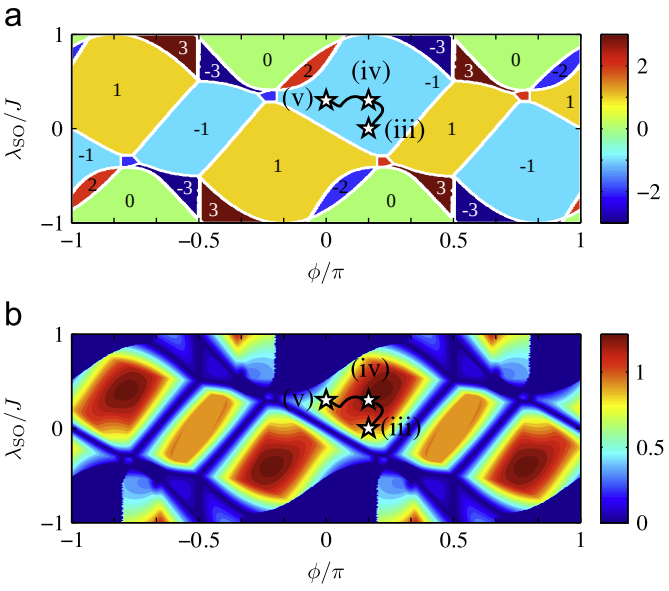

Fig. 5. (Color online) Contour plot of (a) the Chern number and (b) the gap of the model as a function of (ϕ,λ_{SO}) at half-filling for $J=J'$. Here ϕ is the phase angle on the nearest neighbor hopping parameters given in Ref. [84]. Also shown is a possible path which adiabatically connects the flux patterns (iii)–(v) defined in Fig. 4.

procedure is shown in Fig. 4, and the panels in Fig. 5 explicitly show that the Chern number remains unchanged and the gap remains open in this process, establishing the topological equivalence, and the Kitaev–Haldane–Kane–Mele correspondence on the decorated honeycomb lattice [84].

It should be clear from the examples of the decorated honeycomb lattice and the honeycomb lattice above that the Kitaev–Haldane–Kane–Mele correspondence is rather general. However, it is also true that one can invert the argument to use the existence of a TI in an s-band model on a particular lattice to infer a chiral spin liquid with a finite Chern number in a Kitaev-type model. Indeed, we have used the work of Guo and Franz that established a TI on the kagome lattice [87] to motivate the study of a Kitaev-type model on the same lattice [18]. Not only did we find a new exactly solvable chiral spin liquid model with finite Chern number, but also a phase that possess a stable spin Fermi surface [18]. We note that unstable spin Fermi surfaces have been reported in other models [95,100,101].

Because the kagome lattice has sites with four links (as opposed to three on the honeycomb, decorated honeycomb, and decorated square lattice), the effective spin in a Kitaev-type model must be at least 3/2 [96]. These higher-spin Kitaev models require that the spin-1/2 Pauli spin matrices be generalized to Gamma matrices [95]. The spin Hamiltonian we study [18] on the kagome lattice is

$$\mathcal{H}=J_{\triangle}\sum_{\langle ij\rangle\in\triangle}\Gamma_i^1\Gamma_j^2+J_{\nabla}\sum_{\langle ij\rangle\in\nabla}\Gamma_i^3\Gamma_j^4+J_5\sum_i\Gamma_i^5$$
$$+J_{\triangle}'\sum_{\langle ij\rangle\in\triangle}\Gamma_i^{15}\Gamma_j^{25}+J_{\nabla}'\sum_{\langle ij\rangle\in\nabla}\Gamma_i^{35}\Gamma_j^{45}, \quad (11)$$

where we have distinguished the nearest neighbor couplings J_{ij} as $J_{\triangle},J_{\nabla}$ and J'_{ij} as $J_{\triangle}'$ and J_{∇}' based on whether the link $\langle ij\rangle$ belongs to an up ($\triangle$) triangle or down (∇) triangle (the kagome lattice can be viewed as a corner sharing network of up and down triangles), and $\langle ij\rangle$ is taken in the counterclockwise sense for each triangle. Locally, the five Γ-matrices satisfy a Clifford algebra, $\{\Gamma_i^a,\Gamma_i^b\}=2\delta^{ab}$, where $a,b=1,\ldots,5$, and $\Gamma^{ab}\equiv[\Gamma^a,\Gamma^b]/(2i)$. In terms of the components of the spin $S=3/2$ operators [95,102],

$$\Gamma^1=\tfrac{1}{\sqrt{3}}\{S^y,S^z\},\quad \Gamma^2=\tfrac{1}{\sqrt{3}}\{S^z,S^x\},\quad \Gamma^3=\tfrac{1}{\sqrt{3}}\{S^x,S^y\},$$

$$\Gamma^4=\tfrac{1}{\sqrt{3}}[(S^x)^2-(S^y)^2],\quad \Gamma^5=(S^z)^2-\tfrac{5}{4}. \quad (12)$$

With the identification (12), it is clear the model (11) has a global Ising spin symmetry under 180° rotations about the z-axis, and possesses time-reversal symmetry (TRS) (although TRS will be spontaneously broken in the ground state from the triangular plaquettes as we described earlier) in addition to the translational and threefold rotational lattice symmetry mentioned above.

In order to solve the higher-spin Γ-matrix model (11), a Majorana representation similar to that for spin-1/2, (4), is employed

$$\Gamma_i^a=i\xi_i^a c_i,\quad \Gamma_i^5=ic_id_i,\quad \Gamma_i^{a5}=i\xi_i^a d_i, \quad (13)$$

with $a=1,2,3,4$. There are thus six Majorana species on each site i: $\{\xi_i^1,\xi_i^2,\xi_i^3,\xi_i^4,c_i,d_i\}$. The Majorana representation enlarges the spin-3/2 Hilbert space, so that one must enforce the constraint $D_i=-\Gamma_i^1\Gamma_i^2\Gamma_i^3\Gamma_i^4\Gamma_i^5=-i\xi_i^1\xi_i^2\xi_i^3\xi_i^4c_id_i=1$, namely for any physical state $|\Psi\rangle_{\rm phys}$ $D_i|\Psi\rangle_{\rm phys}=|\Psi\rangle_{\rm phys}$ for any i. The remainder of the steps are similar to the spin-1/2 version and one obtains a Majorana tight-binding model on the kagome with imaginary hopping parameters [18]. Solving the model on a strip geometry in the gapped phase with a finite Chern number (±2) yields the results shown in Fig. 6. The *gauge dependent* but *stable* Fermi surface in a gapless phase is shown in Fig. 7.

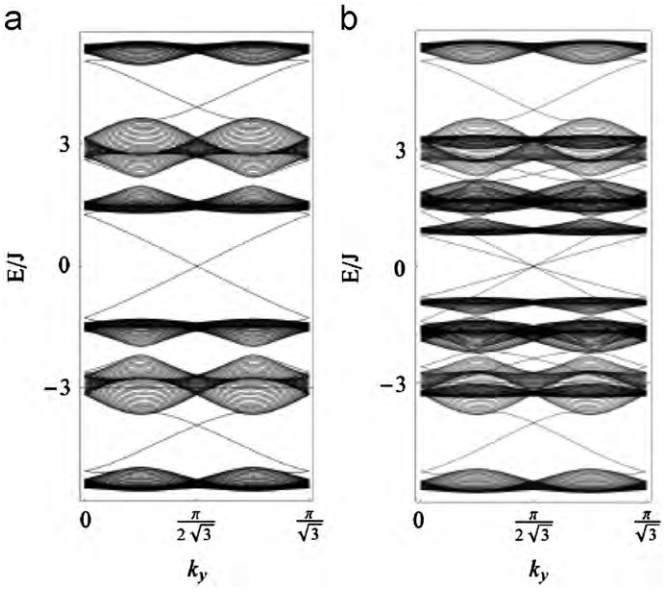

Fig. 6. (a) Band structure on a cylindrical geometry for $J_{\triangle}=J_{\triangle}'=1.0$, $J_{\nabla}=J_{\nabla}'=0.8$, $J_5=0$. There are two gapless chiral Majorana edge states (dotted lines) which overlap on each other. (b) For $J_{\triangle}=1.0$, $J_{\triangle}'=0.6$, $J_{\nabla}=0.9$, $J_{\nabla}'=0.5$, and $J_5=0.1$, the two gapless edge states separate. These ground states are thus CSLs with a spectrum Chern number (±2) and the vortices obey Abelian statistics. From Ref. [18].

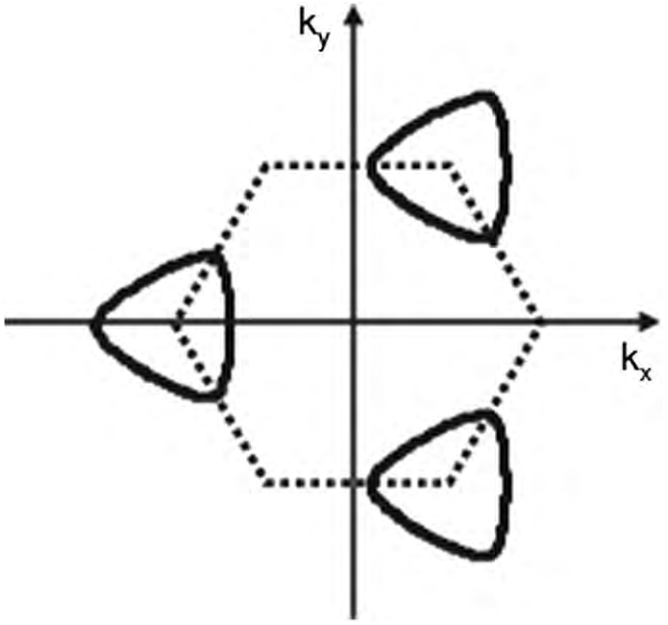

Fig. 7. The Fermi surface (solid line) for the flux configuration $\{\pi/2,\pi/2,\pi\}$ and $\{J_{\triangle}J_{\nabla}J_{\triangle}'J_{\nabla}'J_5\}=\{1.0,0.3,0.8,0.5,1.4\}$. (See Ref. [18] for a description of notation.) The dashed hexagon is the Brillouin zone boundary. Note that there is only one Fermi pocket for this set of parameters and the three pockets shown are related by a reciprocal lattice vector and are thus equivalent.

The results of this subsection have demonstrated the Kitaev–Haldane–Kane–Mele correspondence and illustrated how TIs can be generated from a certain class of QSLs, and vice-a-versa. Thus, we have established a *method* of generating certain types of desired states. Moreover, along the way we have also discovered new QSLs, such as the gapless varieties with a stable spin fermi surface [18]. In all these "non-interacting" models, the topological relationship between the TI and QSL models is based on the Chern number and an underlying band structure of free fermions. In the next subsection we turn to the study of interacting models in two dimensions.

As a final remark, we note there are also deep connections between Kitaev models, the quantum Hall effect, topological insulators, and topological superconductivity [11,58,65,103–107]. The topological Kitaev models [19] and the TI insulators (including the integer quantum Hall effect) [20–24] show that disorder can play a useful role in *stabilizing* topologically ordered states and could play a role in guiding the experimental discovery of topological quantum spin liquids [19]. The non-interacting models discussed in this section can be viewed as mean-field states in a more general interacting model.

3.3. Interacting lattice models

While the Kitaev models are interacting in terms of the underlying electronic degrees of freedom (local moments), we discussed them under the heading of "non-interacting" lattice models because they admit a free (Majorana) fermion representation and therefore can be understood in terms of the properties of their band structure. There are few exactly solvable interacting models in two dimensions, and those that exist often possess special symmetries [108]. Thus, one must look for approximate methods to address the physics of interactions.

For a certain class of Hamiltonians (those without a fermion sign problem), quantum Monte Carlo is a powerful theoretical method. Given the central role the honeycomb lattice has played in the understanding of TIs and QSLs, it is natural to begin an investigation of interacting models on this lattice. In the last year the simplest interacting model, the Hubbard model (no spin–orbit coupling terms), has been shown to possess a (apparently gapped) spin-liquid phase at half-filling and intermediate coupling [109]. Moreover, this spin liquid has been shown to be robust in the presence of a second-neighbor spin–orbit coupling in quantum Monte Carlo [110] and dynamical mean-field [111] studies of the so-called Kane–Mele–Hubbard model. Related quantum Monte Carlo studies on bulk and edge instabilities in the Kane–Mele–Hubbard model have been reported [111–114], as well as closely related exact diagonalization studies in spinless systems with nearest-neighbor interactions for small system sizes [115].

Aside from bosonization studies of interactions in the one-dimensional helical liquids that exist along the boundary of a two-dimensional TI [116–123], most studies of interactions in bulk have relied on some type of mean-field theory [17,59,86,124–127]. One of the most important results to emerge from these studies is that topological insulators can be *spontaneously* generated from interactions at the mean-field level *even when there is no microscopic spin–orbit coupling present*. This was first explicitly shown by Raghu et al. on the honeycomb lattice [17]. In model without any intrinsic spin–orbit coupling, TI phases are produced by the spontaneous generation of spin–orbit coupling from first and second-neighbor interactions treated at the mean-field level [17,30,86,124–126].

The stability of a non-interacting band structure to interactions depends on a large extent on the form of the low-energy dispersions and band crossing points. For example, it is well-known that at 1/2 filling on the honeycomb lattice the non-interacting dispersions are Dirac-like [128]. Dirac points are perturbatively stable to interactions [17,86,88,124]. In practice, this implies that a critical interaction strength is required to drive a phase transition away from the gapless state [86]. This is qualitatively consistent with both mean-field studies [17,124,129] and quantum Monte Carlo studies [109]. By contrast, two bands that touch quadratically or flatter are *infinitesimally* unstable to interactions in two dimensions [86,124]. Quadratic band touching points are known to occur on many of the lattices that support TIs in simple s-band models: decorated honeycomb [84], kagome [87], checkerboard [86], square-octagon [62], and ruby [85]. As we show below, the cases of quadratic band touching points often have topological phases as the leading instabilities with respect to interactions [124]. This effectively enlarges the candidate systems for TI physics to include those *without strong spin–orbit coupling* but with "flat" band touching points in the non-interacting band structure. Another notable example is bilayer and multilayer graphene [130].

The kagome lattice serves as an important example case. Its non-interacting band structure in an s-band nearest neighbor hopping model possess both Dirac points (1/3 filling) and quadratic band touching points (2/3 filling) [87]. We study the following Hamiltonian [124]:

$$\mathcal{H}_{\text{kagome}} = -t\sum_{\langle i,j\rangle} c^\dagger_{i\sigma}c_{j\sigma} + U\sum_i n_{i\uparrow}n_{i\downarrow} + V_1\sum_{\langle i,j\rangle} n_i n_j + V_2\sum_{\langle\langle i,j\rangle\rangle} n_i n_j + V_3\sum_{\langle\langle\langle i,j\rangle\rangle\rangle} n_i n_j \quad (14)$$

at the mean-field level. Here, $c^{(\dagger)}_{i\sigma}$ annihilates (creates) a fermion on site i with spin $\sigma=\uparrow,\downarrow$, $n_{i\sigma}=c^\dagger_{i\sigma}c_{i\sigma}$ and $n_i=\sum_\sigma n_{i\sigma}$. The sums run over nearest-neighbor $\langle i,j\rangle$, second-neighbor $\langle\langle i,j\rangle\rangle$, or third-neighbor bonds $\langle\langle\langle i,j\rangle\rangle\rangle$. The hopping amplitude is denoted by t and the parameters V_1, V_2, and V_3 quantify the nearest-neighbor, second-neighbor and third-neighbor repulsion, respectively.

To perform the mean-field calculation, we decouple the on-site interaction according to [124]

$$n_{i\uparrow}n_{i\downarrow} \approx n_{i\uparrow}\langle n_{i\downarrow}\rangle + \langle n_{i\uparrow}\rangle n_{i\downarrow} - \langle n_{i\uparrow}\rangle\langle n_{i\downarrow}\rangle - c^\dagger_{i\uparrow}c_{i\downarrow}\langle c^\dagger_{i\downarrow}c_{i\uparrow}\rangle - \langle c^\dagger_{i\uparrow}c_{i\downarrow}\rangle c^\dagger_{i\downarrow}c_{i\uparrow} + \langle c^\dagger_{i\uparrow}c_{i\downarrow}\rangle\langle c^\dagger_{i\downarrow}c_{i\uparrow}\rangle. \quad (15)$$

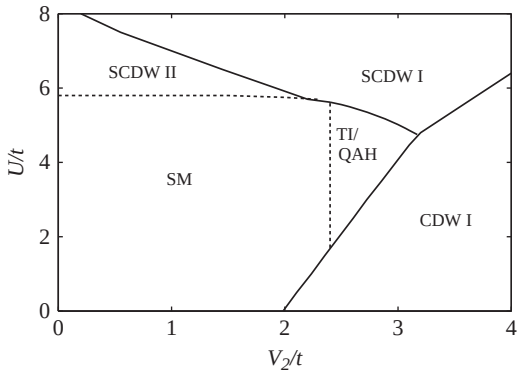

Fig. 8. Filling fraction 1/3 on the kagome lattice with Dirac points in the non-interacting band structure. The U–V_2 phase diagram for $V_1=0$ and $V_3=0.4t$ in Eq. (14). An interaction-driven TI appears for finite U and V_2 and requires a critical interaction strength to appear, and some fine-tuning of parameters. Solid lines indicate first order and dashed lines second order transitions. From Ref. [124].

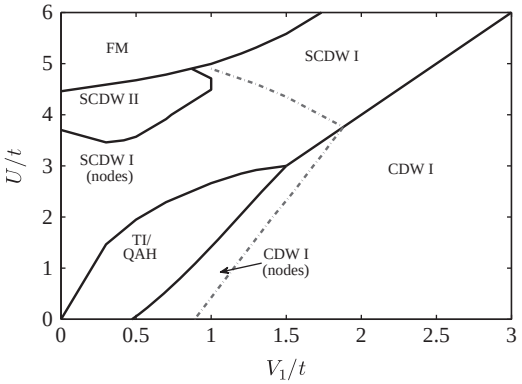

Fig. 9. The U–V_1 phase diagram for $V_2=V_3=0$ at 2/3 filling fraction (quadratic band touching point) in Eq. (14). Note that for small *generic* interactions the leading instability is a topological phase, either TI or the quantum anomalous Hall phase (QAH). From Ref. [124].

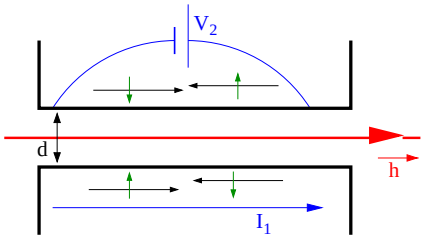

Fig. 10. (Color online) Schematic of a drag measurement between two QSH systems from Ref. [121]. A current I_1 is driven along the upper edge of the lower QSH system and through electron–electron interactions a voltage V_2 is induced in the lower edge of the upper QSH system. A magnetic field $\vec{h}$ is applied in the plane of wires, perpendicular to the spin quantization axis (assumed perpendicular to the plane of QSH systems). Time-reversed Kramer's pairs are indicated for the two edges. A QSH on top of QSH geometry could also be used.

We assume the mean-field solutions are described by a collinear spin alignment and therefore, without loss of generality, we set $\langle c^\dagger_{i\uparrow} c_{i\downarrow}\rangle = \langle c^\dagger_{i\downarrow} c_{i\uparrow}\rangle = 0$ [124]. The further-neighbor interaction is decoupled in a similar way [124]:

$$n_i n_j \approx n_i \langle n_j\rangle + \langle n_i\rangle n_j - \langle n_i\rangle\langle n_j\rangle - \sum_{\alpha\beta}\Big(c^\dagger_{i\alpha}c_{j\beta}\langle c^\dagger_{j\beta}c_{i\alpha}\rangle + \langle c^\dagger_{i\alpha}c_{j\beta}\rangle c^\dagger_{j\beta}c_{i\alpha} - \langle c^\dagger_{i\alpha}c_{j\beta}\rangle\langle c^\dagger_{j\beta}c_{i\alpha}\rangle\Big). \quad (16)$$

The results of the mean-field calculations are shown in Figs. 8 and 9. For a detailed description of the phases appearing in the phase diagrams, see Ref. [124].

The important message we would like to emphasize is that for Dirac points, Fig. 8, topological phases require a critical interaction strength that can be rather large, and appear to require some amount of "fine tuning" [125]. For example, note that $V_1 = 0$ in Fig. 8. On the other hand, when quadratic band touching points are present in the non-interacting band structure, Fig. 9, topological phases can appear as the leading instabilities, without any "fine tuning" of the interactions. Thus, two-dimensional band structures with flat band touching points but small (or even vanishing) spin–orbit coupling are excellent candidates for topological phases [130]. General arguments and functional renormalization group studies (that treat fluctuations) suggest the mean-field results may be reliable and that the TI phase is likely preferred over the quantum anomalous Hall (QAH) state when they are degenerate at the mean-field level [17].

A final point on which we would like to remark concerning interacting topological insulators in two dimensions is how interactions may help identify the phase itself. For example, if two edges of different quantum spin Hall systems are brought close to one another the edges will interact via the Coulomb interactions of the electrons in each edge (See Fig. 10). Under some circumstances, this can lead to novel quasi-one dimensional phases [122]. However, if the interactions are not too strong (the edges are far enough apart), a current driven in one edge will result in a voltage drop along the other edge in the so-called "Coulomb drag" effect [131–137]. The properties of the edge are reflected in the temperature and magnetic field dependence of the drag. For identical edges described by a helical liquid [68,69], the Coulomb drag has a novel magnetic field dependence that is "turned on" in the presence of a time-reversal symmetry breaking magnetic field [121],

$$r_D \propto h^4 T^{4K-3}, \quad (17)$$

where h is the strength of the applied magnetic field and K is the Luttinger parameter of the helical edge system [121]. The role of the finite magnetic field is to open a back-scattering channel for electrons. There is also a weak field dependence of the Luttinger parameter K [121].

3.4. Fractional topological insulators and flat band fractional quantum Hall effect

The discussion in Section 3.2 which related the integer quantum Hall effect to TIs immediately raises the question of whether there is a "fractional" analog to TIs that depends on an intrinsic way on electron–electron interactions in the same way the fractional quantum Hall effect does. In particular, is there a time-reversal invariant topological insulator that is not adiabatically connected to a free electron model? Theoretically, the answer is affirmative [13–15].

In two dimensions, we are guided in a study of fractional topological insulators by the fractional quantum Hall effect. If one has in hand a spinless fermion model that realizes a fractional quantum Hall effect, an S^z conserving, time-reversal invariant model can be straightforwardly constructed by generalizing the Haldane–Kane–Mele correspondence to the interacting case [13,14]. Only very recently has the explicit construction been understood for the non-S^z conserving case (in the presence of Rashba spin–orbit coupling, for example) [15].

A key to understanding lattice models of fractional topological insulators in two dimensions is thus understanding the fractional quantum Hall effect in lattice models. (While this appears necessary, it is not sufficient for constructing a general many-body wavefunction [15,138–141]). For a while, this understanding eluded the community whose picture was based on trial wavefunctions and effective low-energy theories [58], but in the past year important progress has been made.

Attention has focused on a class of insulators with nearly flat bands that possess finite Chern numbers. With a finite Chern number, a partial filling of the flat bands can lead to a fractional quantum Hall effect because interaction energy will always dominate kinetic energy [142]. To date, only a few lattice models have been proposed which are expected to lead to a fractional quantum Hall effect [85,138–141]. The relevant figure of merit in such models is the ratio of the band gap to the bandwidth of the flat band with a finite Chern number. In the model we discuss below, we find this ratio can be as high as 70, which is among the largest in the models reported in the literature thus far [85,138–141].

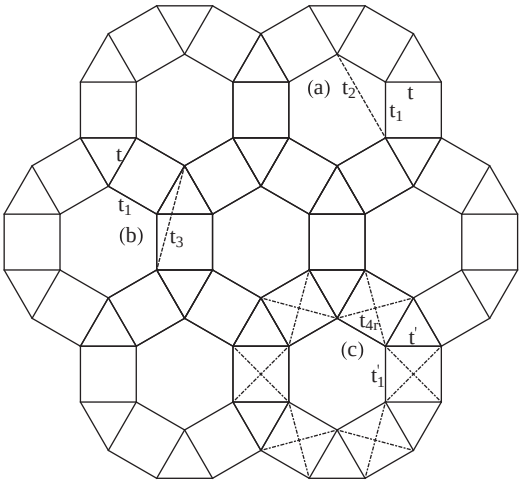

Fig. 11. Schematic of the ruby lattice and illustration of the nearest-neighbor hopping, t,t_1 (real) and t',t_1' (complex), and the three types of "second-neighbor" spin–orbit coupling or hopping indicated by the dashed or dot dashed lines, t_2,t_3 and t_{4r} (from Ref. [85]). (a) The spin–orbit coupling strength t_2 within a hexagon. (b) The spin–orbit coupling strength t_3 within a pentagon composed of one triangle and one square. The hoppings t_2 and t_3 are present on all such bonds of the type shown that are consistent with the symmetry of the lattice. (c) Schematic of the hopping parameters used to obtain a flat band with a finite Chern number and $W/E_g \approx 70$.

We study [85] a simple s-band tight-binding model on the ruby lattice shown in Fig. 11. For fermions with spin, the Hamiltonian is given by $\mathcal{H}=\mathcal{H}_{\text{ruby}}+\mathcal{H}_{\text{ruby-SO}}$, where

$$\mathcal{H}_{\text{ruby}}=-t\sum_{i,j\in\triangle,\sigma}c^{\dagger}_{i\sigma}c_{j\sigma}-t_1\sum_{\triangle\to\triangle,\sigma}c^{\dagger}_{i\sigma}c_{j\sigma} \tag{18}$$

and

$$\mathcal{H}_{\text{ruby-SO}}=it_2\sum_{\langle\langle ij\rangle\rangle,\alpha\beta}v_{ij}s^{z}_{\alpha\beta}c^{\dagger}_{i\alpha}c_{j\beta}+it_3\sum_{\langle\langle ij\rangle\rangle,\alpha\beta}v_{ij}s^{z}_{\alpha\beta}c^{\dagger}_{i\alpha}c_{j\beta} \tag{19}$$

on the ruby lattice shown in Fig. 11. Here $c^{\dagger}_{i\sigma}/c_{i\sigma}$ is the creation/annihilation operator of an electron on site i with spin σ. As indicated in Fig. 11(a,b), t and t_1 are real first-neighbor hopping parameters, and t_2, t_3 are real second-neighbor hoppings (these appear with the imaginary number i in Eq. (19) making the total second-neighbor hopping purely imaginary and time-reversal symmetric). The quantity v_{ij} is equal to 1 if the electron makes a left turn on the lattice links during the second-neighbor hopping, and is equal to -1 if the electron make a right turn during that process. As is clear from Fig. 11, the unit cell of the lattice contains six sites, so six two-fold degenerate bands will result. In addition to the real hopping parameters t,t_1 in Eq. (18), symmetry also allows complex, spin-dependent nearest neighbor hopping with imaginary components t',t_1', as shown in Fig. 11. These parameters lead to a variety of time-reversal invariant phases (including TI) and a rather complex phase diagram [85].

Here we are mainly interested in the spinless case with broken time-reversal symmetry and the hopping parameters described in Fig. 11(c). For spinless fermions we study Eq. (18) with

$$t'=t+i\sigma_z t_i,$$

$$t_1{}'=t_{1r}+i\sigma_z t_{1i}, \tag{20}$$

and add the hopping inside the square in the diagonal directions, labeled t_{4r}. This is shown schematically in Fig. 11(c). A nonzero Chern number and nearly flat band occurs in this case. For example, with $t_i=1.2t,t_{1r}=-1.2t,t_{1i}=2.6t,t_{4r}=-1.2t$ the Chern number is -1 and the gap=$2.398t$, and band width=$0.037t$, which gives $W/E_g\approx 70$, and therefore makes an excellent candidate to realize a fractional topological insulator [85]. The corresponding band structure is shown in Fig. 12(b). The spinless band structure for Eq. (18) with $t'=t=1$ is shown in Fig. 12(a). Note the interesting band crossing/touching points and flat portions of the bands even in this case.

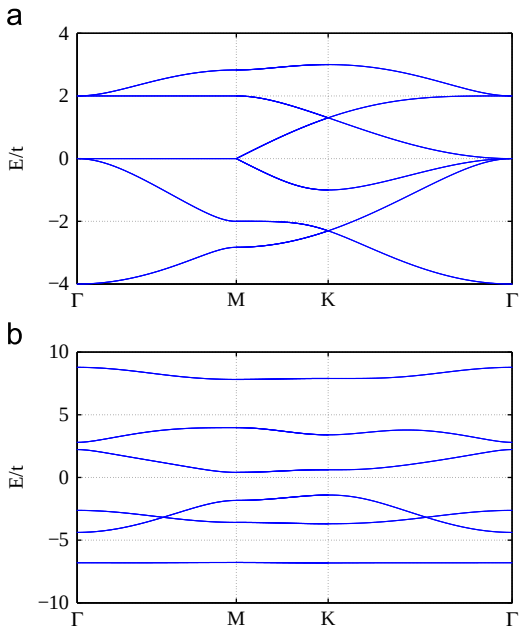

Fig. 12. (a) The energy bands without any spin–orbit coupling and with it tuned on, given by Eq. (18) with $t=t'$ real along high symmetry directions. Note that there is a Dirac point at K for 1/6 and 2/3 filling, and a quadratic band touching point at Γ for 1/2 and 5/6 filling. (The underlying lattice is triangular, as it is for the honeycomb lattice.) Note also the flat bands along the $\Gamma-M$ direction at 1/2 and 5/6 filling. (b) The energy bands with $t_i=1.2t,t_{1r}=-1.2t,t_{1i}=2.6t,t_{4r}=-1.2t$ in Eq. (20). The lowest energy band has Chern number -1. The ratio of the bandwidth to band gap is approximately 70 (from Ref. [85]).

A new direction has emerged in the search for systems with flat bands with conditions favorable to realizing fractional topological insulators or fractional quantum anomalous Hall states—transition metal oxide interfaces [33]. Research in this direction is rapidly evolving with a variety of interesting interaction-driven phases possible [30–32].

As rich as the physics of topological insulators and quantum spin liquids is in two dimensions, the behavior is even richer in three dimensions. This is because the three-dimensional time-reversal invariant topological insulators are qualitatively different from their two-dimensional counter parts, the latter of which can always be viewed as being derived from an underlying quantum Hall effect. The so-called "strong topological" insulators [143] (non-interacting) are an entirely distinct three-dimensional phase with novel response properties [8,51,143–148]. Moreover, once interactions are brought into the picture the physics is richer still. We now turn to three dimensions.

4. Three-dimensional systems

One of the salient features of TIs is that their boundaries possess a topologically protected "metallic" state that is robust to disorder [45,68,69,143,149–151]. Both the two dimensional [116–123] and the three dimensional [8,144–146] boundaries have been shown to exhibit interesting responses to perturbations. In the experimental literature on TIs, the three dimensional systems have dominated. The weakly interacting nature of topological insulators has enabled accurate predictions based on density functional theory [78,147,152,153] for a wide range of two and three dimensional systems [138,154–167], and experiment has followed with confirming data in a large and rapidly growing number of instances [79,80,168–177]. There are also theoretical predictions for systems closely related to TIs with Weyl fermions in their bulk and unusual boundary excitations [32,178–182], as well as crystalline topological insulators [183].

In this section we will describe systems that are too strongly interacting to allow a naive application of density functional theory. On the most exotic side, three-dimensional versions of exotic fractional topological insulators with a non-trivial ground state degeneracy have been proposed [184–187]. For interacting systems treated at the mean-field level, a spontaneous generation of spin–orbit coupling (with topological defects possible) can occur, similar to two dimensions [125].

Here, we will focus on semi-realistic models that are motivated by the physics of transition metal oxides, famous in recent years for high-temperature superconductivity [188,189] and colossal magnetoresistance [190]. These materials typically involve 3d orbitals on the transition metals and lead to strong Coulomb interactions due to their localized nature (compared to 4d and 5d orbitals). However, 4d and 5d orbitals in layered perovskites such as Sr_2RuO_4, Sr_2RhO_4, Sr_2IrO_4, Na_2IrO_3, and the hyperkagome $Na_4Ir_3O_8$ are more spatially extended and thus the Coulomb interaction is typically weaker than those with 3d orbitals [191]. The hyperkagome $Na_4Ir_3O_8$ is an important three-dimensional quantum spin liquid candidate [192–196].

The more extended nature of the 4d and 5d orbitals compared to the 3d orbitals leads to a greater level splitting in a crystal field,

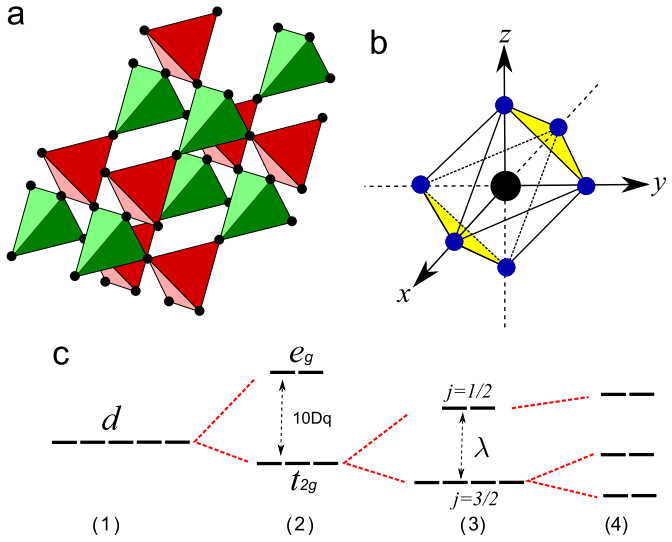

Fig. 13. From Ref. [27]. (a) An illustration of the pyrochlore lattice which is composed of corner sharing tetrahedra. Transition elements are indicated by black solid circles. (b) Each transition ion is surrounded by an oxygen octahedron shown by six solid blue (dark grey) circles. A transition ion is located at the origin of the local coordinate and is shown in black. We study a trigonal distortion preserving C_3 symmetry applied along the [1 1 1] direction (or its equivalent), shown by two yellow (grey) faces, and an elongation preserving C_4 symmetry along the z-axis of the local coordinate. (c) A schematic representation of the splitting of the bare atomic d-levels (1), due to a cubic crystal field arising from the octahedral environment (2), unquenched spin–orbit coupling in the t_{2g} manifold (3), and a distortion of the octahedron (4). The values of the splittings in (4) depend on λ and $\Delta_{3,4}$.

and enhances their sensitivity to lattice distortions [197]. In many oxides, the transition ions are surrounded by an octahedron of oxygen atoms, MO_6, where M represents a transition metal ion. The crystal field splits the five degenerate (neglecting spin for the moment) d-orbitals into two manifolds (see Fig. 13c): a lower lying t_{2g} (d_{xy},d_{yz},d_{zx}) manifold and a higher lying e_g ($d_{3z^2-r^2}$,$d_{x^2-y^2}$) manifold [198,199]. The energy separation between the t_{2g} and e_g levels is conventionally denoted "10Dq" and is typically on the order of $\sim 1-4$ eV, which is large compared to many 3d compounds [200].

Besides the crystal field, the relativistic spin–orbit coupling is another energy scale that results from the large atomic numbers of heavy transition elements. While in the absence of spin–orbit coupling the on-site Coulomb interaction is of the same order as the band width [201,202], inclusion of strong spin–orbit coupling modifies the relative energy scales [203]. Thus, for materials with 4d and particularly 5d electrons, one expects the appearance of novel phases with unconventional electronic structure and order due to the characteristic energy of spin–orbit coupling approaching that of the Coulomb interactions [27,203,204].

In this section we focus on the interplay and competition between strong correlation effects, spin–orbit coupling, and lattice distortion that is expected to be important in heavy transition metal oxides with a pyrochlore lattice [27]. In the heavy transition metal oxides one expects both the spin–orbit coupling [205,206] and the lattice distortion energies [197,207] to be of the order of 0.05–0.5 eV, while the interaction energy is typically at the higher end of this scale to somewhat larger, 0.5–2 eV [178,179,205]. While the phase diagram of an interacting undistorted pyrochlore model with $j=1/2$ has already been studied [203], we expand those results to include the effects of distortions of the local octahedra on the phase diagram [27].

We also investigate pyrochlore oxides at different d-level fillings with the Fermi energy lying in the quadruplet $j=3/2$ manifold, which has not been considered in previous works [27]. One of our motivations is to see if the $j=3/2$ manifold can also realize the interesting Mott phases of the $j=1/2$ manifold [203]. We find that, indeed, these exotic phases can be realized for the $j=3/2$ manifold. Moreover, we find that for the $j=1/2$ manifold "weak" topological variants of the exotic Mott phases can also appear in the phase diagram when certain types of lattice distortion are present.

To study the effects of lattice deformations [197,208], we assume that the octahedron surrounding an ion can be distorted in two ways: (1) a trigonal distortion preserving local C_3 symmetry and (2) an elongation (expansion) of octahedra preserving local C_4 symmetry. (See Fig. 13b.) The former has been argued to be rather common and can be described by the following Hamiltonian on each transition metal ion site [197]:

$$\mathcal{H}_{tri} = -\Delta_3(d^\dagger_{yz}d_{zx} + d^\dagger_{yz}d_{xy} + d^\dagger_{zx}d_{xy}) + \text{H.c.}, \tag{21}$$

where Δ_3 parameterizes the strength and sign of the C_3 preserving distortion, and the C_4 elongation/contraction splitting is described by [204]

$$\mathcal{H}_{el} = \Delta_4 l_z^2 = \Delta_4(n_{yz} + n_{zx}), \tag{22}$$

where Δ_4 parametrizes the strength and sign of the distortion, and l_z is the z component of the effective angular momentum of the t_{2g} orbitals related to the occupation of the d_{xy} orbital by $n_{xy} = n_d - (l_z)^2$ which follows from the constraint $n_d = n_{xy} + n_{yz} + n_{zx}$ [204]. For an elongation of the tetrahedron, $\Delta_4 < 0$, and for a compression of the tetrahedron, $\Delta_4 > 0$. Trigonal distortions appear to be more common in real materials, and the magnitude of the energy splittings can be crudely estimated from density functional theory calculations based on X-ray determined positions of oxygen atoms around the transition metals. We are not aware of detailed calculations of this type for the 4d and 5d pyrochlore oxides, but closely related 3d systems appear to have splittings on the level of 0.01–0.5 eV [207]. We take this as crude estimate, with the larger end of the energy scale probably more likely for the more extended 4d and 5d orbitals.

Thus, the local Hamiltonian describing the t_{2g} orbitals on each site is

$$\mathcal{H}_{local} = \mathcal{H}_{so} + \mathcal{H}_{tri} + \mathcal{H}_{el}, \tag{23}$$

with

$$\mathcal{H}_{so} = -\lambda l \cdot s, \tag{24}$$

where $l=1$ and $s=1/2$ describe the orbital and spin degrees of freedom, and $\lambda > 0$ parameterizes the strength of the spin–orbit coupling. That the t_{2g} orbitals can be effectively described by angular momentum $l=1$ comes from the projection of the d-orbital angular momentum into the local basis of t_{2g} manifold [203,204].

The Hamiltonian (23) can be easily diagonalized and its eigenvectors describe a projection onto the spin–orbit plus distortion basis. We will denote the projection by a matrix M, which contains all the information about the spin–orbit coupling and the distortion of the octahedra (all assumed identical so translational invariance is preserved). Moreover, due to the presence of time-reversal symmetry, the eigenvectors form Kramers pairs. A schematic representation of splitting t_{2g} upon including the terms in Eq. (23) is shown in Fig. 13c.

We now turn to a derivation of the effective Hamiltonian. We first assume $\lambda = \Delta_3 = \Delta_4 = 0$, *i.e.* neglect the contributions in Eq. (23). To obtain the kinetic terms of the Hamiltonian, we need to describe the t_{2g} orbitals of a single ion in the local coordinate system defined by the octahedron of oxygen atoms surrounded the ion, and we need the p-orbitals of oxygen in the global coordinate system [203]. The hopping of electrons from one transition metal ion to a nearest-neighbor transition metal ion is mediated by the oxygen p-orbitals. (We note that for the

relatively extended 5d orbitals direct overlap may also be important, as well as further neighbor hopping [209].) We thus compute the p–d overlaps to determine the hopping matrix elements. The local and global axes are related by a set of rotation matrices [197,203]. The combination of rotation matrices and d–p overlaps gives rise to the following Hamiltonian:

$$\mathcal{H}_d = \varepsilon_d \sum_{i\gamma\sigma} d^\dagger_{i\gamma\sigma} d_{i\gamma\sigma} + t \sum_{\langle i\gamma\sigma, i'\gamma'\sigma'\rangle} T^{ii'}_{\gamma\sigma,\gamma'\sigma'} d^\dagger_{i\gamma\sigma} d_{i'\gamma'\sigma'}, \tag{25}$$

where i, γ, and σ in the sums run over lattice sites, t_{2g} orbitals (xy,yz,zx), and spin degrees of freedom, respectively. The ε_d stands for the on-site energy of the degenerate t_{2g} orbitals, and $t = V^2_{pd\pi}/(\varepsilon_p - \varepsilon_d)$ is the unrotated hopping amplitude depending on the overlap integral $V_{pd\pi}$ and the energy difference between p and d orbitals. The parameter t sets the basic hopping energy scale in the problem. Without loss of generality we set $\varepsilon_d = 0$.

The effect of spin–orbit coupling and distortion are included via the projection of Hamiltonian in Eq. (25) into the eigenvectors of the local Hamiltonian in Eq. (23) using matrix M as follows:

$$\mathcal{H}_{\text{pyro}} = \sum_{i\alpha} \upsilon_\alpha c^\dagger_{i\alpha} c_{i\alpha} + t \sum_{\langle i\alpha, i'\alpha'\rangle} \Gamma^{ii'}_{\alpha,\alpha'} c^\dagger_{i\alpha} c_{i'\alpha'}, \tag{26}$$

where υ_α ($\alpha = 1,\ldots,6$) stands for the six eigenvalues of local Hamiltonian (23), and the matrix Γ describes the hopping between sites given in the local basis via $\Gamma = M^* T M^T$. The $c^\dagger_{i\alpha}(c_{i\alpha})$ is the creation (annihilation) operator of an electron at site i and in local state α. Finally, we add a Coulomb interaction to obtain

$$\mathcal{H} = \mathcal{H}_{\text{pyro}} + \frac{U}{2} \sum_i \left(\sum_\alpha c^\dagger_{i\alpha} c_{i\alpha} - n_d \right)^2, \tag{27}$$

where U is the on-site Coulomb interaction and n_d is the number of electrons on the 5d orbital of the transition metal ion. In the remainder of this section, we investigate the zero-temperature phase diagram of the full Hamiltonian (27), which includes the spin–orbit coupling and lattice distortions in Eq. (23). A full description of our results is given in Ref. [27].

We apply the slave-rotor mean-field theory developed by Florens and Georges [25,26] to treat the effect of weak to intermediate strength Coulomb interactions in the regime where the charge fluctuations remain important. In this theory each electron operator is represented in terms of a collective phase, conjugate to charge, called a rotor and an auxiliary fermion called a spinon as

$$c_{i\alpha} = e^{i\theta_i} f_{i\alpha}, \tag{28}$$

where $c_{i\alpha}$ is the electron destruction operator at site i with quantum number α, representing the states in Eq. (27). The factor $e^{i\theta_i}$ acting on the charge sector is a rotor lowering operator (with θ_i a bosonic field), and $f_{i\alpha}$ is the fermionic spinon operator. The product of the two results in an object with fermi statistics, needed for the electron. Note the rotor part only carries the charge degree of freedom while the spinon part carries the remaining degrees of freedom α. Therefore, an electron has natural spin-charge separation if α is spin in this representation. Substituting Eq. (28) into Eq. (27) and applying mean-field theory results in the phase diagrams shown in Figs. 14 and 15 [27]. The two to three dimensional crossover and issues associated with gauge fluctuations beyond mean-field theory have been discussed in Ref. [210]. The method correctly recovers the $U \to 0$ limit in mean-field theory.

There are several features that are important to emphasize. First, we have identified a new phase—the weak topological Mott insulator (WTMI)—in the regions shown in Fig. 14(b) [27]. This phase is expected to have gapless thermal transport *without charge transport* along a certain class of topological defects, as described in Ref. [28]. Also, we expect a rather rich phenomenology in the spin sector of WTMIs, similar to that recently

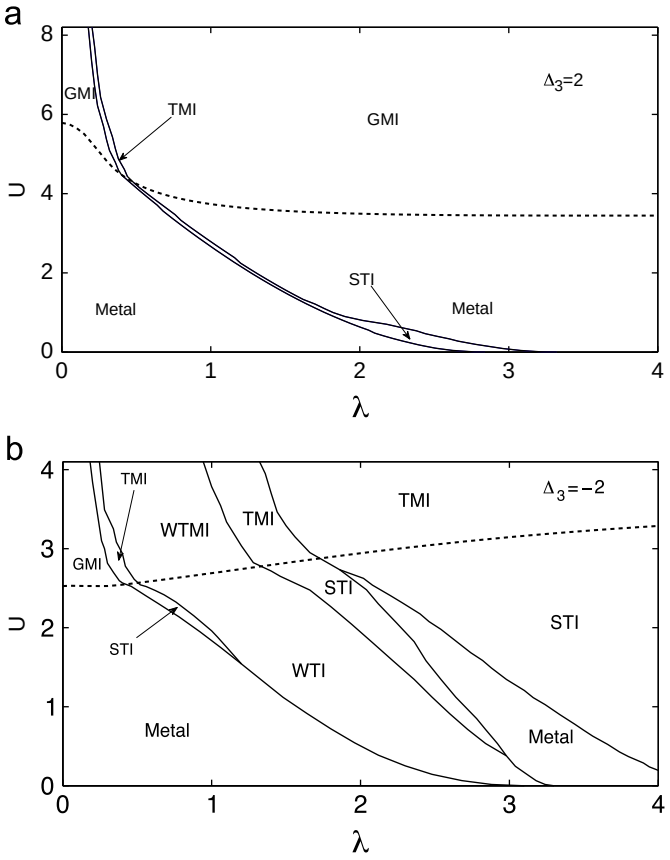

Fig. 14. Phase diagram of the $j = 1/2$-band model corresponding to $n_d = 5$ with positive $\Delta_3 = 2t$ (upper panel) and negative trigonal distortion $\Delta_3 = -2t$ (lower panel). The dashed line separates the rotor condensed phases (below) from the uncondensed phases (above). We set $t = 1$, and the phases labeled are as follows: strong topological insulator (STI), weak topological insulator (WTI), gapless Mott insulator (GMI), topological Mott insulator (TMI), weak topological Mott insulator (WTMI) and metallic phases. From Ref. [27].

emphasized in weak topological insulators (WTI) [211]. Second, it is clear from Fig. 14 that the sign of the trigonal distortion makes a big difference in the complexity of the phase diagram, with the negative trigonal distortion producing a more interesting phase diagram. Third, comparing Figs. 14 and 15 one sees that the $j = 1/2$ and $j = 3/2$ manifolds behave differently for the same distortion. Fourth, the lower panel of Fig. 15 shows the phase diagram in the distortion–spin–orbit coupling plane. The distortion axis can be viewed as a pressure axis. Thus, the application of pressure to transitional metal oxides can drive the system through a complex set of phases, some of which are topological. This is potentially a useful experimental parameter when searching for some of the exotic phases predicted here.

Our slave rotor results make a natural connection to quantum spin liquids in three dimensions described by fermionic excitations: *All the phases above the dashed lines in Figs.*14 and 15 *are time-reversal invariant spin liquids.* These phases have fully gapped charge degrees of freedom and spin degrees of freedom described by the fermionic spinons "$f_{i\alpha}$" in Eq. (28). At the mean-field level, the spinons have an associated band structure that can either be gapped and topological (like a TI) or gapless (like a metal). Thus, the spin sector has an intrinsic single-particle-like nature imposed on it by the formalism. Relaxing this assumption is one of the ingredients needed to obtain the most exotic fractionalized topological insulators in three dimensions [184–187]. Indeed, a fruitful approach to studying and/or discovering exotic fractionalized topological insulators in three dimensions may be to deepen our understanding of quantum spin liquids in three dimensions,

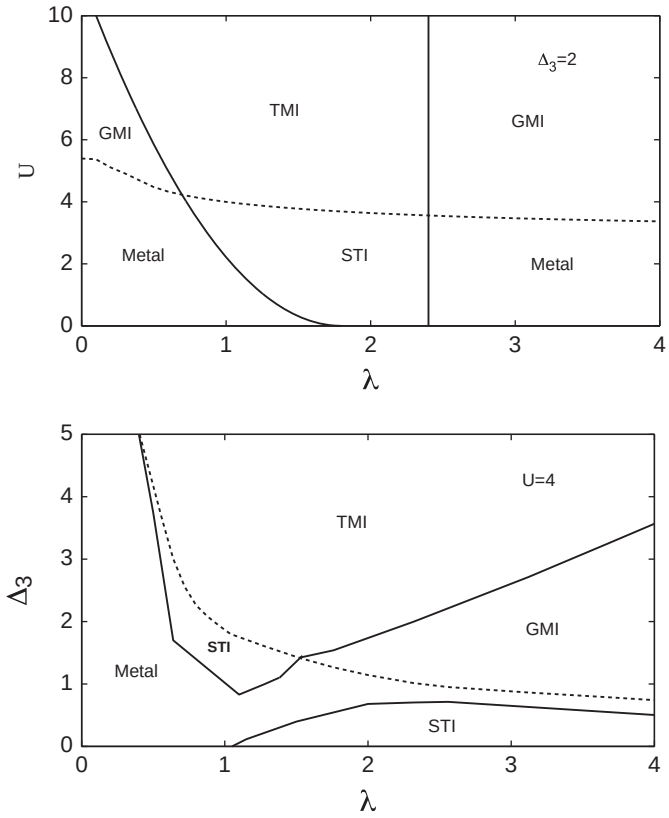

Fig. 15. Phase diagram of the $j=3/2$ band model with $n_d=3$, including the trigonal distortion of the octahedra. The labeling of the phases is the same as that used in Fig. 14. In the upper panel $\Delta_3=2t$. In the lower panel the interaction is fixed at $U=4t$ and the strength Δ_3 of the trigonal distortion is varied, illustrating possible phases that may arise upon the application of pressure to a real system. All energies are expressed in units of t. In both phase diagrams the dashed line separates the rotor uncondensed phase (above) from the condensed phase (below). We note the "pocket" of STI around $\lambda\approx 1, \Delta_3\approx 1.5$ in the lower figure has a numerically difficult to determine boundary with the metallic phase; we have present our best assessment. From Ref. [27].

particularly those whose spinons are strongly correlated and not well described within a single-particle formalism [186]. In a gapless system, these would be "algebraic spin liquids" [4]. One could then "add back" the charge degrees of freedom to obtain an exotic topological insulator [27]. However, it should be emphasized that correspondences between TIs and QSLs described in this paper have all been between QSLs with excitations described by fermions. At the moment, it remains unclear how to relate spin liquids described by bosonic excitations (Schwinger bosons) to the topological insulators, although some interesting parallels have been noted [212].

5. Conclusions

In this work, we have emphasized connections between topological insulators and quantum spin liquids from a variety of viewpoints, with an emphasis on their common topological structure. We have described results from one, two, and three dimensional systems. In one-dimension we have emphasized the important role that quantum entanglement, particularly the entanglement spectrum, can play in studying and classifying phases.

In two dimensions, we have demonstrated the Kitaev–Haldane–Kane–Mele correspondence and shown how it can play a useful role in finding topological insulators and interesting quantum spin liquids. In interacting systems we have described the different roles Dirac points and quadratic band crossing points play in the instability to spontaneously generated topological phases, even when there is no intrinsic spin–orbit coupling. We have given an example of a lattice model of spinless fermions that possesses a very flat band with a finite Chern number. This model and related ones can be used to help guide the discovery of fractional topological insulators in two dimensions. We have also emphasized transition metal oxide interfaces as a promising experimental system for the realization of interaction-driven topological phases.

In three dimensions, we have focused on semi-realistic models appropriate for transition metal oxides with 4d and 5d electrons. We have studied the interplay of distortion, interactions, and spin–orbit coupling and presented rich phase diagrams for different d-shell fillings. We have also found a new phase, the "weak topological Mott insulator", which is expected to reveal itself via topologically protected gapless modes along certain classes of defects [28].

Looking ahead, it is clear that two of the chief challenges with three-dimensional TIs (which are most likely to appear in applications) are sample quality and reliable tunability [29]. To date, the most pressing issue is to obtain samples that have a highly insulating bulk (so that most electrical conductance is along the boundary). In recent months important advances have been made on this front. Both Bi_2Te_2Se [213,214] and $Bi_{1.5}Sb_{0.5}Te_{1.7}Se_{1.3}$ [215,216] are reported to have more than 70% of their conductivity on the surface, and there are indications that TI "work horses" like Bi_2Se_3 are improving in quality, too [217].

In the regime of very strong electron interactions (beyond where the slave-rotor formalism should apply), magnetic phases with broken time-reversal symmetry become more likely [203]. When spin–orbit coupling is strong in this regime, exotic, conventionally ordered phases are also expected to appear [195,196,204,218], including spin–orbital liquid states [219,220]. It seems likely that the new-found capability to engineer gauge fields in cold-atom systems will play a role in our understanding of TIs and QSLs, too [221–226]. Many novel behaviors certainly await identification, and keeping in mind the "connections" between various topological phases seems a good strategy to help guide discovery.

Acknowledgments

We gratefully acknowledge helpful discussions with numerous colleagues, including Xiang Hu, Hong Yao, and C.-C. Joseph Wang who collaborated with us on some of the work presented here, and funding from ARO Grant W911NF-09-1-0527 and NSF Grant DMR-0955778. G.A.F. is grateful for support from the Banff International Research Station where an abbreviated version of this manuscript was presented in the form of a talk. The authors acknowledge the Texas Advanced Computing Center (TACC) at The University of Texas at Austin for providing computing resources that have contributed to the research results reported within this paper. URL: http://www.tacc.utexas.edu

References

[1] X.-L. Qi, S.-C. Zhang, Physics Today 63 (2010) 33.
[2] J.E. Moore, Nature 464 (2010) 194.
[3] M.Z. Hasan, C.L. Kane, Reviews of Modern Physics 82 (2010) 3045.
[4] L. Balents, Nature 464 (2010) 199.
[5] X.-G. Wen, Quantum Field Theory of Many-Body Systems, Oxford, New York, 2004.
[6] R.B. Laughlin, Reviews of Modern Physics 71 (1999) 863.
[7] W.P. Su, J.R. Schrieer, A.J. Heeger, Physical Review Letters 42 (June) (1979) 1698.
[8] X.-L. Qi, T.L. Hughes, S.-C. Zhang, Physical Review B 78 (2008) 195424.

[9] X.-L. Qi, T.L. Hughes, S.-C. Zhang, Nature Physics 4 (2008) 273.
[10] A. Kitaev, Annals of Physics 303 (2003) 2.
[11] A. Kitaev, Annals of Physics 321 (2006) 2.
[12] D.-H. Lee, G.-M. Zhang, T. Xiang, Physical Review Letters 99 (2007) 196805.
[13] B.A. Bernevig, S.-C. Zhang, Physical Review Letters 96 (2006) 106802.
[14] M. Levin, A. Stern, Physical Review Letters 103 (November) (2009) 196803.
[15] X.-L. Qi, Physical Review Letters 107 (2011) 126803.
[16] Y.-M. Lu, Y. Ran, Symmetry protected fractional Chern insulators and fractional topological insulators, 2011, ⟨arXiv:1109.0226⟩.
[17] S. Raghu, X.-L. Qi, C. Honerkamp, S.-C. Zhang, Physical Review Letters 100 (2008) 156401.
[18] V. Chua, H. Yao, G.A. Fiete, Physical Review B 83 (2011) 180412.
[19] V. Chua, G.A. Fiete, Physical Review B 84 (2011) 195129. doi:10.1103/PhysRevB.84.195129.
[20] J. Li, R.-L. Chu, J.K. Jain, S.-Q. Shen, Physical Review Letters 102 (2009) 136806.
[21] C.W. Groth, M. Wimmer, A.R. Akhmerov, J. Tworzydło, C.W.J. Beenakker, Physical Review Letters 103 (2009) 196805.
[22] E. Prodan, Physical Review B 83 (2011) 195119.
[23] H.-M. Guo, G. Rosenberg, G. Refael, M. Franz, Physical Review Letters 105 (2010) 216601.
[24] E. Prodan, T.L. Hughes, B.A. Bernevig, Physical Review Letters 105 (2010) 115501.
[25] S. Florens, A. Georges, Physical Review B 66 (October) (2002) 165111.
[26] S. Florens, A. Georges, Physical Review B 70 (July) (2004) 035114.
[27] M. Kargarian, J. Wen, G.A. Fiete, Physical Review B 83 (2011) 165112.
[28] Y. Ran, Y. Xhang, A. Vishwanath, Nature Physics 5 (2009) 298.
[29] G.A. Fiete, Science 332 (2011) 546.
[30] A. Rüegg, G.A. Fiete, Physical Review B 84 (2011) 201103. doi:10.1103/PhysRevB.84.201103.
[31] F. Wang, Y. Ran, Phys. Rev. B 84 (2011) 241103. doi:10.1103/PhysRevB.84.241103.
[32] K.-Y. Yang, W. Zhu, D. Xiao, S. Okamoto, Z. Wang, Y. Ran, Phys. Rev. B 84 (2011) 201104. doi:10.1103/PhysRevB.84.201104.
[33] D. Xiao, W. Zhu, Y. Ran, N. Nagaosa, S. Okamoto Nature Communications 2 (2011) 596, doi:10.138/ncomms1602.
[34] G.E. Volovik, The Universe in a Helium Droplet, Clarendon Press, Oxford, 2003.
[35] T.H. Hansson, V. Oganesyan, S.L. Sondhi, Annals of Physics 313 (2004) 497.
[36] T. Giamarchi, Quantum Physics in One Dimension, Clarendon Press, Oxford, 2004.
[37] A.O. Gogolin, A.A. Nersesyan, A.M. Tsvelik, Bosonization and Strongly Correlated Systems, Cambridge University Press, Cambridge, England, 1998.
[38] F.D.M. Haldane, Journal of Physics C 14 (1981) 2585.
[39] G.A. Fiete, Reviews of Modern Physics 79 (2007) 801.
[40] G.A. Fiete, Journal of Physics: Condensed Matter 21 (2009) 193201.
[41] A.E. Feiguin, G.A. Fiete, Physical Review Letters 106 (2011) 146401.
[42] S. Ryu, A.P. Schnyder, A. Furusaki, A.W.W. Ludwig, New Journal of Physics 12 (2010) 065010.
[43] A. Kitaev, Periodic table for topological insulators and superconductors, 2009, ⟨arXiv:0901.2686⟩.
[44] A. Altland, M.R. Zirnbauer, Physical Review B 55 (1997) 1142.
[45] A.P. Schnyder, S. Ryu, A. Furusaki, A.W.W. Ludwig, Physical Review B 78 (2008) 195125.
[46] L. Fidkowski, A. Kitaev, Physical Review B 81 (2010) 134509.
[47] L. Fidkowski, A. Kitaev, Physical Review B 83 (2011) 075103.
[48] V. Gurarie, Physical Review B 83 (2011) 085426.
[49] G.D. Mahan, Many-Particle Physics, 2nd ed., Plenum Press, New York, 1990.
[50] W.-K. Tse, A.H. MacDonald, Physical Review Letters 105 (2010) 057401.
[51] G. Rosenberg, M. Franz, Physical Review B 82 (2010) 035105.
[52] J. Eisert, M. Cramer, M.B. Plenio, Reviews of Modern Physics 82 (2010) 277.
[53] L. Amico, R. Fazio, A. Osterloh, V. Vedral, Reviews of Modern Physics 80 (2008) 517.
[54] G. Vidal, J.I. Latorre, E. Rico, A. Kitaev, Physical Review Letters 90 (2003) 227902.
[55] A. Kitaev, J. Preskill, Physical Review Letters 96 (2006) 110404.
[56] M. Levin, X.-G. Wen, Physical Review Letters 96 (2006) 110405.
[57] H. Li, F.D.M. Haldane, Physical Review Letters 101 (2008) 010504.
[58] C. Nayak, S.H. Simon, A. Stern, M. Freedman, S. Das Sarma, Reviews of Modern Physics 80 (2008) 1083.
[59] A. Ruegg, G.A. Fiete, Phys. Rev. Lett. 108 (2012) 046401. doi:10.1103/PhysRevLett.108.046401.
[60] A.M. Turner, Y. Zhang, A. Vishwanath, Physical Review B 82 (2010) 241102.
[61] A. M. Turner, Y. Zhang, A. Vishwanath, Band topology of insulators via the entanglement spectrum, 2009, ⟨arXiv:0909.3119⟩.
[62] M. Kargarian, G.A. Fiete, Physical Review B 82 (2010) 085106.
[63] T.L. Hughes, E. Prodan, B.A. Bernevig, Physical Review B 83 (2011) 245132.
[64] R. Thomale, A. Sterdyniak, N. Regnault, B.A. Bernevig, Physical Review Letters 104 (2010) 180502.
[65] L. Fidkowski, Physical Review Letters 104 (2010) 130502.
[66] A. Chandran, M. Hermanns, N. Regnault, B. Bernevig, Phys. Rev. B 84 (2011) 205136. doi:10.1103/PhysRevB.84.205136.
[67] X.-L. Qi, H. Katsura, A. Ludwig, General relationship between the entanglement spectrum and the edge state spectrum of topological quantum states, 2011, ⟨arXiv:1103.5437⟩.
[68] C. Wu, B.A. Bernevig, S.-C. Zhang, Physical Review Letters 96 (2006) 106401.
[69] C. Xu, J.E. Moore, Physical Review B 73 (2006) 045322.
[70] L. Fu, C.L. Kane, Physical Review B 74 (2006) 195312.
[71] A.M. Turner, F. Pollmann, E. Berg, Physical Review B 83 (2011) 075102.
[72] F.D.M. Haldane, Physical Review Letters 50 (1983) 1153.
[73] M. den Nijs, K. Rommelse, Physical Review B 40 (1989) 4709.
[74] T. Kennedy, H. Tasaki, Physical Review B 45 (1992) 304.
[75] F. Pollmann, A.M. Turner, E. Berg, M. Oshikawa, Physical Review B 81 (2010) 064439.
[76] R. Thomale, D.P. Arovas, B.A. Bernevig, Physical Review Letters 105 (2010) 116805.
[77] X. Chen, Z.-C. Gu, X.-G. Wen, Physical Review B 83 (2011) 035107.
[78] B.A. Bernevig, T.L. Hughes, S.-C. Zhang, Science 314 (2006) 1757.
[79] M. König, S. Wiedmann, C. Brune, A. Roth, H. Buhmann, L. Molenkamp, X.-L. Qi, S.-C. Zhang, Science 318 (2007) 766.
[80] A. Roth, C. Brüne, H. Buhmann, L.W. Molenkamp, J. Maciejko, X.-L. Qi, S.-C. Zhang, Science 325 (2009) 294.
[81] C.L. Kane, E.J. Mele, Physical Review Letters 95 (2005) 146802.
[82] C.L. Kane, E.J. Mele, Physical Review Letters 95 (2005) 226801.
[83] F.D.M. Haldane, Physical Review Letters 61 (1988) 2015.
[84] A. Rüegg, J. Wen, G.A. Fiete, Physical Review B 81 (2010) 205115.
[85] X. Hu, M. Kargarian, G.A. Fiete, Physical Review B 84 (2011) 155116. doi:10.1103/PhysRevB.84.155116.
[86] K. Sun, H. Yao, E. Fradkin, S.A. Kivelson, Physical Review Letters 103 (2009) 046811.
[87] H.-M. Guo, M. Franz, Physical Review B 80 (2009) 113102.
[88] C. Weeks, M. Franz, Physical Review B 82 (2010) 085310.
[89] V. Kalmeyer, R.B. Laughlin, Physical Review Letters 59 (1987) 2095.
[90] H. Yao, S.A. Kivelson, Physical Review Letters 99 (2007) 247203.
[91] G. Kells, D. Mehta, J.K. Slingerland, J. Vala, Physical Review B 81 (2010) 104429.
[92] F. Wang, Physical Review B 81 (May) (2010) 184416.
[93] G. Jackeli, G. Khaliullin, Physical Review Letters 102 (January) (2009) 017205.
[94] E.H. Lieb, Physical Review Letters 73 (1994) 2158.
[95] H. Yao, S.-C. Zhang, S.A. Kivelson, Physical Review Letters 102 (May) (2009) 217202.
[96] C. Wu, D. Arovas, H.-H. Hung, Physical Review B 79 (2009) 134427.
[97] G.-W. Chern, Physical Review B 81 (March) (2010) 125134.
[98] S. Ryu, Physical Review B 79 (February) (2009) 075124.
[99] S. Mandal, N. Surendran, Physical Review B 79 (January) (2009) 024426.
[100] G. Baskaran, G. Santhosh, R. Shankar, Exact quantum spin liquids with fermi surfaces in spin-half models, 2009, ⟨arXiv:0908.1614⟩.
[101] K.S. Tikhonov, M.V. Feigel'man, Physical Review Letters 105 (2010) 067207.
[102] S. Murakami, N. Nagosa, S.C. Zhang, Physical Review B 69 (2004) 235206.
[103] W. DeGottardi, D. Sen, S. Vishveshwara, New Journal of Physics 13 (2011) 065028.
[104] T. Grover, T. Senthil, Physical Review Letters 100 (2008) 156804.
[105] X.-L. Qi, T.L. Hughes, S. Raghu, S.-C. Zhang, Physical Review Letters 102 (2009) 187001.
[106] M. Sato, S. Fujimoto, Physical Review B 79 (2009) 094504.
[107] A.P. Schnyder, S. Ryu, A.W.W. Ludwig, Physical Review Letters 102 (2009) 196804.
[108] L. Huijse, N. Moran, J. Vala, K. Schoutens, Physical Review B 84 (2011) 115124.
[109] Z.Y. Meng, T.C. Lang, S. Wessel, F.F. Assaad, A. Muramatsu, Nature 464 (2010) 847.
[110] M. Hohenadler, T.C. Lang, F.F. Assaad, Physical Review Letters 106 (2011) 100403.
[111] W. Wu, S. Rachel, W.-M. Liu, K. Le Hur, Quantum spin hall insulators with interactions and lattice anisotropy, 2011, ⟨arXiv:1106.0943⟩.
[112] D. Zheng, C. Wu, G.-M. Zhang, Phys. Rev. B 84 (2011) 205121. doi:10.1103/PhysRevB.84.205121.
[113] Y. Yamaji, M. Imada, Physical Review B 83 (2011) 205122.
[114] S.-L. Yu, X.C. Xie, J.-X. Li, Physical Review Letters 107 (2011) 010401.
[115] C.N. Varney, K. Sun, M. Rigol, V. Galitski, Physical Review B 82 (September) (2010) 115125.
[116] A. Ström, H. Johannesson, Physical Review Letters 102 (2009) 096806.
[117] C.-Y. Hou, E.-A. Kim, C. Chamon, Physical Review Letters 102 (2009) 076602.
[118] C. Xu, L. Fu, Physical Review B 81 (2010) 134435.
[119] J.C.Y. Teo, C.L. Kane, Physical Review B 79 (2009) 235321.
[120] K.T. Law, C.Y. Seng, P.A. Lee, T.K. Ng, Physical Review B 81 (2010) 041305.
[121] V.A. Zyuzin, G.A. Fiete, Physical Review B 82 (2010) 113305.
[122] Y. Tanaka, N. Nagaosa, Physical Review Letters 103 (2009) 166403.
[123] J. Maciejko, C. Liu, Y. Oreg, X.-L. Qi, C. Wu, S.-C. Zhang, Physical Review Letters 102 (2009) 256803.
[124] J. Wen, A. Rüegg, C.-C.J. Wang, G.A. Fiete, Physical Review B 82 (2010) 075125.
[125] Y. Zhang, Y. Ran, A. Vishwanath, Physical Review B 79 (2009) 245331.
[126] Q. Liu, H. Yao, T. Ma, Physical Review B 82 (2010) 045102.
[127] A. Rüegg, G.A. Fiete, Physical Review B 83 (2011) 165118.
[128] A.H. Castro Neto, F. Guinea, N.M.R. Peres, K.S. Novoselov, A.K. Geim, Reviews of Modern Physics 81 (January) (2009) 109.
[129] S. Rachel, K. Le Hur, Physical Review B 82 (2010) 075106.
[130] F. Zhang, J. Jung, G.A. Fiete, Q. Niu, A.H. Mac-Donald, Physical Review Letters 106 (2011) 156801.
[131] V.V. Ponomarenko, D.V. Averin, Physical Review Letters 85 (2000) 4928.
[132] V. Yakovenko, JETP 56 (1992) 510.
[133] R. Klesse, A. Stern, Physical Review B 62 (2000) 16912.
[134] T. Fuchs, R. Klesse, A. Stern, Physical Review B 71 (2005) 045321.

[135] M. Pustilnik, E.G. Mishchenko, L.I. Glazman, A.V. Andreev, Physical Review Letters 91 (2003) 126805.
[136] D.N. Aristov, Physical Review B 76 (2007) 085327.
[137] G.A. Fiete, K. Le Hur, L. Balents, Physical Review B 73 (2006) 165104.
[138] J. Wang, R. Li, S.-C. Zhang, X.-L. Qi, Physical Review Letters 106 (2011) 126403.
[139] K. Sun, Z. Gu, H. Katsura, S. Das Sarma, Physical Review Letters 106 (2011) 236803.
[140] T. Neupert, L. Santos, C. Chamon, C. Mudry, Physical Review Letters 106 (2011) 236804.
[141] E. Tang, J.-W. Mei, X.-G. Wen, Physical Review Letters 106 (2011) 236802.
[142] D.N. Sheng, Z.-C. Gu, K. Sun, L. Sheng, Nature Communications 2 (2011) 389.
[143] L. Fu, C.L. Kane, E.J. Mele, Physical Review Letters 98 (2007) 106803.
[144] X.-L. Qi, J. Zang, S.-C. Zhang, Science 323 (2009) 1184.
[145] A.M. Essin, J.E. Moore, D. Vanderbilt, Physical Review Letters 102 (April) (2009) 146805.
[146] A.M. Essin, A.M. Turner, J.E. Moore, D. Vanderbilt, Physical Review B 81 (May) (2010) 205104.
[147] J.C.Y. Teo, L. Fu, C.L. Kane, Physical Review B 78 (2008) 045426.
[148] G. Rosenberg, H.-M. Guo, M. Franz, Physical Review B 82 (2010) 041104.
[149] R. Roy, Physical Review B 79 (2009) 195321.
[150] R. Roy, Physical Review B 79 (May) (2009) 195322.
[151] J.E. Moore, L. Balents, Physical Review B 75 (2007) 121306.
[152] L. Fu, C.L. Kane, Physical Review B 76 (2007) 045302.
[153] H. Zhang, C.-X. Liu, X.-L. Qi, X. Dai, Z. Fang, S.-C. Zhang, Nature Physics 5 (2009) 438.
[154] S. Chadov, X.-L. Qi, J. Kübler, G.H. Fecher, C. Felser, S.-C. Zhang, Nature Materials 9 (2010) 541.
[155] W. Feng, D. Xiao, J. Ding, Y. Yao, Physical Review Letters 106 (2011) 016402.
[156] H.-J. Zhang, S. Chadov, L. Müchler, B. Yan, X.-L. Qi, J. Kübler, S.-C. Zhang, C. Felser, Physical Review Letters 106 (2011) 156402.
[157] D. Xiao, Y. Yao, W. Feng, J. Wen, W. Zhu, X.-Q. Chen, G.M. Stocks, Z. Zhang, Physical Review Letters 105 (2010) 096404.
[158] H. Lin, R.S. Markiewicz, L.A. Wray, L. Fu, M.Z. Hasan, A. Bansil, Physical Review Letters 105 (2010) 036404.
[159] Y.L. Chen, Z.K. Liu, J.G. Analytis, J.-H. Chu, H.J. Zhang, B.H. Yan, S.-K. Mo, R.G. Moore, D.H. Lu, I.R. Fisher, S.C. Zhang, Z. Hussain, Z.-X. Shen, Physical Review Letters 105 (2010) 266401.
[160] B. Yan, C.-X. Liu, H.-J. Zhang, C.-Y. Yam, X.-L. Qi, T. Frauenheim, S.-C. Zhang, Europhysics Letters 90 (2010) 37002.
[161] B. Yan, H.-J. Zhang, C.-X. Liu, X.-L. Qi, T. Frauenheim, S.-C. Zhang, Physical Review B 82 (2010) 161108.
[162] H. Lin, L. Wray, Y. Xia, S.-Y. Xu, S. Jia, R. Cava, A. Bansil, M. Hasan, Single-dirac-cone Z2 topological insulator phases in distorted li2agsb-class and related quantum critical li-based spin–orbit compounds, 2010, ⟨arXiv:1004.0999⟩.
[163] B. Yan, L. Mchler, X.-L. Qi, S.-C. Zhang, C. Felser, Topological insulators in filled skutterudites, 2011, ⟨arXiv:1104.0641⟩.
[164] H. Lin, L. Wray, Y. Xia, S. Jia, R. Cava, A. Bansil, M. Hasan, Nature Materials 9 (2010) 546.
[165] Y. Sun, X.-Q. Chen, S. Yunoki, D. Li, Y. Li, Physical Review Letters 105 (2010) 216406.
[166] W. Feng, D. Xiao, Y. Zhang, Y. Yao, Physical Review B 82 (2010) 235121.
[167] W. Al-Sawai, H. Lin, R.S. Markiewicz, L.A. Wray, Y. Xia, S.-Y. Xu, M.Z. Hasan, A. Bansil, Physical Review B 82 (2010) 125208.
[168] D. Hsieh, D. Qian, L. Wray, Y. Xia, Y. Hor, R.J. Cava, M.Z. Hasan, Nature 452 (2008) 970.
[169] D. Hsieh, Y. Xia, L. Wray, D. Qian, A. Pal, J.H. Dil, J. Osterwalder, F. Meier, B. Bihlmayer, C.L. Kane, Y. Hor, R.J. Cava, M.Z. Hasan, Science 323 (2009) 919.
[170] Y. Xia, D. Qian, D. Hsieh, L. Wray, A. Pal, H. Lin, A. Bansil, D. Grauer, Y.S. Hor, R.J. Cava, M.Z. Hasan, Nature Physics 5 (2009) 398.
[171] Y.L. Chen, G. Analytis, J.-H. Chu, Z.K. Liu, S.-K. Mo, X.L. Qi, H.J. Zhang, D.H. Lu, X. Dai, Z. Fang, S.C. Zhang, I.R. Fisher, Z. Hussain, Z.-X. Shen, Science 325 (2009) 178.
[172] D. Hsieh, Y. Xia, D. Qian, L. Wray, J.H. Dil, F. Meier, L. Patthey, J. Osterwalder, A. Fedorov, H. Lin, A. Bansil, D. Grauer, Y. Hor, R. Cava, M. Hasan, Nature 460 (2009) 1101.
[173] D. Hsieh, Y. Xia, D. Qian, L. Wray, F. Meier, J.H. Dil, J. Osterwalder, L. Patthey, A.V. Fedorov, H. Lin, A. Bansil, D. Grauer, Y.S. Hor, R.J. Cava, M.Z. Hasan, Physical Review Letters 103 (2009) 146401.
[174] Y.S. Hor, A. Richardella, P. Roushan, Y. Xia, J.G. Checkelsky, A. Yazdani, M.Z. Hasan, N.P. Ong, R.J. Cava, Physical Review B 79 (2009) 195208.
[175] T. Sato, K. Segawa, H. Guo, K. Sugawara, S. Souma, T. Takahashi, Y. Ando, Physical Review Letters 105 (2010) 136802.
[176] K. Kuroda, M. Ye, A. Kimura, S.V. Eremeev, E.E. Krasovskii, E.V. Chulkov, Y. Ueda, K. Miyamoto, T. Okuda, K. Shimada, H. Namatame, M. Taniguchi, Physical Review Letters 105 (2010) 146801.
[177] A. Nishide, A.A. Taskin, Y. Takeichi, T. Okuda, A. Kakizaki, T. Hirahara, K. Nakatsuji, F. Komori, Y. Ando, I. Matsuda, Physical Review B 81 (2010) 041309.
[178] X. Wan, A.M. Turner, A. Vishwanath, S.Y. Savrasov, Physical Review B 83 (2011) 205101.
[179] X. Wan, A. Vishwanath, S.Y. Savrasov, Computational design of axion insulators based on 5d spinels compounds, 2011, ⟨arXiv:1103.4634⟩.
[180] A.A. Burkov, L. Balents, Physical Review Letters 107 (2011) 127205.
[181] A.A. Burkov, H.D. Hook, L. Balents, Phys. Rev. B 84 (2011) 235126. doi:10.1103/PhysRevB.84.235126.
[182] G.B. Halasz, L. Balents, Phys. Rev. B 85 (2012) 035103. doi:10.1103/PhysRevB.85.035103.
[183] L. Fu, Physical Review Letters 106 (2011) 106802.
[184] J. Maciejko, X.-L. Qi, A. Karch, S.-C. Zhang, Physical Review Letters 105 (2010) 246809.
[185] B. Swingle, M. Barkeshli, J. McGreevy, T. Senthil, Physical Review B 83 (2011) 195139.
[186] G.Y. Cho, J.E. Moore, Annals of Physics 326 (2011) 1515.
[187] M. Levin, F.J. Burnell, M. Koch-Janusz, A. Stern, Exactly soluble models for fractional topological insulators in 2 and 3 dimensions, 2011, ⟨arXiv:1108.4954⟩.
[188] P.A. Lee, N. Nagaosa, X.-G. Wen, Reviews of Modern Physics 78 (January) (2006) 17.
[189] E. Dagotto, Reviews of Modern Physics 66 (July) (1994) 763.
[190] M.B. Salamon, M. Jaime, Reviews of Modern Physics 73 (August) (2001) 583.
[191] W.D. Ryden, A.W. Lawson, C.C. Sartain, Physical Review B 1 (February) (1970) 1494.
[192] Y. Okamoto, M. Nohara, H. Aruga-Katori, H. Takagi, Physical Review Letters 99 (2007) 137207.
[193] Y. Zhou, P.A. Lee, T.-K. Ng, F.-C. Zhang, Physical Review Letters 101 (2008) 197201.
[194] M.J. Lawler, A. Paramekanti, Y.B. Kim, L. Balents, Physical Review Letters 101 (2008) 197202.
[195] D. Podolsky, Y.B. Kim, Physical Review B 83 (2011) 054401.
[196] D. Podolsky, A. Paramekanti, Y.B. Kim, T. Senthil, Physical Review Letters 102 (2009) 186401.
[197] B.-J. Yang, Y.B. Kim, Physical Review B 82 (2010) 085111.
[198] S. Maekawa, T. Tohyama, S.E. Barnes, S. Ishihara, W. Koshibae, G. Khaliullin, Physics of Transition Metal Oxides, Springer, Heidelberg, Germany, 2004.
[199] Y. Tokura, Colossal Magnetoresistive Oxides, Gordon and Beach, New York, 2000.
[200] S.J. Moon, M.W. Kim, K.W. Kim, Y.S. Lee, J.-Y. Kim, J.-H. Park, B.J. Kim, S.-J. Oh, S. Nakatsuji, Y. Maeno, I. Nagai, S.I. Ikeda, G. Cao, T.W. Noh, Physical Review B 74 (September) (2006) 113104.
[201] S. Nakatsuji, Y. Maeno, Physical Review Letters 84 (March) (2000) 2666.
[202] J.S. Lee, Y.S. Lee, T.W. Noh, K. Char, J. Park, S.-J. Oh, J.-H. Park, C.B. Eom, T. Takeda, R. Kanno, Physical Review B 64 (December) (2001) 245107.
[203] D. Pesin, L. Balents, Nature Physics 6 (2010) 376.
[204] G. Chen, R. Pereira, L. Balents, Physical Review B 82 (2010) 174440.
[205] A. Shitade, H. Katsura, J. Kuneš, X.-L. Qi, S.-C. Zhang, N. Nagaosa, Physical Review Letters 102 (2009) 256403.
[206] T. Dodds, T.-P. Choy, Y.B. Kim, Physical Review B 84 (2011) 104439.
[207] S. Landron, M.-B. Lepetit, Physical Review B 77 (2008) 125106.
[208] D.L. Bergman, R. Shindou, G.A. Fiete, L. Balents, Physical Review B 74 (October) (2006) 134409.
[209] H. Jin, H. Kim, H. Jeong, C. H. Kim, J. Yu, ⟨arXiv:0907.0743⟩, 2009.
[210] W. Witczak-Krempa, T.P. Choy, Y.B. Kim, Physical Review B 82 (2010) 165122.
[211] Z. Ringel, Y. Kraus, A. Stern, The strong side of weak topological insulators, 2011, ⟨arXiv:1105.4351⟩.
[212] B. Scharfenberger, R. Thomale, M. Greiter, Physical Review B 84 (2011) 140404.
[213] Z. Ren, A.A. Taskin, S. Sasaki, K. Segawa, Y. Ando, Physical Review B 82 (2010) 241306.
[214] J. Xiong, A.C. Petersen, D. Qu, R.J. Cava, N.P. Ong, Quantum oscillations in a topological insulator Bi_2Te_2Se with large bulk resistivity (6 Ωcm), 2011, ⟨arXiv:1101.1315⟩.
[215] A.A. Taskin, Z. Ren, S. Sasaki, K. Segawa, Y. Ando, Physical Review Letters 107 (2011) 016801.
[216] Z. Ren, A.A. Taskin, S. Sasaki, K. Segawa, Y. Ando, Physical Review B 84 (2011) 165311.
[217] N. Bansal, Y.S. Kim, M. Brahlek, E. Edrey, S. Oh, Giant surface transport in topological insulator bi2se3 thin films, 2011, ⟨arXiv:1104.5709⟩.
[218] G. Chen, L. Balents, Physical Review B 78 (September) (2008) 094403.
[219] G. Chen, A.P. Schnyder, L. Balents, Physical Review B 80 (2009) 224409.
[220] G. Chen, L. Balents, A.P. Schnyder, Physical Review Letters 102 (2009) 096406.
[221] Y.-J. Lin, R.L. Compton, A.R. Perry, W.D. Phillips, J.V. Porto, I.B. Spielman, Physical Review Letters 102 (2009) 130401.
[222] I.B. Spielman, Physical Review A 79 (2009) 063613.
[223] Y.-J. Lin, R.L. Compton, K. Jimenez-Garcia, J.V. Porto, I.B. Spielman, Nature 462 (2009) 628.
[224] N. Goldman, I. Satija, P. Nikolic, A. Bermudez, M. Martin-Delgado, M. Lewenstein, I.B. Spielman, Engineering time-reversal invariant topological insulators with ultra-cold atoms, 2010, ⟨arXiv:1002.0219⟩.
[225] A. Bermudez, L. Mazza, M. Rizzi, N. Goldman, M. Lewenstein, M.A. Martin-Delgado, Physical Review Letters 105 (2010) 190404.
[226] T.D. Stanescu, V. Galitski, S. Das Sarma, Physical Review A 82 (2010) 013608.